EVALUATION OF THREE DRYING MODELS FOR DRY-CURED HAM

Karoline Husevåg Kvalsvik

Academic Supervisor:

Prof. Trygve Magne Eikevik, NTNU

Research Advisors:

PhD. Michael Bantle, SINTEF Energy,

PhD. cand. Inna Petrova, NTNU

Fall 2014

NTNU

Department of Energy and Process Engineering

Norwegian University of Science and Technology

Norwegian University of Science and Technology

Faculty of Engineering Science and Technology
Department of Energy and Process Engineering

EPT-P-2014-60

NTNU

PROJECT WORK

for

student Karoline Kvalsvik

Autumn 2014

Energy efficiency in thermal process industry

Energieffektivitet i industrielle næringsmiddel prosesser

Background and objective

In order to reach EU climate goal (20-20-20) it is necessary to reduce emission of climate gases, increase the use of renewable energy and decrease energy consumption, especially in energy intensive industry and processes.

The focus of the work will be on coupled heat- and mass transfer processes, which are applied in the production of dry-cured ham. Drying is the most important step in the dry-cured ham manufacture; during this period the hams obtain their distinctive quality. At the same time it is the most time and energy consuming step and that is why it is of a special interest for optimization. The mass transfer will directly influence the product quality and the energy consumption (~production costs) of the process. The correct estimation of the drying rate is therefore the most important parameter for processing of dry-cured ham.

The aim of the project work is to identify suitable models for drying process of dry-cured ham, determine the mass transfer controlling parameters and verify the model. The focus shall be on physical models which are more suitable for upscaling and variation of drying conditions, compare to empirical models.

The work will be connected to the research group Industrial Processes at the Department of Energy and Process Engineering at NTNU and to a larger competence research project "Sustainable production of traditional and novel cured dried meat products – DryMeat", coordinated by SINTEF Energy Research.

The following tasks are to be considered:

1. Literature review about drying and curing of ham
2. Determine the mass transfer controlling parameters
3. Evaluate the different models with respect to stability and accuracy
4. Identify a suitable for model process simulation
5. Program a tunnel drier model in Dymola (optional)
6. Draft a scientific paper of the main results from the work (optional)
7. Make proposal for the further work in a Master thesis

-- " --

Address
N-7034 Trondheim
Norway

Location
K. Hejes vei 1b

Tel. +47 73 59 38 60
Fax +47 73 59 35 80
Org. no. NO 974 767 880

The project work comprises 15 ECTS credits.

The work shall be edited as a scientific report, including a table of contents, a summary in Norwegian, conclusion, an index of literature etc. When writing the report, the candidate must emphasise a clearly arranged and well-written text. To facilitate the reading of the report, it is important that references for corresponding text, tables and figures are clearly stated both places.
By the evaluation of the work the following will be greatly emphasised: The results should be thoroughly treated, presented in clearly arranged tables and/or graphics and discussed in detail.

The candidate is responsible for keeping contact with the subject teacher and teaching supervisors.

Risk assessment of the candidate's work shall be carried out according to the department's procedures. The risk assessment must be documented and included as part of the final report. Events related to the candidate's work adversely affecting the health, safety or security, must be documented and included as part of the final report. If the documentation on risk assessment represents a large number of pages, the full version is to be submitted electronically to the supervisor and an excerpt is included in the report.

According to "Utfyllende regler til studieforskriften for teknologistudiet/sivilingeniørstudiet ved NTNU" § 20, the Department of Energy and Process Engineering reserves all rights to use the results and data for lectures, research and future publications.

The report shall be submitted to the department in 3 complete, bound copies.

An executive summary of the thesis including title, student's name, supervisor's name, year, department name, and NTNU's logo and name, shall be submitted to the department as a separate pdf file. The final report in Word and PDF format, scientific paper and all other material and documents should be given to the academic supervisor in digital format on a DVD/CD-rom or memory stick at the delivery of the project report.

Submission deadline: *December 19, 2014.*

☐ Work to be done in lab (Water power lab, Fluids engineering lab, Thermal engineering lab)
☐ Field work

Department for Energy and Process Engineering, 22 August 2014.

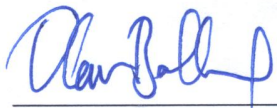

Prof. Olav Bolland
Department Head

Prof Trygve M. Eikevik
Academic Supervisor
e-mail: Trygve.m.eikevik@ntnu.no

Research Advisor:
PhD Michael Bantle, SINTEF Energy
PhD-student Inna Petrova, NTNU

e-mails
michael.bantle@ntnu.no
inna.petrova@ntnu.no

Abstract

Modelling drying of dry-cured ham accurately is necessary for the simulation, and thereby inexpensive optimization, of energy use in production, which is highly energy intensive. Important factors are temperature, salt content and air humidity. Three drying models were compared to two highly different experimental drying curves, for salted and unsalted ham. The most promising was then compared to more curves from experiments to find and include the effects of the important process parameters.

The Fickean model is often successfully applied, but the required model parameter varies between studies and the model is based on some unrealistic assumptions. This model only predicted one of the curves well, even with more realistic assumptions. The Weibull model is simple, requires short computation time and showed accurate results. However it is not based on physics, thus its dependence on physical parameters is problematic to incorporate. The Strømmen model has not previously succeeded in modelling ham drying, but new, realistic modifications concerning dry layer thickness and vapour pressure enabled it to be very accurate. Model parameters were internal resistance, which was 2.013 for salted and for 0.281 unsalted meat at temperature 13 ^{o}C and relative humidity 68 %, and initial dry layer thickness, which was 3.7 mm for salted, and 0.0 mm for unsalted meat. This model was chosen for further investigation.

No model that includes salt content as a parameter is known, and attempts to model it were conducted without success. Too few data were available for this purpose and realistic inclusion of salt content requires further research. Uncertainty about the true mass transfer coefficient and growth of the dry layer make the obtained parameters equally uncertain and was a challenge. Some results indicated that the model could be unrealistic. However, with the new, realistic assumptions, the Strømmen model predicted drying quite well under various conditions and better than the Fickean model. The modified Strømmen model is thus suited for simulations to save energy and reduce environmental impacts and cost of dry-cured hams, and a dynamic model was developed in DYMOLA for this purpose.

SAMANDRAG

Ein grannsam modell for turking av spekeskinke er naudsynt for simulering, og dermed billeg optimalisering av energibruken i produksjonen, som er svært høg. Temperatur, saltinnhald og luftfukt er viktige faktorar. Tre turkemodellar vart samanlikna med to svært ulike turkekurver frå forsøk for salta og usalta skinke. Den mest lovande vart so samanlikna med resultat frå fleire forsøk for å finne og inkludere effekten av dei viktige faktorane.

Ofte vert Fick-modellen brukt med suksess, men modellparameteren som trengst varierer frå artikkel til artikkel og modellen har ein del urealistiske føresetnader. Weibull-modellen er enkel, krev kort reknetid og ga grannsame resultat. Likevel er han problematisk fordi han ikkje avheng av fysiske parametrar, so det er vrient å inkludere effekten av dei. Modellering av skinketurking med Strømmen-modellen har ikkje lukkast før, men nye, realistiske endringar for turrsjiktet og vassdamptrykket gjorde han svært presis. Modellparametrar var intern motstand som var 2,013 for salta og 0,281 for usalta kjøt ved 13 ^{o}C og 68 % relativ fukt, og turrsjikt før turking, som var 3,7 mm for salta og 0,0 mm for usalta kjøt. Denne modellen vart valt til vidare undersøkingar.

Ingen modell som inkluderer salt er funnen, og forsøk på å modellere dette var mislukka. Der var for få tilgjengelege data og dette treng å forskast meir på. Kor stort masseovergongstalet eigentleg er og korleis turrsjiktet veks var usikkert og ei utfordring gjennom heile arbeidet. Parametrane som er funne er like usikre. Somme funn tydde på at modellen var urealistisk, men med dei nye, realistiske føresetnadane passa Strømmen modellen ganske godt saman med turkekurver for ulike forhold, og betre enn Fick-modellen. Den modifiserte Strømmen-modellen er dermed eigna til simuleringar for å spare energi, miljøpåverknader og kostnader for spekeskinke, og det vart lagd ein dynamisk modell i DYMOLA til dette.

Preface

The work with this project was carried out at NTNU during the fall 2014, in the subject TEP4550, as a preparation to my planned master's thesis during the spring 2015. It is part of a larger project, DryMeat, at SINTEF Energi AS, and I am very grateful for that they have let me take a small part in it. My supervisor from SINTEF, PhD. Michael Bantle, among other things arranged it so that SINTEF let me go to a local production site, join a meeting regarding this project and see how the production is. All the employees at SINTEF have been very helpful and friendly in this respect. Thanks to them for that.

I thank all who have helped me with finding relevant literature and data, especially my supervisors Prof. Trygve Magne Eikevik, PhD. Michael Bantle and PhD. candidate Inna Petrova, and the library at NTNU. They have given me access to books and articles that I otherwise would not have had possibility to read. The library also have held courses in the use of search engines and critique. This has been very valuable in the work.

I am also very grateful to Inna Petrova for having supplied all the experimental data for this work, thereby saving me much time in the laboratory and making the work easier for me. Trygve Magne Eikevik has been very helpful in questions regarding heat transfer, salt effects and how to face unexpected challenges in the work. He has spent much of his time on discussing this project with me, and I thank him for that.

Michael Bantle should also have thanks for helping me with programming in DYMOLA, and Nicolas Fidorra have been very helpful in the same, showing me how the model could be made more flexible and convenient to use. Thanks to them both, and to Fredrik Hildrum, who have helped me extensively with writing this in LaTeX, so that it looks quite good even though I have never touched LaTeX before, and for having calmed my nerves many times this semester.

Trondheim, December, 2014

Karoline K. Kvalsvik

Contents

List of Figures

List of Tables

Nomenclature

`0`	initial value, at time=0
`a`	air
`act`	activation (energy)
`core`	the undried core of the sample, inside the dry layer
`dry`	completely dry ham with 0 water content
`db`	dry basis
`e`	equilibrium
`eff`	effective or overall or appearent parameter
`end`	at the end of drying
`ham`	property of the ham
`j`	counting index
`lm`	logarithmic mean
`mix`	mixture of components
`s`	surface
`T`	thermal
`tot`	total, all effects or components together
`w`	water, water vapour
`wb`	wet basis
`wet`	wet bulb (temperature)

Table 1: Nomenclature: Subscripts

α	parameter of the Weibull model	s
β	mass transfer coefficient or	$\frac{m}{s}$
β	parameter of the Weibull model	-
Δ	change in the parameter to follow	
ϵ	porosity	- or %
μ	reduction in diffusion coefficient	-
ν	kinematic viscosity	$\frac{m^2}{s}$
ρ	density	$\frac{kg}{m^3}$
ϕ	relative humidity	- or %
Ψ	dimensionless moisture content	-

Table 2: Nomenclature: Greek letters

Symbol	Parameter	Unit
A	area	m^2
a	activity	-
B, C, D	unknown constants	-
b	scaling facor	$\frac{kg}{m^3}$
C	concentration	$\frac{kg}{m^3}$
c_p	specific heat capacity at constant pressure	$\frac{J}{kgK}$
d	diameter	m
D	diffusivity	$\frac{m^2}{s}$
E	energy	J
f	fugacity	Pa
h	heat transfer coefficient	$\frac{W}{m^2K}$
i	square root of -1	-
k	thermal conductivity	$\frac{W}{mK}$
L	length of meat sample in experiments	m
Le	Lewis number	-
M	molecular mass	$\frac{kg}{kmol}$
MR	moisture ratio (Weibull model)	-
m	mass	kg
Nu	Nusselt number	-
P	power, effect	W
p	total pressure	Pa
p_i	partial pressure of species i	Pa
p^o	saturation pressure	Pa
Pr	Prandtl number	-
$\dot{Q}$	heat flow per time, effect	W
R	universal gas constant	$\frac{J}{kmolK}$
R_g	geometric factor of the Weibull model	-
Re	Reynolds number	-
s	dry layer thickness	m
Sc	Schmidt number	-
Sh	Sherwood number	-
St	Stanton number	-
T	temperature	K or ^{o}
t	time	s
V	volume	m^3
v	velocity	$\frac{m}{s}$
w	constant	m^-2
X	moisture content	$\frac{kgH_2O}{kgdrymass}$, $\frac{kgH_2O}{kgham}$
x	absolute humidity	$\frac{kgH_2O}{kgdryair}$
y	molar fraction	-
z	position coordinate	m

Table 3: Nomenclature: Latin letters

Chapter 1

Introduction

This work will investigate how to model the drying of hams in the production of dry-cured hams. Curing refers to adding a curing agent, generally a salt, to develop certain flavours and desired colour [Toldrà, 2002, p. 27]. This process is very energy intensive and therefore, it is desirable to investigate potentials for energy reduction [Bantle et al., 2014]. In order to do so, accurate modelling of the drying taking place is necessary. How parameters are affecting the process is essential in order to optimize it. Time is one of the main factors contributing to the high energy demand, as long process times are needed for several chemical processes taking place within the hams, which are necessary to achieve desired quality. A small reduction in processing time means a huge reduction in energy use due to the high energy need [Okos et al., 2006].

Hams are dry-cured for different purposes. Earlier, the main reason was the preservation of food, as the raw ham would grow yeast and mould, bacteria, and other microorganisms could feast in it unless the conditions within the hams were changed [Parolari, 1996, Toldrà, 2002, Raiser, 2014]. To achieve this, a low pH creating a sour environment, low temperature, slowing down chemical reactions and thereby bacterial growth, high salt content could be utilized. The hams were stored for long times, allowing certain slow ripening processes to develop special texture and aroma [Petrova, 2015]. Cool climates like northern countries or mountain regions with natural ventilation of outdoor air were used for drying, and the type of ham, the animal feed, salt content, temperature and drying time highly determined the flavour developed. These conditions were uncontrolled and today, hams are therefore produced in drying chambers with regulated temperature and humidity of the air. The main purpose for dry-curing hams nowadays is to achieve the traditional flavour [Toldrà, 2002, p. 27].

This work will focus on evaluating and comparing three model equations describing the drying of hams, in order to find a suitable one for simulation. This model could then be used to test, and compare different drying conditions and various energy systems by applying inexpensive computer simulation. This cheap, easy solution could then give an idea of which conditions are optimal for drying with respect to energy use. Of course, other aspects, like quality, are of high importance and must be evaluated together with such results. However, before this can be done, a realistic model of the hams must be found.

It is desirable to use a physically correct model, that describes the actual processes taking place, without adding too much complexity. This is because a physiological model will depend on temperature, time, air humidity and other factors in a correct manner, so that different drying conditions could be simulated with realistic results.

Any model will be a simplification. A completely realistic model would be extremely complex, and is therefore not desirable. Complex models require longer simulation times and a good

model should be as easy as it is possible without seriously affecting the result. For this reason, it would be useful to determine which factors that influence drying, and include only the most important ones.

This work therefore starts with some definitions of key terms (Chapter 2), followed by a description of the dry-curing process (Chapter 3) and literature review (Chapter 4) to give a theoretical background. Then, controlling factors and promising models for evaluation are chosen, and the theory of the models is given (Chapter 6) before comparison of the models and choice of the most suitable one (Chapter 7). This will then be then further developed and used to develop a simulation model in DYMOLA, which is a computer environment highly suitable for process simulation. Heat calculations will also be considered (Section 7.7). The main points and some conclusions are drawn (Chapter 8), before finally, proposals for further work in a master's thesis are given (Chapter 9).

Chapter 2

DEFINITIONS

In order to describe drying, some parameters should be defined. The **water activity** a_w is defined at the surface of the product as

$$a_w = \frac{\overline{f_w}}{f_w^o(T)}, \tag{2.1}$$

where $\overline{f_w}$ is the fugacity of water vapour in mixture with other components, $f_w^o(T)$ is the fugacity of water vapour alone at the process temperature T and a reference pressure. In the theoretical, ideal case, the activity would be equal to the molar fraction y_w of water in the air, times the total pressure p, divided by the saturated water vapour pressure at the temperature:

$$a_{w,ideal} = \frac{y_w p}{p_w^o(T)} = \frac{p_w}{p_w^o(T)}. \tag{2.2}$$

Here p_w is the partial pressure of the water vapour. Fugacity is a way to account for that gases, like water vapour, do not behave in an ideal manner, and is therefore often described as an «effective pressure» [Moran and Shapiro, 2006]. The water activity is then described as a measure of the amount of water free to take part in reactions and thereby a measure of how easily the product will be destroyed by microorganisms [Raiser, 2014]. In many cases the ideal behaviour is assumed, as this is convenient and almost true. This was also also done in this work.

The **relative humidity**, denoted by ϕ, is defined in the same way as the ideal water activity (2.2), except that it is not only defined at the product surface, but everywhere in the air and inside the pores of the product. Since the relative humidity equals the ratio of vapour pressure to the saturated vapour pressure, $\phi \in [0, 1]$, normally expressed as a percentage.

Water can be firmly bound to the product structure, more loosely bound or not bound at all. The latter is called «free water.» Water can be bound in different ways, which are further explained in Section 4.5. An example is the loose bond between a water molecule and a surface that it rests on, which is called **adsorption**. Energy is required to remove the molecule. All effects that bind water to the structure are called **sorption** effects [Strømmen, 1980, p. 15].

A **driving potential** is an imbalance that will start a process, acting as a driving force. In the case of ham drying, the driving potential is assumed to be the difference in local vapour pressures inside and outside the hams [Song, 1990]. In the inner, undried region of the ham, the vapour pressure is assumed to be equal to the saturated water pressure [Bantle et al., 2014] or somewhat lower due to the sorption of the water. Sorption, binding the water more strongly to the structure, lowers the satured pressure in the ham compared to that of pure water [Luikov, 1966, p. 192].

The ham structure and sorption effects slow down the rate of vaporization in ham relative to that in pure water. Everything that slows down evaporation can be classified as a resistance to the mass transfer. **Internal resistance** to mass transport is what slows down the transport inside the ham, **external resistance** the resitance to transport mass from the surface to the air. In some cases, a gradient (in temperature, air velocity and/or species concentration) can develop in the air outside the product. The air layer close to the ham that differs more than 1 % from the surrounding air is then called the **boundary layer**. This layer is the reason why external resistance develops, as the local differences in for example vapour pressure will be gradual and small in the boundary layer, slowing down the drying.

Water content can be expressed in two different ways: on wet or dry basis. The first is the ratio of the mass of water in the product divided by total mass, typically around 75 % in hams, the second is mass of water divided by the rest of the mass, or the dry mass $m_{dry} = m_{tot,ham} - m_w$. The latter will be used in this text and denoted by X:

$$X = \frac{m_w}{m_{dry}} = \frac{m_w}{m_{tot,ham} - m_w}. \tag{2.3}$$

The **equilibrium water content** is the water content when drying stops by itself and the remaining mass is stable. In other words, when no more net transport of water occurs because the driving potential is zero. This happens when the local vapour pressures are equal everywhere, or when $a_w = \phi_a$. Thus, the relative humidity of the air determines the equilibrium water content of the hams [Comaposada et al., 2000]. The relation between equilibrium water content and water activity is given by graphs called **sorption isotherms** [Raiser, 2014].

Osmotic dehydration is a phenomenon that occurs because hams normally are salted before drying [Petrova, 2015]. The addition of salt to the surface creates a higher salt concentration in the outer part of the product than in the inner. This creates a concentration gradient for salt, and hence, there will be a driving potential to transport salt towards the inner regions with less salt. The meat acts as a semi-permeable membrane, and salt travels through it much faster and much more easliy than the water [Costa-Corredor et al., 2010]. This affects the water activity of the ham. Salt binds water. The activity of pure water is 1, but lower when solutes are present. Hence the water activity, or the effective pressure of the water, decreases in the part of the meat where salt is added. As a result, water will experience a higher pressure inside the ham than in the outer layer and due to this be transported towards the surface. This pressure difference is called osmotic pressure (or salt pressure in greek). Both driving potentials are present until the salt and water concentrations are equal everywhere.

The outwards water transport will contribute to drying out the product, but as the process continues, more of the water in the ham contains salt, and thus, the water activity and driving potential decreases. Thus salt increases the drying rate initially, but then retards it. Higher salt contents in clip fish led to faster dehydration [Strømmen, 1980], while studies on ham imply that higher salt content slows down the overall drying so much that even with higher initial water contents, unsaltet samples are faster dried than salted [Bantle et al., 2014, Raiser, 2014, Gou et al., 2003]. The longer processing time for hams might be the main reason for this difference. Salt is initially mainly in the outer layers, but the salt distribution will be quite even

after four to five months and later there will be more salt in the core than in the outer layers due to the higher water content in the core [Toldrà, 2002, p. 47].

Diffusion is a transport phenomenon, where the flux of a specimen is proportional to a gradient the concentration gradient related to it. The gradient is an expression for an imblance or driving potential. The flux is also proportional to a coefficient, called the **diffusion coefficient,** $D_{specimen,medium}$. This is described by Fick's laws in Section 6.2. This phenomenon is affected by the media in which it occurs, chemical reactions and composition, temperature and pressure. There are more types of diffusion: gaseous or vapour diffusion, liquid diffusion and surface diffusion of adsorbed molecules [Okos et al., 2006]. The first two explain themselves, the last involves that adsorbed molecules distribute evenly on the surfaces they are adsorbed to, without really desorbing [Waananena et al., 1993].**Knudsen diffusion** is gaseous diffusion in pores of smaller diameter than the mean free path (about 0.07 μm), so that the molecules hit the walls and bounce through the channel [Nesse,]. The possibility of adsorption slows down this type of diffusion. **Stefan diffusion** is diffusion in multicomponent mixtures, where the species flow due to differences in speed and a concentration or chemical potential gradient [Max, 2013]:

$$\frac{\nabla \mu_i}{RT} = \nabla \ln(a_i) = \frac{\sum_{j=1, j\neq i}^{n} y_i y_j}{D_{ij}(v_i - v_i)}. \tag{2.4}$$

Mutual diffusion is brownian motion or Fickan diffusion, also called self diffusion. It brings concentration gradients to zero or species distributions to equilibrium, and is caused by the larger probability of a specimen to move away from an area with high concentration of the specimen, than from an area with lower concentration [Scalettar et al., 1988].

A similar transport phenomenon for heat is **conduction**, where heat flux is proportional to a temperature gradient and a constant which depends on the medium the heat flows through. This is called the thermal conductivity, k_{medium} [Bergman et al., 2011, p. 3].

Convection is another transport phenomenon, where a bulk flow (such as air circulating in contact with hams) drives the transport. Since diffusion of mass creates a mass flow, mass diffusion always creates some convection, but normally this is negligible [Bergman et al., 2011, p. 6]. The rate at which the transport happens can be looked upon as dependent on some conducting property of the medium, or inversely as dependent on the resistance of the medium, which is then the inverse of the conducting property.

Capillary flow driven by capillary forces are forces arising due to pressure differences over water surfaces in the pores or capillaries in a product. This can create a driving force for liqiud flow. The so called two pore model explains this phenomenon by two connected pores, initially filled with water. The water wets the capillary walls and curves due to its surface tension. If some water is evaporated, a change in pressure over the surfaces occur. This causes the whole surface to curve and different radii in the pores will give different surface curvatures and pressures, which will drive the water from the wider to the narrower pore. This will continue as long as water is evaporated to maintain the pressure difference, but is only normal in the initial part of drying. All information in this paragraph was found in [Song, 1990, p. 19-27].

Some products can be in one of two states [Moyne and Degiovanni, 1985]: the **funicular**

state where water is continuously distributed in the solid and flows by capillary forces; or the **pendular state**, which is reached after the funicular state, when much of the water has evaporated. It is characterized by that the water is no longer continuously distributed, only some droplets remain and most of the H_2O is in the vapour phase. In this case pressure matters more than capillary forces (capillary forces affect only water transport, not vapour transport) [Moyne and Degiovanni, 1985].

Drying is often described by three **drying steps** [Okos et al., 2006], [Song, 1990, p. 4-5], [Strømmen, 1980, p. 6-7 and 97], [Raiser, 2014]: initially the free water near the surface evaporates like pure water. Said in another way; the ham has no effect on the drying rate, which is constant, and determined solely of external condtions. This step was not observed in ham [Bantle et al., 2014, Raiser, 2014] or clipfish [Strømmen, 1980, p. 7]. [Raiser, 2014] explained this by the osmotic dehydration before the convective drying, which removes the free water close to the surface, so that this step one cannot occur. The second step is characterized by a falling drying rate as the outer layer of the product is dried and properties in this region altered. The outer, drier layer creates a larger resistance to mass flow than a wet product, as water keeps the pores in the ham open [Okos et al., 2006]. As the dry layer grows, this internal resistance increases and drying rate falls. Another drop in drying rate characterizes the third step, when more firmly bound water (chemically bound water and capillary water, see Section 4.5) is removed [Okos et al., 2006, sec. 10.2.0], [Song, 1990, p. 5].

Ham initially consists mainly of water [Toldrà, 2002, p. 9-10], the other main component is protein, which is mainly found in the muscle fibres, also called the myofibrils, and they are placed as parallel threads in the meat. The breakdown or degradation of these proteins is called **proteolysis** and is performed by enzymes called proteases [Toldrà, 2002, Petrova, 2015, p. 9-10]. Proteolysis leads to the formation of amino acids and improves the texture as it breaks down the muscle fibres.

Between the different muscles in the hams there are fat tissues, which are barriers for water [Gou et al., 2004]. In fat, **lipids** are the main constituent, and the breakdown of these, by a set of reactions called **lipolysis**, is very important for flavour development. Proteolysis and lipolysis are the most important groups of biochemical reactions occurring according to [Toldrà, 2002, p. 12-18]. Too much of these reactions is however not desirable [Toldrà, 2002, p.135].

Excessive degradation of proteins (proteolysis) creates more amino acids than desirable. This affects the flavour to the worse, but also leads to the formation of a tyrosin **crystal layer** on the ham surface. This white layer can be brushed off, but is a visual sign of an undesired reaction and a too tender product. The reason is often related to the age and breed of the pig [Toldrà, 2002, p. 116 and 122].

In the same way, excessive lipolysis, or lipid oxidation, affects the product quality to a large extent. Some oxidation elabourates the flavour, too much causes rancidity and is highly unwanted [Toldrà, 2002, p. 135-7]. These reactions are mainly active during the first five months of the ripening period, hence it extends over the whole drying stage. Therefore, fat content and the degree of lipolysis and rancidity is higly important for the final taste and quality [Toldrà, 2002, p. 135-7]. All these chemical processes depend on water and salt content, pH

and temperature, and the key to a high quality product involves low temperature and decrease of a_w [Okos et al., 2006, Marinos-Kouris and Maroulis, 2006]. Optimal pH for desired flavour development is around 5.7 [Ruiz-Cabrera et al., 2004].

Other concerns in dry-curing ham are those affecting quality. These are caused by too high temperatures or too fast or too slow dehydration, which can result in a burnt surface, microorganism or a hard dried out surface which prevents drying of the inner parts of the ham [Strømmen, 1980, Parolari, 1996, Bantle et al., 2014]. Another concern is **non-enzymatic browning** or maillard browning, which is the reduction of proteins and/or their components with sugars and ascorbic acid (vitamin C). This is desirable in some amount, but too much is bad and can be a danger to the kidneys [Friedman, 1996]. It is normally accompanied by brown colour, which gives it its name [Friedman, 1996]. It can be prevented by ensuring the temperature and water activity are not too high.

Chapter 3

The production of dry-cured ham

3.1 Why dry-cure hams?

Hams are dry-cured for different purposes. Earlier, the main reason was the preservation. The main purpose for dry-curing hams nowadays is rather to achieve the traditional flavour [Toldrà, 2002, p. 27]. Health considerations are affecting the product slightly, and all the old and new methods and ideas have also led to the development of standards for some of the more famous types of ham like Parma ham [Parolari, 1996]. Some of the most important hams are Iberian and Serrano ham (Spain), Parma ham and San Daniele prosciutto (Italy) and Bayonne (France) [Toldrà, 2002] and Celta (Spain), Toscano (Italy), Jinhua, Xuanwei (China) [Petrova, 2015].

It is important in the dry-curing of ham that the ripening develops the desired texture and flavour. Actually, this is what takes most of the production time [Petrova, 2015], but also requires that the water content is not too low for reactions to occur. Unlike other dried products, the goal is not to remove as much water as possible as quickly as possible, since many processes need time to take place. These processes need water, and it is only in order to prevent microorganism contamination during the ripening that the hams are dried. The weight loss is an economic loss. Therefore excessive drying is unwanted, and there is a fine balance between economic loss and safety of microorganism.

The ripening does not anly affect taste, but also texture, and the degradation of the proteins by proteolysis is the main reason for the texture changes in dry-curing of ham. These are important for quality [Petrova, 2015], and so is the lipolysis (see Chapter 2). Lipolysis is highly affecting the development of desirable aromas, but excessive lipolysis can also destroy product quality [Toldrà, 2002, p. 135-7]. The main muscles of hams are biceps femoris and semimembranosus, and these, along with gluteus medius are the most commonly used in experiments for ham [Clemente et al., 2011], and the type of ham, the animal feed, salt content, temperature and drying and ripening time highly determines the flavour developed [Toldrà, 2002, p. 27].

3.2 Manufacture

The hams are supplied to the production site and, if necessary, thawed and eventually pressed. Pressing is done to bleed out any blood left in the hams and to create and/or open pores within

the meat to enhance transport of water and salt in the product [Raiser, 2014, Strømmen, 1980, Toldrà, 2002, p. 30-32 and 40-41]. A water loss occurs upon thawing, and another loss due to pressing. These are only a few percent of total mass [Raiser, 2014, Toldrà, 2002, p. 30-32].

Normally, some additives like nitrate, nitrite, potassium chloride or other salts are added before the hams are salted and sent to rest, dry and ripen [Raiser, 2014, Toldrà, 2002, p. 37-38]. The salt can be added in undecided amounts by a bath in salt solution or storage in containers filled with salt for a period of two-three weeks. Eventually, the specific desired amount of salt is rubbed onto the surface before the hams are packed in plastic and stored. Larger hams are salted twice; the second time about 1 day per kg ham is needed [Toldrà, 2002, p. 37-39]. Osmotic dehydration then occurs, see Chapter 2, and due to this, $3-4$ % of the water is withdrawn. [Toldrà, 2002, p. 37]. During the salting stage, the environment must be moist, in order to prevent dehydration of the surface and creation of a hard crust on the outside that might prevent transport of water. The temperature must be low, typically $4-6\,^{\circ}\mathrm{C}$, since, at this stage, the hams are wet and the salt content in the core of the hams low: Bacteria growth must be prevented [Raiser, 2014].

The surface salt is then washed or brushed off and the hams are stored again for two to nine weeks to obtain a more evenly distributed salt content. Another $4-6$ % of the mass is lost during these weeks [Raiser, 2014, Toldrà, 2002, p. 39]. In some processes more additives are used to prevent growth of microorganism [Raiser, 2014] before the hams are hanged in ranks to dry. The hams should not touch each other to have as much surface area open to the free stream air blowing above them as possible [Toldrà, 2002, p. 40]. The drying period normally lasts for about two months. Production time takes between two months and two years depending on desired quality.

The drying is the most energy intensive part of the process [Clemente et al., 2011]. During this time, temperature can be kept constant at $10-18\,^{\circ}\mathrm{C}$ or varied. Some processes have one week with temperatures as high as $22-26\,^{\circ}\mathrm{C}$ to enhance drying and enzymatic reactions, but this cannot be done safely for a longer period for previously mentioned reasons [Toldrà, 2002, p. 40-41]. The humidity of the air should be low in order to dry the products, but as in the salting process, there is a danger of drying out the surface that must be avoided [Bantle et al., 2014], thus imposing a lower limit to the humidity of the drying air. Normally, the relative humidity is at least 60 % [Toldrà, 2002, p. 36].

Ripning takes place both during and after drying, and is the real goal with behnd dry-curing. The reactions taking place depend on the type of pork breed, gender, diet and age at slaughter [Toldrà, 2002, p. 167, 196]. The amount and type of lipids and the degradation of lipids and proteins are important for the flavour development and required time. Flavour also depends on temperature and additives like nitrate, nitrite, salt, etc [Cassens, 1995]. They decide colour, texture, flavour, pH and many of them need much time to reach the desired state. An increase of some components, like certain lipids, have been found to enhance both flavour development, but water removal tends to be slower [Ruiz-Cabrera et al., 2004].

Some enzymatic reactions take place only in sour environments, created by the amino acids formed by proteolysis [Toldrà, 2002, p. 93 and 113-122]. The best conditions for proteolysis

involves long time and low salt content, and most of it occurs during the forth to tenth month or so. Lipolysis is most important the first five months [Toldrà, 2002, p. 93 and 113-122].

Some drying processes start already in the resting period, after the first salting, and are conducted in two stages: one with high temperature or very low relative humidity (50-60 %) so that the drying rate increases. The production rate can then be higher. After two weeks, a lower temperature and higher humidity must be used, in order not to dry out the outer layer. Drying it out destroys the outer layer, as it becomes hard with almost no water content. Parolari describes it by the word «crust.» Also, this creates a barrier for further water loss from inside, so that water pockets and bacteria can develop [Parolari, 1996].

Drying ends when the moisture content has reached a desired value. At this point, the water activity a_w, defined in Chapter 2 is normally in the range [0.87, 0.94], and normally the drying has then lasted for two to four months [Petrova, 2015]. When $a_w < 0.9$ the hams are safe of bacteria, microbial activity and reactions, for example by enzymes, that could impair the taste [Raiser, 2014, Okos et al., 2006]. However, mould and yeast could be a problem unless $a_w < 0.80$, according to [Okos et al., 2006].

The total mass loss throughout the entire process is about 33-36 % on wet basis [Toldrà, 2002, Raiser, 2014, p. 40-41]. After drying the hams are covered with lard, fat with salt and pepper, which prevents attack of mould, yeast and further drying, especially dehydration of the outer layer [Toldrà, 2002, p. 40-41]. This is done since any additional mass loss is a purely economic loss. The hams are then left to rest and further ripening forseveral months so that salt and water balances and the final desired taste develops. The different qualities of the hams mainly depend on the length of this step. Total production time can be up to three years. After this, the hams are boned pressed in shapes [Toldrà, 2002, Raiser, 2014, p. 41] and ready for consumers.

Chapter 4

Literature review

4.1 Introduction

Dry-curing of ham is a way to preserve the meat. Drying means to remove water by evaporation [Marinos-Kouris and Maroulis, 2006]. Curing means adding a salt or curing agent like NaCl and normally nitrate or nitrite [Toldrà, 2002, p. 3]. The addition of these bind water, and together with drying, reduces water activity or the amount of free water available for bacteria and microorganisms. The term «water activity» was introduced to describe the conditions for microorganisms according to [Kapsalis, 1987]. This was useful because water activity, unlike moisture content, says something about the availability of water that organisms can utilize, and hence what degree of drying that is required to preserve the food.

Drying involves mass transfer of water through the ham and from the ham to the surrounding air. There are several mechanisms for mass transfer: diffusion of different types, capillary flow and bulk flow. Diffusion and capillary flow are described in Chapter 2, bulk flow is due to a pressure gradient created at high temperatures [Moyne and Degiovanni, 1985]. Normally, only one or a few of the mechanisms are dominating [Waananena et al., 1993, Okos et al., 2006]. Eventually they dominate at different times in the drying process [Whitaker, 1977, p. 121], [Song, 1990, p. 26], [Okos et al., 2006].

Attempts to mathematically model the drying process seems to have been carried out for about a century. The models are physiological, empirical or phenomenological. The first ones aim to describe what is physically taking place during drying. Phenomenological models do not consider which mechanism is dominating, but looks only at some thermodynamically driving force created by imbalances. They use gradients (both concentration, temperature and pressure gradients can be used) and express mass flux from this [Okos et al., 2006]. Empirical models are based purely on fitting a mathematical expression to results, applying parameters without physical meaning. These models have the advantage that they are easy to use [Corzo et al., 2010].

4.2 Early drying

Preservation of food has been important for several thousand years, and when salting and drying was first used is unknown[Toldrà, 2002, p. 1]. [Toldrà, 2002, p. 2] writes that the origin probably was around the Mediterranean sea due to the access to salt from the sea and the climate that

allowed for drying. From the Sumerian culture, texts from 2000 B.C mention how pork was an important part of the diet. Also northern Europe has traditions for dry-cured meat. In this region, smoking the meat was more usual due to the cold climate, and smoking and drying meat has been done for at least 1000 years [Toldrà, 2002, Petrova, 2015, p. 2].

In the early drying processes, the hams were stored for long times, allowing certain slow ripening processes to develop special texture and aroma [Toldrà, 2002, p. 113-122 and 135]. Cool climates like those in northern countries or mountain regions with natural ventilation of outdoor air were used for drying. Salting, post-salting and final drying and ripening both are and were the main steps in the production. The drying and ripening conditions were badly controlled, since the regulation mainly consisted in opening or closing the windows. Today, hams are therefore produced in drying chambers with regulated temperature and humidity of the air [Toldrà, 2002, p. 40].

4.3 EARLY STUDIES

The effect of salting has been known for very long times. The earliest detected study of how sodium chloride and potassium nitrate are distributed in such a product was performed in 1911 [McBryde, 1911] in [Besley, 1942]. The need for conservation is demonstrated by that [Milroy, 1917] writes about attempts to transport meat safely on ships by freezing it as early as 1861, and includes a list over imported meat, among other products salted and frozen ham.

Additives that prevent microorganism contamination and thereby preserve the food are called curing agents. Curing agents are salts, typically NaCl and one salt containing nitrate and/or nitrite [Toldrà, 2002, p. 3]. All hams contain NaCl, which also gives it taste and make up 4-9 % of weight inside the ham [Raiser, 2014]. The role of muscle structure and content has also been known for many years. The role of lipids, protein has been studied since before 1937, when [Anderson and Williams, 1937] wrote about «The role of fat in diet» and mentioned among other factors whether ham is good or bad for the human diet. A study of meat products [Hankins, 1945] then reported that pork infection is a problem, but

> *«... certain procedures in freezer storage and curing are now known to kill the organism ... Except in farm and home curing and canning, spoilage of meat does not present a serious problem ...»* [Hankins, 1945]

> *«... rancidity in fat is accompanied by a change to a yellowish color. Pork is especially predisposed to such changes.»* [Hankins, 1945]

It is mentioned that meat can have different shades of red, dark or light, but why was not clear. Concerns were, and are still, those of browning, nutrient degradation, rancidity and formation of a crystal layer [Hankins, 1945, Parolari, 1996, Toldrà, 2002, p. 116].

4.4 Early modelling

The most widely used model for drying of food is probably Fick's law of diffusion [Gou et al., 2004, Ruiz-Cabrera et al., 2004, Waananena et al., 1993, Okos et al., 2006] as described in Section 6.2. Adolf Eugen Fick developed Fick's law of diffusion in 1855 for gases, but there are also other types of diffusion [Waananena et al., 1993], which were explained later in Chapter 2.

Diffusion models make use of a diffusion coefficient to describe the mass transport. It also is and has been usual to swop the diffusion coefficient with an effective diffusion coefficient that takes hand of all the deviations from pure, true Fickean diffusion, which, if such a thing exists, would occur in pure media [Whitaker, 1977]. The effective diffusion coefficient therefore depends on which mechanisms that control the drying [Whitaker, 1977]. Which mechanisms these are and how they should be modelled has been discussed for about a century.

[Lewis, 1921] looked into mass transfer during drying of solids. He described the drying process as liquid transport by diffusion to the surface and then evaporation from the surface [Whitaker, 1977]. [Sherwood, 1929] followed these ideas in his investigations from 1929 and onward. He also mentioned that heat transfer might play a role and diffusion might be in both vapour and liquid phase, but did not investigate this further [Whitaker, 1977].

On the other side, scientists working with moisture in soil, clay and ceramics, [Richards, 1931, Gardner and Widtsoe, 1920] according to [Whitaker, 1977], found from 1920 and onward that liquid transport in unsaturated solids cannot be explained by diffusion alone: the surface tension of water must be included. The surface tension of water creates capillary forces, which transport liquid. Gases were assumed to be transported by diffusion or other mechanisms in their study. Capillary flow is pressure driven according to [Richards, 1931], who also modelled this mechanism by Darcey's law. He wrote that capillary flow:

> *« . . . is distinguished from other cases of liquid flow only because of the relation of surface tension and curvature to the pressure and to the effective cross-sectional area of the liquid-transmitting region.»*

Using surface tension and curvature to describe pressure difference between the two sides of a curved liquid surface in a pore, he found an equation for the capillary flow potential Ψ, which is the sum of gravity and pressure forces, derived from the momentum equation. This is the driving potential to move the liquid. Results showed that the potential depends on moisture content.

The moisture content at equilibrium versus the relative humidity of the air, which at equilibrium equals the water activity of the product, can be described by sorption isotherms [Comaposada et al., 2000]. These are graphs having water content as the ordinate and water activity as the abscissa. A mathematical model for these is Bradley's equation from 1936, given in [Okos et al., 2006], who also list several others that developed models for sorption isotherms during the 20th century.

[Ceaglske and Hougen, 1937] stated, according to [Whitaker, 1977], that capillary flow was the main drying mechanism for bodies saturated with water. They successfully modelled capillary

forces coupled to liquid content for both sand, clay, soap, paper and more, whereas the diffusion model clearly failed at the same. For wood however, the capillary model failed and the diffusion model performed well.

Other factors affecting the drying have been studied later, like heat transfer along with mass transfer that [Krischer, 1940] included as the first [Whitaker, 1977, p. 124]. The first one to study the dependence on the other factors according to [Katekawa and Silva, 2006], was Luikov in 1950 (reference was not given). One such factor is temperature, which is often modelled by the Arrhenius equation (see (6.10)). The earliest mentioned study that applied this equation in [Okos et al., 2006] is [H.Burton, 1954].

4.5 QUALITY AND ITS RELATION TO WATER

Quality is a major factor for studies on ham, and the role of water is important for this purpose. According to [Kuprianoff, 1958] in [Okos et al., 2006], not all water in products is free to take part in reactions; some of it is bound. «Bound water» desorbs less easily than unbound water, and he defined it as water that does not freeze below the freezing point of water. This partially explains some of the findings in the 1960's, when some studies revealed that some pork meat easily loses much water. Such meat was characterized as pale soft and exudative, or PSE. It has high drying rates and low quality, because the water is mainly dried from the surface, hence, the inside is not safe for bacteria and the outer layer is rancid [Cassens, 2000]. It was also recognized that pigs can have PSS, porcine stress syndrome, and this was considered as one reason for PSE [Cassens, 2000].

The colour of PSE meat is pale, but there is also a similar type of meat, that has the desired red colour, RSE (red, soft and exudative) which causes similar problems, but this is less recognizable due to the colour [Warner et al., 1997] in [Toldrà, 2002].

Pork can also be DFD, dark, firm and dry [Cassens, 2000]. This looks good, but should not be used at all, because it binds water and has a neutral pH (ideally meat should have pH 5.6-6.2 [Toldrà, 2002, Gou et al., 2002, p. 12 and 29]) which allows for bacterial growth. The problem is more rear, but also more severe than PSE [Toldrà, 2002, p. 24]. 18 % of the pork in the USA were PSE in 1963, and 16 % in 1992. 16 % had high quality and 10 % DFD the rest was RSE [Cassens, 2000].

In 1966, Luikov invented a model that coupled heat and mass transfer by including both temperature and concentration gradients in both the mass and heat transfer equations [Luikov, 1966]. Except for this, it is quite similar to the Fickean diffusion equation, but it allows water to evaporate within the solid and is based on thermodynamic irreversibility. The model has been applied to wood drying by several researchers [Thomas et al., 1980, Kulasiri and Samarasinghe, 1996]. One of the findings was that the temperature gradients were negligible.

4.6 Sorption

Luikov also described how water is bound to the product structure in the same book. He wrote that water in hams or other products can be present in several ways [Strømmen, 1980, p. 15], [Luikov, 1966, p. 193-197]:

- chemically combined water
- adsorbed water (which is assumed to constitute a monomolecular layer on the inside of the ham structure, called the monolayer. [Okos et al., 2006] discuss its existence.)
- capillary bound water (which is bound by the surface tension and wetting properties of water)
- osmotically bound water (which is bound by ionic /polar attraction)
- free water

The first four types are bound water, and all the binding phenomena together are called sorption [Strømmen, 1980, p. 15]. [Luikov, 1966, p. 192 and 198] wrote that due to the sorption, more energy than the latent heat of evaporation is needed to remove the water, and therefore, the vapour pressure in the ham will be slightly lower than that of vapour above pure saturated water. This decreases the driving forces in drying. Solids that have water bound to it by adsorption, like hams, are called hygroscopic [Raiser, 2014].

The bound water content in protein was studied by [Berlin et al., 1970]. 50-60 % of dry mass was bound water. Studying the water content and profile was previously cumbersome and lacked accuracy. A sample would have to be removed from the experiment and the water content measured, hence different samples would be studied at each observation [Gou et al., 2004, Okos et al., 2006]. Around 1970 however, studies using nuclear magnetic resonance spectroscopy, or NMR were performed [Okos et al., 2006]. NMR allows the study of water content without interrupting the drying process. For hams, no study with NMR before [Ruiz-Cabrera et al., 2004] was detected.

Studying the sorption and desorption characteristics of solids, often displays a tendency of hysteresis, which means that different equilibrium water contents are detected for sorption and desorption. The hysteresis for cooked pork was found to be small and present from water activities between 0 and 0.85 [Wolf et al., 1972].

4.7 Controlling drying mechanism

Unlike the soil scientist who found the diffusion mechanism non-satisfactory to describe drying in several materials, those who looked at biological material [Berger and Pei, 1973] got good results by applying the diffusion equation when the effective diffusion coefficient D_{eff} was a function of

moisture content [Whitaker, 1977]. Recall the diffusion coefficient is called «effective» when all other effects than diffusion only are accounted for through the allowed variation of D_{eff}.

Which mechanisms that were mainly responsible for water transport in meat was investigated by [Radford, 1976], and he concluded that Fickean diffusion was the most important one in his study on lean mutton[Trujillo et al., 2007]. Then, [Radford et al., 1976] were also some of the first to model mass diffusivity by means of the «effective» diffusion coefficient in meat, and heat transfer was also included in their modelling [Trujillo et al., 2007].

The 70's was also the time when controlled drying environment with coolers to prevent microorganisms became usual [Parolari, 1996]. Before that, more meat was destroyed because both temperature and water content were high, and at least one of them should be low to prevent contamination. Hence, some production sites could not operate all year [Parolari, 1996].

In Whitaker's work from 1977, he strongly criticized every model not based on the fundamental laws of physics, and developed a model that is based on these [Whitaker, 1977]. He criticized diffusion, stating that the success of this model is due to that the diffusion coefficient is allowed to vary, in a completely intuitive and empirical manner, with all other parameters. His work includes examples where clearly the capillary effect, not diffusion, is the controlling mechanism for drying of granular media, but he also wrote that there is «definite evidence» for diffusion and convection to control when water content is so low that the pendular state is reached [Whitaker, 1977, p. 125], especially in biological material. [Whitaker, 1977, p. 123-126] and [Song, 1990, p. 26] write that for both granular and biological material, the capillary effect is important in the start of drying, when the surface is wet, but when it is dry *«the convection and diffusion in the vapour phase are the only mechanisms by which the moisture content can be reduced.»* As a result, he stated that the capillary effect is dominant for porous media, whereas the diffusion is a better mechanism for biological material.

Drying normally displays three different stages, as explained in Chapter 2. [Strømmen, 1980] observed no sign of the first drying phase in his doctor thesis about clip fish, but found that most of the moisture transport happens in vapour phase, about 75 %. In this work, Strømmen developed a model based on the analogy between heat and mass transfer, which, applied to the drying of clip fish, gave good fits.

A temperature and a concentration gradient both can cause mass transfer, and both can cause heat transfer and they affect each other as in for example the Luikov model [Luikov, 1966]. These are called Soret and Dufor effects [Okos et al., 2006]. The coupling between heat and mass transfer, or how they interfere, was investigated by [Fortes and Okos, 1981] and [Crapiste et al., 1988] according to [Okos et al., 2006]. [Fortes and Okos, 1981] looked at irreversible thermodynamics together with phenomenological models to model this dependence. [Crapiste et al., 1988] performed a similar study. They all concluded that the effect on mass transfer due to temperature gradients was very small compared to mass transfer due to concentration gradients [Okos et al., 2006]. Thus, the inclusion of temperature gradients in mass transfer equations seemed unimportant.

The influence of moisture and the importance of the capillary effect is related to the pores in the substance being dried. [Gal, 1983] in [Okos et al., 2006] concluded that most food products do

not have any firm pore structure for water. This can explain why the diffusion mechanism rather than the capillary flow often models biological material better as [Whitaker, 1977] commented, and also why D_{eff} changes with moisture content, as the pores might exist only when water is present. It is not clear whether this is true for hams, which always contain much water, also after drying.

4.8 PROCESS MANIPULATIONS

Several researchers in the 80's found that thawed meat is dried faster than unthawed meat [16, 2003, Toldrà, 2002, p. 47] . They found that frozen and thawed hams had salt diffusion coefficient $2.9 \cdot 10^{-10}$ and green ham had $2.2 \cdot 10^{-10}$. Pressing the meat mechanically had the same effect as freezing and thawing, as all these processes make cracks and open up pores for mass transport [Toldrà, 2002, p. 203-4], [Strømmen, 1980]. One drawback is that yeast and mould can start growing in such pores, thereby closing them and lower water transport.[Toldrà, 2002, p. 47] No final conclusions about the relationship between structure and moisture content has been found.

The addition of nitrate and nitrite to hams prevents botulism and hence quality degradation [Richard, 1981]. This is the only function these additives have and one should avoid more than necessary due to health [Cassens, 1995, Cingi et al., 1992]. When added, potassium nitrate and/or sodium nitrate dissolve in the water in the hams. The nitrate ions (NO_3^-) can then be reduced to nitrite (NO_2^-) [Toldrà, 2002, p. 30]. For health reasons, there are maximum allowed amounts of these components [Cassens, 1995].

The reduction rate of nitrate is high at pH 5.6-6.0 and ascorbic or erythorbic acid is often added simultaneously to reduce the nitrate. Nitrite can further be reduced to nitric oxide (NO). This is very important, as nitric oxide reacts with myoglobin in the meat to nitromyoglobin and this gives the meat the desired red colour typical for cured meat [Toldrà, 2002, p. 30]. However, the prevention of oxidation processes also affects the flavour. These additives were forbidden in Parma from 1993 [Parolari, 1996].

Attempts to reduce energy usage by speeding up the process has been performed by several authors. Boning and skinning the hams before drying-ripening did not affect the eating experience, while salt penetration, shrinkage, moisture loss rate and proteolysis was enhanced [Montgomery et al., 1976]. Making cuts in the meat to enhance diffusion gave higher salt penetration, but did not increase ripening or water loss rate [Marriott et al., 1983] in [Toldrà, 2002]. Tumbling the meat before curing resulted in higher salt content and moisture removal [Marriott et al., 1987].

4.9 STUDIES ON QUALITY IMPROVEMENT

During the 80's, many scientists looked into the enzymatic reactions in ham during ripening. The focus on understanding why PSE and DFD occurred and controlling the drying environment has first happened during the last decades: Almost no studies before the 80's on ham are found. [Parolari, 1996] has earliest reference from 1978. [Okos et al., 2006] have one reference to a ham study from 2004 and mentions a study on hysteresis in pork isotherms from 1972, but no other pork study is mentioned despite a long list of products. In their review article, [Waananena et al., 1993] also only mention one.

Problems with destroyed, contaminated meat have become fewer the last decades due to the controlled drying environments with cooled air and studies revealing necessary salt and water activity levels [Parolari, 1996]. This has not been enough to prevent surface problems of Parma ham, which requires high drying rates and cold air in the first resting period before the main drying. Although many of these requirements were met during the 1980's, problems with microorganism and mould are far from over [Raiser, 2014, Parolari, 1996, Toldrà, 2002, p. 40-41].

Air conditioning is extremely important to avoid quality problems: If the air velocity is not high enough, the surface will be wet and mould grow on the outside [Raiser, 2014]. In order to test the quality inside the hams, a probe and sniff method has been used. A probe (horse bone) is then inserted into the meat and trained experts smell whether the inside is acceptable or not [Parolari, 1996, Toldrà, 2002]. The type of problem depends on the season. Surface problems typically occur in the summer and the inside is a challenge in the winter [Parolari, 1994] in [Parolari, 1996].

[Marriott et al., 1992] concluded that

> *«Dry-curing can be accelerated through production techniques such as tumbling, blade tenderizing, microbial inoculation, use of nitric oxide and processing as skinned and/or boneless legs,»*

but more research was necessary to ensure quality was satisfactory. Freezing accelerated lipolysis and proteolysis by three to six months, and only the salt taste was affected in a study of [Motilva et al., 1994] in [Toldrà, 2002], but adjusting the amount of salt should not be too difficult. Since the main part of the production consists in ripening, not drying, the enhancement of these processes is more important in order to save energy than enhancing the drying rate. Also, sufficiently high water content is needed for several ripening processes to find place [Bantle et al., 2014, Petrova, 2015], so a too fast drying is not really desirable.

4.10 Factors influencing the process

The required amount of energy to desorb water and evaporate it is often described by the activation energy E_{act} in the Arrhenius equation. Instead of modelling D_{eff} intuitively as proportional to moisture or salt content, some authors allow the activation energy to vary: [Palmia et al., 1993] in [Gou et al., 2002] found that E_{act} decreased with increasing moisture content in pork loins. Since this parameter is supposed to represent the energy to desorb and evaporate water, it should change with the composition of the ham. Water is bound more tightly to the structure if more salt ions are present and when little water is left, so that all the loosely bound water is gone.

Due to research on genetics and molecules, [Cassens, 2000] stated that the problems with PSE hams can be overcome. Research around 2000 A.D. seems to be mainly on which parameters affect the process and how. In addition, new methods for imaging and studying the actual processes are applied. [Comaposada et al., 2000] found D_{eff} to depend on salt content in a study of raw ham. [Gou et al., 2002] looked at how pH and fibre direction affects D_{eff} and the year after they considered temperature, salt content and muscle type [Gou et al., 2003]. The conclusions were that pH and muscle type are unimportant, but diffusion parallel to muscle fibres is 31 % higher than when it is perpendicular. Diffusion in these (and other) studies decreased with salt content and increased with temperature. The Arrhenius equation described its temperature dependence, but this equation alone did not describe D_{eff} well enough, since for example salt affects D_{eff} and salt content is not a part of this equation. In addition, it might be that proteolysis affects the drying process[Gou et al., 2004].

The temperature influence on D_{eff} appeared to be well described by the Arrhenius equation along with a moisture dependent expression [Ruiz-Cabrera et al., 2004, Gou et al., 2004]. The effect of fat content on diffusion was found to be unimportant by [Gou et al., 2002] and [Gou et al., 2003], whereas it is highly important for ripening and flavour development [Toldrà, 2002, p. 11-12 and 196]. Others have found that fibre direction has negligible effect, whereas increased lipid content decreased diffusion dramatically [Ruiz-Cabrera et al., 2004]. Neither did they find any effect of temperature, but attributed this to different compositions of the samples, so this result was not regarded as reliable. [Ruiz-Cabrera et al., 2004, Gou et al., 2004] also found that the moisture profiles in ham are Fickean. All these references used the Fickean diffusion model with good results.

[Toldrà, 2002, p. 58-59] stated that shortening production time requires that conditions for ripening are optimized, so that ripening becomes faster, or extra enzymes could be rubbed onto the surface to enhance ripening. These could then penetrate the meat along with the curing agents. However, the method is not fully developed as it gave a poorer taste.[Schilling et al., 2004] presented a study in which PSE meat was treated with soy protein, sodium casienate and food starch and quality improved. [Álvarez et al., 2009] looked at how the animals are treated directly before slaughter affects the meat quality, and found that quality was reduced when the animals were stressed.

In their work, [Okos et al., 2006] wrote that the capillary forces in pork has an effect for

water activities between zero and 0.85, which can be found from the sorption isotherm for pork: Capillary forces dominate where the curve is flatter and the hysteresis present.

[Clemente et al., 2011] looked at external resistance of ham, and shrinkage, they found shrinkage unimportant in hams, as it was 25 % instead of 70.3 % as for beef where shrinkage was found to be significant [Trujillo et al., 2007]. External resistance was important at velocity of $v = 0.6$ m/s unlike at $v = 2.0$ m/s, and muscle type was always unimportant [Clemente et al., 2011].

4.11 MOST RECENT STUDIES

Many studies on the chemical components are still performed, in order to find out which components affect flavour, speed of ripening and quality in which way, utilizing techniques like chromatography [Mora et al., 2014, Herrmann et al., 2014] and infrared spectroscopy [Prevolnik et al., 2011] to determine composition. Improving energy efficiency has been tested by ultrasound [McDonnell et al., 2014], which gave faster curing. [Bekhit et al., 2014] investigated applying an electric field to beef loin, and concluded tenderness was improved. [Jaeger et al., 2008] stated that pulsing electric fields creates pores and availability for mass flow within food, and that the technique improved tenderness of hams.

The model developed by [Strømmen, 1980] for clip fish was applied to drying of ham by [Raiser, 2014, Bantle et al., 2014], but performed worse than the Fickean model to which it was compared. This is somewhat surprising as it fitted the clip fish results very well, but fish and hams are quite different products, for example regarding drying time and pore structure. The main problem with Strømmen's model was that the predicted drying rate was very high in the beginning, as it then assumes no internal resistance to mass transfer. In the model, the internal resistance develops as a dry layer grows from the surface of the ham during drying.

However, the measured water profiles of hams show an inital dry layer [Gou et al., 2004], which could be due to osmotic dehydration or drying during resting. This would cause an initial internal resistance. If this was not included in the mathematics, the predicted drying rate certainly would be too high in the beginning, and hence, this model could need further investigation. [Bantle et al., 2014] also reported that no first drying phase was discovered for ham, temperature had no effect in the range 10-16 ^{o}C, and that relative humidity of the drying air had a major influence.

[Okos et al., 2006] presented several studies on chemical development in food products. These are never coupled with the mass transfer, but studied separately from the drying studies, even though their interaction might be important. Investigation of dry-cured meat has traditionally been divided into two parts, one studying the chemistry and development of taste and structure, and another studying drying of ham alone. The coupling has, as far as the author knows, never been done, but is planned in a study of [Petrova, 2015].

4.12 SUMMING UP

To achieve a safe, high quality product, a low pH creating a sour environment, a relatively low humidity, low temperature that slows down chemical reactions and thereby bacterial growth and/or a high salt content could be utilized. The raw material is also important. DFD meat should not be used, but PSE can be treated.

Dry-curing of ham is not simply a drying process, but mainly a ripening process, and ripening takes much longer time than drying. Shortening the drying time would therefore not significantly reduce energy consumption. The use of long time is simply necessary to obtain high quality, and a faster drying alone could rather be detrimental than beneficial. Hence, to reduce production time one must speed up lipolysis, proteolysis and salt penetration. Freezing and tumbling seems to be the most promising techniques so far.

An alternative is to set the focus on increasing the energy efficiency of the plant, so that heating and cooling of air requires less energy, rather than applying faster drying methods. Another idea could be to based on that about half of the hams are sold as sliced ham [Toldrà, 2002, p. 43]. Drying thin slices requires much shorter drying times than drying whole hams, and this could be utilized for saving time and energy without big process changes. However, ripening still requires longer time, and sufficient water content [Petrova, 2015], so this cannot be applied without loss of quality.

Different materials are dominated by different mechanisms of mass transfer during drying, and this might vary with time. The pressure gradient driven bulk flow is not relevant for hams as they cannot handle high temperatures [Bantle et al., 2014, Gou et al., 2004]. The capillary flow has been suggested as a mechanism, but the findings indicate that they are of low importance in ham drying, but might be important when the surface is wet or at activities below 0.85, which is drier than in any process reported.

The diffusion mechanism seems to be the widely accepted one for hams, but external resistance, time dependence of parameters and realistic initial moisture profiles are often neglected in this model. Chemical composition, water content and hence how dry the product should be influence the drying. Chemical reactions are probably influencing the process, but little is known of how. Shrinkage is negligible for hams. The main parameters controlling mass transport in ham seems to be humidity of the air, moisture and salt content, and perhaps temperature, although this is not clear in the range of interest. pH matters, but probably not in the practically applied range. To reduce time, optimum pH for ripening, about 5.7 [Ruiz-Cabrera et al., 2004], should be chosen and hence, it is not of interest to adjust it for better drying. This might also be true for temperature.

Chapter 5

EXPERIMENTALS

The evaluation of the models was performed by comparing them to experimental data found by Michael Bantle and Inna Petrova. All data were supplied by Inna Petrova. Cubic samples of ham form the muscle semimembranosus, with lengths of 4 to 6 cm were dried in a laboratory drying chamber. The samples were carefully cut parallell and perpendicular to the muscle fibers, and packed in lard on five of the six sides. Lard is fat with salt and pepper, and creates a barriere for water and vapour transport, allowing drying only from one side. This forced mass transfer to be one-dimensional and parallel to the myofibrils. Salting was conducted for one day and all samples were rested in two days before drying.

The initial water content was 301 % on dry basis. Salt content, temperature and relative humiity were varied and are shown in Table 5.1. The two first, Unsalted and Salted, were arranged by Michael Bantle and each of the two experiments involved drying of ten cubic samples. These were used to evaluate the three models, whereas the other experiments were modelled only by the most promising of the models, based on how well it modelled the to first. This was done in order to limit the scope of this work and effectively screen all the models without exhausting amounts of labour. Another reason was that the results for the samples called Salt and Unsalt in Table 5.1 were supplied early in the work, whereas the last samples were supplied less than a month before the end of the project, thus it ws impractical to model all experiments by all methods. Heat calculations were also only performed for these two first samples. Since they showed highly different drying curves, only a model which can model two such different curves could be chosen.

Name of sample	T $[^oC]$	ϕ [%]	**Length** [cm]	**Salt content** [%]
`Unsalted`	13	68	5	0.2
`Salted`	13	68	5	8.1
`NotSalt68`	13	68	6	0.2
`LowSalt68`	13	68	6	3.2
`MedSalt68`	13	68	6	5.0
`NotSalt80`	4	80	4	0.2
`LowSalt80`	4	80	4	3.2
`MedSalt80`	4	80	4	5.0

Table 5.1: Samples used in experiments, the names of each experiment and conditions for drying are given. ϕ is the applied relative humidity and T the temperature. All experiments had air velocity of 0.4 $\frac{m}{s}$. Salt content is given on wet basis.

The samples of 4 and 6 cm were all dried by Inna Petrova. They were prepared like in the two first experiments, but were measured at different time intervals and without the weight of a metal track to be subtracted. Fat content has been excluded in all modelling. Three different salt concentrations were used, and the samples will be referred to as not salted or unsalted, low salted and medium salted samples. They were named after salt content and relative humidity, as shown in Table 5.1. Different drying conditions were applied. Temperature and relative humidity are shown in the same table. Each of the six last experiments (rows three to eight) involved three samples at each salt concentration.

Chapter 6

Theory

Three different models for drying were chosen for investigation and will be presented in this chapter. They are:

- the phenomenological Fickean model
- the empirical Weibull model
- the physiological Strømmen model

These were chosen for the following reasons: The Fickean model is the most often applied model. It usually gives good results and is based on diffusion which is stated to be the dominant drying mechanism in hams by several studies [Ruiz-Cabrera et al., 2004, Gou et al., 2004] as reported moisture distributions have Fickean shapes. It is similar to Darcy's law which is derived from physics, and therefore it might be a realistic description of the actual mechanisms taking place. However, it is almost always assumed that the initial water distribution is uniform [Gou et al., 2002, Gou et al., 2003, Clemente et al., 2011] which it clearly is not [Gou et al., 2004]. The effect of this and external resistance, which found to be important at low velocities like the one applied here [Clemente et al., 2011], was investigated in this work. The model assumes other effects are negligible or can be baked into a effective diffusion coefficient, but the obtained values for this differ with an order of magnitude [Bantle et al., 2014, Raiser, 2014, Gou et al., 2002, Gou et al., 2003]. This could indicate that the model does not reflect reality.

The Strømmen model is based on physics as it uses the pressure difference for water vapour inside and outside the hams as the driving force for mass flow. This model performed very well for clip fish drying but has not previously succeeded in modelling ham [Strømmen, 1980, Raiser, 2014, Bantle et al., 2014]. However, in previous studies it was assumed that there is no initial internal resistance. Yet, osmotic drying might have occurred before measurements started, and in any case the surface can have lost some of its moisture before the experiment, as shown by [Gou et al., 2004]. It was therefore investigated whether the model is applicable if an initial dry layer, s_0, was assumed.

Both the above-mentioned models are complicated and involve many parameters that depend on each other in complicated ways. The ease, and therefore short computational time, of the empirical Weibull model has therefore also been investigated. All modelling was performed in MATLAB, version 2012b, both for calculations and to display the results. But since the aim of this work was to find a model suitable for later energy simulations, a model of a drying tunnel was developed in DYMOLA, version 2014, 64-bit. This program is made for simulation

of physical processes like for example drying. The model programmed in DYMOLA was based on the results from the MATLAB files.

To evaluate their performance, the models were applied to two highly different drying curves (that is, the measured weight of hams during drying) from two experiments, referred to as Unsalt and Salt, to see if they could fit both these well. Since the experimental curves were so different, it would be challenging for the models to fit both, and therefore this would hopefully reveal which models that were not suitable. See Table 5.1 for details on these two first experiments.

That a model «fits» and «is suitable» should involve a small deviation between model and measurement, but also that the shapes of the modelled curves are similar to the measured ones, not only close (the red curve in figure Figure 7.1 is an example of a not suitable curve with small error). Based on the results for these first experiments, one model was chosen as the best performing and used in further modelling.

6.1 FACTORS THAT INFLUENCE DRYING

The model selected for further investigation should include or be upgraded to include, drying and product conditions. Relevant parameters for drying are salt content [Raiser, 2014, Gou et al., 2002, Gou et al., 2003], temperature (given that the tested temperature range is wide enough, at small ranges it has negligible effect [Bantle et al., 2014, Ruiz-Cabrera et al., 2004]) and relative humidity [Bantle et al., 2014, Raiser, 2014].

pH has no effect on drying in the normal range in ham production[Gou et al., 2002], and this range is not likely to be changed as the normally applied range is close to optimal and important for ripening [Petrova, 2015]. No reports on other pressures than atmospheric was found for ham drying, but production sites normally prefer small, not expensive investments, and thus, it is not likely that pressure is a relevant parameter. It should not be anything but $\approx$ 101325 Pa. Air velocity also matters in some cases with low air velocity [Clemente et al., 2011], but normally only at the start [Strømmen, 1980]. It will only be included through the heat and mass transport coefficients, h and β, which depend on it. In total then, this study considers three parameters and three models.

6.2 FICKEAN DIFFUSION MODEL

The phenomenon of diffusion is described by Fick's laws [Okos et al., 2006, Bergman et al., 2011]. Analogously to heat, mass tends to flow if the distribution of it is not equal. A concentration gradient creates a driving force for mass transfer, and this mechanism is called diffusion. Fick's first law in a system of several component is [Bergman et al., 2011, p. 941]:

$$\dot{m}''_w = -\rho_{dry} D_{w,mix} \nabla X. \tag{6.1}$$

The subscript w denotes H_2O. In words, this expression is: the local flux of water per unit area equals the density of the dry matter times a constant times the local gradient of water content (mass of water per dry mass), or the concentration gradient. The constant $D_{w,mix}$ is then the diffusion coefficient of water in the mixture. Often, it is assumed that the diffusion in hams is one-dimensional. In one dimension this is:

$$\dot{m}''_w = -\rho_{dry} D_{w,mix} \frac{\delta X}{\delta z}.$$

Here z is the space coordinate of the direction in which the diffusion occurs. The rate of change of water content within a volume $dx\ dy\ dz$ will then be the difference between water diffusion into it on one side ($z = z_0$) and out on the other ($z = z_0 + dz$). If the sides both have area $dx\ dy$, the rate of change of moisture in the volume is:

$$\begin{aligned}\frac{\delta X}{\delta t} dx\ dy\ dz = \quad & dx\ dy \left(-D_{w,mix} \frac{\delta X}{\delta z}\right)_{z=z_0} \\ & - dx\ dy \left(\left(-D_{w,mix} \frac{\delta X}{\delta z}\right)_{z=z_0} + \frac{\delta}{\delta z}\left(-D_{w,mix} \frac{\delta X}{\delta z}\right)_{z=z_0} dz\right).\end{aligned}$$

This gives

$$\frac{\delta X}{\delta t} = D_{w,mix} \frac{\delta^2 X}{\delta z^2}. \tag{6.2}$$

Here the expression has also been divided by the dry matter density, and is called Fick's second law. The ham is assumed to be homogenous and isentropic in this model and properties were assumed to be constant, and hence the diffusion coefficient could be placed outside the differential. This is not really true in hams. Diffusion coefficients can be found for water in air and oxygen in pure water etc., but hams are not isentropic, consists of many different types of components (protein, lipids, salt) and the composition alters as the drying and ripening processes proceed. Hence this is a rough simplification and finding the relationship between $D_{w,mix}$ and temperature, moisture and salt content, pH, etc. is an unsolved challenge, especially since the composition of the ham, and therefore the coefficient, changes with both time and position. Nevertheless, this equation is widely used in modelling the diffusion of water in hams. An effective diffusion coefficient D_{eff} is used to account for all the mentioned uncertainties, and found in each study by curve fitting. This is done by varying the parameter until a value is found that minimizes the difference between model and measurement.

The solution to (6.2) is often found in [Crank, 1975]. This solution assumes, in addition to a isentropic, homogenous ham, that the initial moisture distribution is uniform. This is not so far away from the truth, which can be seen in [Gou et al., 2004], but it is not correct. One could avoid this assumption by applying an initial condition to the solution that approximates the initial water profile. In this work, a flat and a sine-shaped initial profile were compared.

Since relative humidity of the drying air is of high importance for drying, it was also desirable to try to apply a boundary condition on the surface of the ham that includes this parameter. The boundary condition on the surface can be modelled as either a known water content on the surface in equilibrium with the humidity of the applied air, or by a convection

condition[Clemente et al., 2011]. The first requires known sorption isotherms, often modelled by an empirical equation like the GAB, Peleg or Lipwick relations [Costa-Corredor et al., 2010], the second condition assumes that [Clemente et al., 2011, Bergman et al., 2011, p. 955-960]:

$$\dot{m}_{surface\,to\,air} = \frac{\beta A}{R_w T}(p_{w,s} - p_{w,a}). \tag{6.3}$$

Here A is the lean surface area of the ham; R_w is the gas constant; T the temperature in Kelvin and p the pressure. The subscripts refer to the water (w) at the surface (s) and in the air (a). β is the mass transfer coefficient. Defining

$$\Psi(z,t) = \frac{X(z,t) - X_e}{X_0 - X_e}$$

where t is time, X is water content (dry or wet basis would be the same in this case), X_e and X_0 constants, e stands for «equilibrium» and 0 for start time $t = 0$ and z the distance from the surface inside the ham, the solution to the one-dimensional solution to Fick's second law must be on the form:

$$\Psi = \sum_{j=0}^{\infty} \left[C_j e^{\sqrt{B_j} z} + D_j e^{-\sqrt{B_j} z} \right] e^{D_{eff} B_j t} + \text{constant}.$$

where B_j, C_j and D_j are unknown constants, and the boundary conditions for a flat profile in equilibrium with the drying air should be:

$$a) \lim_{t\to\infty} \Psi(z,t) = 0,\ b)\ \Psi(z,0) = 1,\ c)\ \Psi(0,0) = 0. \tag{6.4}$$

The first requirement ensures that the water content becomes the one at equilibrium after sufficiently long time. This means that the constant must be zero and B_j must be negative, and then e is raised to the power of a complex number. Using the Euler's formula:

$$e^{iz} = \cos z + i \sin z, e^{-iz} = \cos(z) - i \sin(z)$$

$$\Psi(z,t) = \sum_{j=0}^{\infty} \left[(C_j + D_j) \cos\left(\sqrt{-B_j} z\right) + i(C_j - D_j) \sin\left(\sqrt{-B_j} z\right) \right] e^{B_j D_{eff} t} \tag{6.5}$$

From (6.4) c) the terms in front of the cosine must be zero, and from b) the solution at t=0 should then make use of Fourier series to make a sum of sines equal to a constant. The solution normally applied from [Crank, 1975] is then [Gou et al., 2003, Gou et al., 2002, Gou et al., 2004]:

$$\Psi = \sum_{j=0}^{\infty} \frac{8(-1)^j}{\pi^2(2j+1)^2} \sin\left(\frac{(2j+1)\pi z}{2L}\right) e^{-D_{eff} \frac{(2j+1)\pi}{2L}^2 t} \tag{6.6}$$

In this work, (6.6) was applied with the first 50 terms ($j \in [0, 49]$) because this was done by the given references who applied it. A modified version applying a non-uniform initial moisture content was also used and these two were compared. Considering the results from [Gou et al., 2004], the initial moisture profile might be relatively well approximated by a single

sine as:

$$\Psi(z,0) = \frac{1}{\int_0^L \sin\left(\frac{\pi z}{2L}\right) e^{-(\frac{\pi}{2L})^2 D_{eff} t} dz} \sin\left(\frac{\pi z}{2L}\right) e^{-(\frac{\pi}{2L})^2 D_{eff} t}.$$

Hence

$$\Psi = \frac{\pi}{2} \sin\left(\frac{\pi z}{2L}\right) e^{-D_{eff}(\frac{\pi}{2L})^2 t}, \tag{6.7}$$

where the factor $\frac{\pi}{2}$ is necessary to make the average moisture content equal to X_0, which must here be the average initial water content (a constant, for convenience). The average value of Ψ at $t = 0$ is then 1, as it should be.

Both these two expressions assume that the surface moisture content always will be the equilibrium moisture content. This appears to be unrealistic from studies that have taken pictures or measured the moisture distribution in hams during drying [Ruiz-Cabrera et al., 2004, Gou et al., 2004]. In addition, the relative humidity of the air affects drying to a high extent [Raiser, 2014, Bantle et al., 2014]. Except for that equilibrium moisture content depends on it, the relative humidity has no other influence on the drying, and in particular, no influence on the drying rate, with these initial conditions. This might be a limitation, as [Bantle et al., 2014] found different values of the diffusion coefficient at different humidities, even though D_eff is not a property of the air.

To include the vapour concentration in the drying air as a factor, and also account for external resistance to mass transfer, one should apply the boundary condition from (6.3):

$$m_{dry}\left(X_e + (X_i - X_e)\frac{\delta\Psi}{\delta t}_{z=0}\right) = \beta A(C_{w,a} - C_{w,surf}), \tag{6.8}$$

where $C_{w,a}$ is the concentration of water vapour in the drying air, depending directly on the relative humidity. Air velocity influences through β, and matters when it is low, as it was in this work, creating an external resistance to mass transfer[Clemente et al., 2011].

From (6.8), it is clear that a relation between the moisture content and vapour concentration in the air is needed. Assuming that $C_{w,surf} = b(X_e+(X_i-X_e)\Psi(t,0))$ is reasonable in the applied drying range (this is seen from sorption isotherms in [Okos et al., 2006, Comaposada et al., 2000] and Figure 6.1).

From equilibrium conditions one must then demand $C_{w,a} = bX_e$. However, with the model equations above, the water content at $z = 0$ is always the equilibrium water content, hence, there is always equilibrium at the surface. This makes the driving force constant and equal to zero. Thus, the boundary condition is not valid together with the two assumed initial moisture distributions. Then one should use the boundary condition (6.8) along with the general

expression for Ψ on the surface ($z = 0$) to get

$$\begin{aligned}
&\rho_{dry} D_{eff} \Big((X_i - X_e) \sum_{j=0}^{\infty} \sqrt{-B_j} \left[-(C_j + D_j) \sin(0) + i(C_j - D_j) \cos(0) \right] e^{B_j D_{eff} t} \Big) \\
&= \rho_{dry} D_{eff} \Big((X_i - X_e) \sum_{j=0}^{\infty} \sqrt{-B_j} i (C_j - D_j) e^{B_j D_{eff} t} \Big) \\
&= \beta \Big(C_{w,a} - b(X_e + (X_i - X_e)\Psi(t, 0)) \Big) \\
&= \beta \Big(C_{w,a} - b \Big(X_e + (X_i - X_e) \sum_{j=0}^{\infty} [(C_j + D_j) \cos(0) + i(C_j - D_j) \sin(0)] e^{B_j D_{eff} t} \Big) \Big) \\
&= \beta \Big(C_{w,a} - b \Big(X_e + (X_i - X_e) \sum_{j=0}^{\infty} (C_j + D_j) e^{B_j D_{eff} t} \Big) \Big).
\end{aligned} \tag{6.9}$$

Gathering the constants at one side gives

$$\beta(C_{w,a} - bX_e) = (X_i - Xe) \sum_{j=0}^{\infty} \left(\rho_{dry} D_{eff} \sqrt{-B_j} i (C_j - D_j) + \beta b (C_j + D_j) \right) e^{B_j D_{eff} t}.$$

As noted earlier, $C_{w,a} = bX_e$, and thus:

$$0 = \sum_{j=0}^{\infty} \left(\rho_{dry} D_{eff} \sqrt{-B_j} i (C_j - D_j) + \beta b (C_j + D_j) \right) e^{B_j D_{eff} t}.$$

But now all dependence on vapour concentration in the air is lost, and the inclusion of this was the main motivation for using this approach. It is of course possible that $C_{w,s}$ should be a more complicated function of the surface water content, but a boundary condition should not pose a limit to a physical relationship, and this relation is very close to the truth in the relevant range of water activities.

All attempts to follow this further concluded that the solution is too complex to be found, and this is given in Section A.3.

Models using Fickean diffusion achieve good fits. The main problem is that D_{eff} differs from the diffusion coefficients for water in air or other homogenous, «pure» isotropic mediums, is unknown and changing. The reported values differ, although they are mostly in the same range. D_{eff} must be found experimentally for each production process and it is difficult to optimize a process as long as its dependence on process conditions remains unsolved.

As the process is very slow, it is in semi-equilibrium, and one can assume D_{eff} to be constant, and then obtain different coefficients for different conditions. From this, one can incorporate the effect of process conditions empirically. The effect of temperature for example, is often modelled by an Arrhenius expression, (6.10) b), where it is assumed that the water requires the activation energy E_{act} for vaporization and for desorption [Okos et al., 2006, Pakowski and Adamski, 2007]. Sometimes this is combined with a model related to moisture content [Okos et al., 2006, Costa-Corredor et al., 2010]. [Pakowski and Adamski, 2007] applied

four different models for D_{eff}:

$$\begin{aligned} &a)\ D_{eff} = D_0,\ b)\ D_{eff} = D_0 e^{-\frac{E_{act}}{RT}}, \\ &c)\ D_{eff} = D_0 X^{d_1} e^{-\frac{E_{act}}{RT}},\ d)\ D_{eff} = D_0(1 + d_2 X^{d_1}) e^{-\frac{E_{act}}{RT}}, \end{aligned} \tag{6.10}$$

where X is the moisture content. In their study of apples, the model accuracy improved significantly by using c) and d) compared to a) and b). The best fit was obtained by d), but the improvement was small compared to c). Similarly to studies of ham [Ruiz-Cabrera et al., 2004], this shows that temperature alone is not sufficient to model the change in D_{eff}, they mentioned that salt content should be included.

In this work, the temperature did not change within each experiment, so no dependence temperature was necessary in the equations, but D_{eff} was allowed to vary between experiments, and this allowed for temperature dependence.

The dependence on water content for apples was weak, but the results became significantly better by including this weak dependence [Pakowski and Adamski, 2007]. Most studies on food drying have found that water content seems to be important [Okos et al., 2006]. Studies on ham on the contrary, have performed very well without dependency on X [Gou et al., 2003, Raiser, 2014, Bantle et al., 2014, Gou et al., 2004]. Therefore, no influence of moisture content on the diffusion coefficient was included in this work.

[Costa-Corredor et al., 2010] modelled salt and water diffusion simultaneously by the GSM model. This really is a matrix form using Fickean expressions for both species, but also allowing interaction between them, arguing that the species affect each other, which, in theory, they do [Bergman et al., 2011]. Therefore modelling both salt and water diffusion and their interference, should be more physically realistic than modelling water diffusion alone.

Other authors [Clemente et al., 2011] point out that although a model can be more realistic, the added complexity should yield added accuracy in the predictions, if not, a simplification of reality is better, even if it is less realistic. This is after all the point with models, and necessary due to for example computation time for computers. The results obtained by [Costa-Corredor et al., 2010] where not more accurate than those not using this effect, and hence it is usually not applied. Therefore, interaction between salt and water diffusion was not included in this work, but D_{eff} was allowed to vary with salt content, as this has been important [Ruiz-Cabrera et al., 2004, Bantle et al., 2014, Raiser, 2014]. Both humidity and salt effects are accounted for through the equilibrium moisture content.

6.3 THE WEIBULL MODEL

[Corzo et al., 2010] investigated the Weibull model to predict drying of mango. The model is based on the Weibull distribution from statistics, and the moisture content X is expressed as a moisture ratio (MR):

$$\mathrm{MR} = \frac{X - X_e}{X_0 - X_e} = e^{-(\frac{t}{\alpha})^{\beta}}. \tag{6.11}$$

This is actually the same as Ψ in the Fickean model, but it will be denoted MR to follow [Corzo et al., 2010] and keep the models apart. The parameters to be determined are α and β. The initial and equilibrium moisture contents, X_0 and X_e must be known.

The parameter β (not to be confused with the mass transfer coefficient β in the Fickean and the Strømmen model) is related to the drying rate, especially in the start phase, and mainly determines the shape of the curve; high values make mass increase, low values makes the mass loss quick. Furhtermore, the parameter α must have units time and is considered as the time to reach a certain percentage of the mass loss. In [Corzo et al., 2010] this was 63 % for mango. They applied a normalized version of the model, developed by [Marabi et al., 2003] in addition to the not normalized version, and this was also done in this project.

Following [Corzo et al., 2010] the equilibrium water content was first set equal to the one corresponding to the last measured weight, but this was later adjusted as the salted sample for model comparison (named Salt in Chapter 5) was not dried to equilibrium. The final research was conducted with an assumed equilibrium moisture content for a salted sample of 0.55 (wet basis). This value was taken from [Comaposada et al., 2000, figure 2], assuming 8 % salt. One result using the final weight as equilibrium weight was also be reported for comparison.

Since the unsalted sample (Unsalt) was dried to equilibrium, and the parameter α should be a part of the time to reach equilibrium, denoted by t_{tot}, the lower and upper limits for this parameter should not exceed 0 and 1 times t_{tot}. For the salted sample, t_{tot} was unknown and no upper limit was set on α. Several methods were used to find the parameters:

6.3.1 GRID METHOD

This method involved an interactive grid search, where a range of values were tried for α and for each of these a range of values were tried for β. The ranges were adjusted until a minimum within both ranges was found. Initial limits for β was between 0.5 and 1.5. If no minimum was found in the range (that is, the β that yielded the smallest error at 0.5 or 1.5) the limits were changed. It is expected that $\beta \in (0, 1]$ in drying experiments, since the initial slope curves the wrong way for higher values (the curve becomes concave at the start, whereas it is convex in all plots that have been found).

A grid with 24 values of each parameters that tried totally $24^2 = 576$ combinations was applied. The step size for β was 0.033, for α it was $0.033 \cdot t_{tot}$. This can be seen as the measure of highest possible error or uncertainty in the parameters. For each pair of parameters, the deviation from the experimental results was found and the best parameters, if they were within their ranges, were chosen. If not the grid ranges were adjusted.

6.3.2 LINEAR REGRESSION METHOD

The other method applied was a more analytical one. It consists in manipulating the equation by taking the natural logarithm of it twice and obtain an equation for a linear Weibull plot:

$$\ln(\mathrm{MR}) = \ln\left(e^{-\left(\frac{t}{\alpha}\right)^{\beta}}\right) = -\left(\frac{t}{\alpha}\right)^{\beta},$$

$$\ln(-\ln(\mathrm{MR})) = \beta \ln(t) - \beta \ln(\alpha).$$

Hence a plot of the logarithm of the negative logarithm of experimental values for MR versus ln(t), should yield a straight line from which the slope, β could be read. This line would intersect the ordinate axis at -$\beta \ln(\alpha)$, and thus both parameters could be read from the plot.

6.3.3 NORMALIZED WEIBULL MODEL

In the normalized Weibull model, the parameters were found as described by [Corzo et al., 2010]: Three simulations of drying curves using the four first terms of the normally applied solution to Fick's second law from [Crank, 1975]:

$$\mathrm{MR} = \frac{8}{\pi^2} \sum_{n=0}^{\infty} \frac{1}{(2n+1)^2} \exp\left(-\frac{(2n+1)^2 \pi^2 D_{eff} t}{L^2}\right)$$

with values of 10^{-10}, 10^{-11} and $10^{-12} \frac{m^2}{s}$ for D_{eff} were made. The moisture ratios were calculated from these and an artificial disturbance was introduced by changing each point of the modelled ratios with a percentage determined by a random number generated in MATLAB, with maximum value of 3.33 %. From this, the grid method described previously was used to find suitable values for α and β for the simulated curves. In the normalized version of this model, α was modelled as:

$$\alpha = \frac{L^2}{D} = \frac{L^2 R_g}{D_{eff}}.$$

In this way, it is related to the effective diffusion coefficient D_{eff}. The symbol R_g is a geometric factor that describes the change of diffusion due to the geometry of the product, not so different from the models used by [Bantle et al., 2014, Raiser, 2014, Strømmen, 1980, Song, 1990] where a factor describes the change in diffusion due to the presence of the meat. The coefficient D should then be the effective diffusion coefficient of water in ham regardless of geometry. The inverse of α is also sometimes reported to be related to temperature by an Arrhenius expression[Corzo et al., 2010], just as D_{eff}, the inverse of α is.

With $L = 0.025$ m for the two first experiments and D_{eff} known in each case, R_g could be found. An average of the three obtained values was then used. In [Corzo et al., 2010] the values of R_g were similar for all curves, a value representative for all cases was used when the model was applied to experimental data. In this case, both R_g and L were known, and D_{eff} could be determined.

6.4 THE STRØMMEN MODEL

A major question in modelling is how and in which phase H_2O is transported in the hams. In sausages it is transported as vapour only[Costa-Corredor et al., 2010]. In fish, at least 75 % is vapour [Strømmen, 1980], but both vapour and liquid has pressure as their driving force, so a

physical model could account for both by applying pressure rather than concentration. This model is based on the analogy between heat and mass transfer. The heat conduction in a material subject to convective conditions can be described by [Strømmen, 1980, Bergman et al., 2011]:

$$\dot{Q}_{air\ to\ surface} = \alpha A(T_a - T_s),$$

$$\dot{Q}_{surface\ to\ core} = \frac{kA}{s}(T_s - T_{core}),$$

where the subscripts s denotes the surface, core the undried product core and a denotes the air. The parameter s is the thickness of the dry layer [Bantle et al., 2014, Strømmen, 1980, Raiser, 2014] which varies with time, k is the thermal conductivity (often denoted λ in other texts) and A the surface area of the material. In the drying process this heat flow is normally stabilized early so that the two expressions are equal which leads to:

$$\dot{Q} = \frac{A(T_a - T_{core})}{\frac{1}{\alpha} + \frac{k}{s}}. \tag{6.12}$$

The heat flow in must equal the heat needed to evaporate and desorb water on the surface of the core, which [Strømmen, 1980] calls the humidity front. When this is true, one can apply the Lewis relation:

$$\dot{Q} = \dot{m}\mathrm{Le},$$

where Le is the Lewis number, equal to the ratio between the thermal diffusivity and the mass diffusivity [Bergman et al., 2011, p. 409]. This analogy made it possible for [Strømmen, 1980] to apply a similar model for mass transfer as for heat transfer. The driving potential for mass is always the difference in local vapour pressure. In the core, this was assumed to be equal to 99 % of the saturated water vapour pressure, an approximation first used by Michael Bantle. This was used as the partial pressure of the water vapour in the ham will be somewhat lower due to the sorption effects [Luikov, 1966, p. 192], [Strømmen, 1980, p. 15]. The analogy then gives:

$$\dot{m}_{surface\ to\ air} = \frac{\beta A}{R_w T_a}(p_{w,s} - p_{w,a})$$

$$\dot{m}_{core\ to\ surface} = \frac{D_{w,a}A}{s\mu R_w T_h am}(p_{w,core} - p_{w,s})$$

where w denotes H_2O, $D_{w,a}$ the diffusion coefficient of water in air and R is the gas constant. μ is a resistance, representing the decrease in water vapour transport compared to that in air due to the presence of the product structure, impurity of the water and diffusion of salt in the opposite direction. This must be found experimentally [Raiser, 2014]. β is the mass transfer coefficient from the surface to the air.

It is important to note that water only is removed through the lean side of the ham [Toldrà, 2002, p. 42], and hence the area in this equation must be the area of the lean side of the ham and smaller than the total surface area of the ham. Heat can in theory be conducted from all sides of the ham, but since all vaporization takes place on or close to the lean side, and this side is closer to the convective air than the backside of the ham/the samples, it was assumed

that all heat transfer also occurred only on this surface, thus the same area was used in both the heat and the mass transfer equations.

If the water transport to the surface equals that from the surface to the air, then just as for heat:

$$\dot{m} = \frac{A(p_{w,s} - p_{w,a})}{R_w T_a(\frac{1}{\beta} + \frac{s\mu}{D_{w,a}})}. \tag{6.13}$$

The temperature was taken as that of the air, partly for simplicity, partly because the difference between this and the temperature in the ham will be very small, and partly because heat supply was assumed to be sufficient. This is normally a reasonable assumption [Okos et al., 2006], and heat calculations revealed that this was likely to be true during most of the process.

6.4.1 CONVECTIVE VAPOUR FLOW

If one also considers that the mass flow due to diffusion is a mass flow that could cause convection of vapour inside the ham, this must be accounted for by a slight increase in mass flow. Inclusion of convection is modelled as follows [Bergman et al., 2011, Raiser, 2014, Bantle et al., 2014, p. 943]:

$$\dot{m}_{core\,to\,surface} = \frac{D_{w,a}A}{s\mu\left(1 - \frac{p_{w,lm}}{p}\right)}(p_{w,core} - p_{w,s})$$

where $p_{w,lm}$ is the logarithmic mean of vapour pressure in the dry layer, and p the total pressure, making this a logarithmic mean of the mass fraction of water vapour. This was included in the modelling, simplified to:

$$\frac{p_{w,lm}}{p_w^o} = \frac{\phi - 0.99}{\ln(\phi) - \ln(0.99)}.$$

Here 0.99 is the assumed value of the relative humidity within the ham (not given in percent as this was more convenient).

It must be noted that heat and mass transfer, although having many similarities and that they are often used in analogy with one another, differ in several important manners. For example, temperature is a continuous function, mass distribution need not be. This means that the assumption that mass flow to and from the surface need not be in balance: mass can accumulate. The mass flow of water cannot travel through the fat layer [Gou et al., 2004, Toldrà, 2002, p. 42], whereas temperature can.

This could make this model invalid, since mass can accumulate. However, the diffusion resistance is normally the largest one, except from at the very start the process when the surface is wet [Strømmen, 1980, Clemente et al., 2011], hence, water is not likely to accumulate on the surface and this is in accordance with observations. Rather, the surface is dried out and external resistance can sometimes be neglected. One could then argue for a model of the form:

$$\dot{m} = \max(\dot{m}_{surface\,to\,air}, \dot{m}_{core\,to\,surface}).$$

However, when the resistances are comparable, (6.13) should be more appropriate, and when one resistance dominates over the other, it will be so in the equation too. Calculations were

therefore simplified by including both resistances in this case.

6.4.2 Decreasing drying rate

The Strømmen model is based on physical processes, but lacks one very important feature: the drying rate does not diminish with time. It seems reasonable that after some time, the driving forces should decrease to zero, because the ham reaches its equilibrium state, and one can measure that the vapour pressure of the ham is equal to that of the surrounding air [Comaposada et al., 2000]. Eventually the resistance should become infinitely large, but then the dry layer must become infinitely large as well, and this cannot be the case.

To describe the physical processes taking place, one must ask what happens when the dry layer is fully developed. If the dry layer for example spans the whole sample or a fat tissue is reached, a new barrier for mass transfer must occur, a new mechanism should be limiting. Either, all free water is removed, and the water is bound more tightly to the structure, thus the vapour pressure in the ham would decrease until it equals that of the surrounding air, creating the equilibrium condition; or the internal resistance should depend more strongly on the dry layer thickness, and thus become very large when the dry layer s reaches its final value. Both these alternatives were investigated. A third option is that another new mechanism becomes dominating in mass transfer, but this will not be considered in this work, to limit its scope.

Decreasing the pressure was done by assuming that the vapour pressure in the ham was the product of the saturated vapour pressure at the wet bulb temperature and the water activity in equilibrium with the moisture content. This was found from the sorption isotherm in Section 6.5.2. This also required knowledge of the final equilibrium moisture content at 68 % humidity and 13 ^oC, which was modelled from the actual measured value of lean meat at the end of the process, corresponding to 24.25 % on dry basis, similar to the value in figure 2 reported by [Comaposada et al., 2000]. Pressure was not increased before a certain amount of water was removed and several attempts with various criteria were conducted.

6.4.3 Dry layer

[Strømmen, 1980] pointed pout that this model is not completely physically correct, since this would require more knowledge than practically obtainable and be far too complex. Despite this, the model yielded very good and accurate results when applied to experiments on clip fish [Strømmen, 1980]. This could mean that the most important mechanisms are accounted for, and thus that this is a simplification, but a good one. On the other side, [Bantle et al., 2014] and [Raiser, 2014] concluded that this model did not fit the experimental data as well as the Fickean diffusion model, even though it should be more physically realistic. The main reason was that it predicted a much higher initial drying rate than the real one. However, it was assumed that the initial thickness of the dry layer was zero, as no water had been removed yet at the start. This means that the only resistance to heat transfer initially is $\frac{1}{\beta}$. But from [Ruiz-Cabrera et al., 2004] it is clear that the initial moisture profile might show a starting dry layer already before the beginning of the drying process. Before entering the drying chamber,

the hams are treated with salt, and thereby lose 3-4 % weight by osmotic dehydration from the surface [Raiser, 2014]. It is also seen in [Bantle et al., 2014, Raiser, 2014] that the initial water contents decreased with increasing salt content, as if water was already removed.

In drying processes there are three phases, in the first one, the free unbound water in the outer layer evaporates without internal resistance, so that the drying rate is constant, and all properties are equal to those of water [Okos et al., 2006]. In hams, this first period was not observed[Raiser, 2014] maybe because it already has occurred during salting and eventually resting, causing the initial dry layer observed by [Ruiz-Cabrera et al., 2004] and the different initial water contents in [Raiser, 2014, Bantle et al., 2014]. Whatever the reason may be, assuming a non-zero initial dry-layer thickness would lower the initial rate. This could cause the entire profile to approach the real one, and was therefore investigated in this project.

The approximate length of the dry layer is necessary to use the model. It should be a function of removed water, and [Bantle et al., 2014] modelled it as

$$s = \frac{m(0) - m(t)}{A\rho_w(1-\epsilon)},$$

where s is dry layer thickness, ϵ the porosity of the ham and ρ_w the density of water. However, the porosity of ham is unknown and might change during drying due to shrinkage and collapse in the structure when water is removed [Marinos-Kouris and Maroulis, 2006, Clemente et al., 2011]. Assuming no shrinkage, an equation for the dry layer can be found from the following [Raiser, 2014]: The dry layer thickness s times the area of the ham through which the drying takes place creates a dry volume, consisting of the meat matrix and the empty pores of the ham. In addition, there is an undried core. Since shrinkage is small and negligible according to [Clemente et al., 2011], the volume of the whole ham is considered constant and equal to:

$$V_{tot} = V_{core} + V_{dry}. \tag{6.14}$$

Denoting the removed amount of water by Δm, the volume of removed water is $\frac{\Delta m}{\rho_w}$. Due to the meat this is only a portion of the total volume that the water is present in. Initially, denoted by 0, the water fills a fraction of

$$\frac{V_{w,0}}{V_{tot,0}} = \frac{\frac{m_{w,0}}{\rho_w}}{\frac{m_{tot,0}}{\rho_{tot,0}}} = \frac{m_{w,0}\rho_{tot,0}}{m_{tot,0}\rho_w} = X_{wb,0}\frac{\rho_{tot,0}}{\rho_{w,0}}$$

of the ham, and this is then related to the void fraction or porosity of the ham. The samples that were dried and used for model evaluation in this work were cubic, and if the length of a side is L and the area A:

$$V_{dry} = \frac{\Delta m}{\rho_w \frac{V_{w,0}}{V_{tot,0}}} = \frac{\Delta m}{\rho_w X_{wb,0}\frac{\rho_{tot,0}}{\rho_{w,0}}} = \frac{\Delta m}{\rho_{tot,0}X_{wb,0}}.$$

Inserting this in (6.14) yields:

$$AL = A(L - s) + \frac{\Delta m}{\rho_{tot,0} X_{wb,0}},$$

and so

$$s = \frac{\Delta m}{\rho_{tot,0} A X_{wb,0}}. \tag{6.15}$$

The advantage with this method is that it does not require knowledge about the porosity of ham. If in addition dry layer existed at the start of drying, this was denoted by s_0. Its value was adjusted to make the modelled curve fit the experimental curve, since it could not be measured in any other way. The dry layer was modelled not to grow any further when pressure started to decrease. At this point, the internal resistance due to the dry layer was regarded as fully developed, because the desoption of more strongly bound water took over, so all free water was removed, and the dry layer should not grow any more.

Some initial investigations (Figure 7.9 to Figure 7.12) indicated that the resistance parameter μ was not constant, but changed with time, linearly with s. This was not regarded as unreasonable, as diffusion depends on water content [Okos et al., 2006], and thus, μ could increase as long as the dry layer develops. Some of the modelling therefore applied (6.13) with s to the second power.

[Strømmen, 1980] reported that the dry layer was 1 mm in clip fish. Similar values are seen in the figures found by [Ruiz-Cabrera et al., 2004]. During this work, it was discovered that the dry layer thickness could become about ten times larger than this. In addition, since the internal resistance dominates during most of the process, the use of (6.15) for s essentially makes the drying rate proportional to the surface area to the second power (this is easily seen in (6.21)), which seemed unrealistic. This called for another method to model the development of inner resistance, which clearly varied during the experiments (as can be seen in Figure 7.9 to Figure 7.12). Following [Strømmen, 1980] and assuming that the dry layer is 1 mm, the resistance μ must vary. Again, it was assumed to be a linear function of removed water with an initial value μ_0:

$$\mu = \mu_0 + d\mu(m(0) - m(t)). \tag{6.16}$$

It was then a question about whether μ_0 could be smaller than one. If it is, then diffusion in the ham is higher than it would have been in air, which clearly should be wrong. However, when the surface is wet, there should not be any internal resistance at all, thus either μ or s should be zero, and then increase as the surface becomes dry. If capillary forces are present, then they might enhance the initial, but only the initial, drying[Song, 1990, p. 19-27]. The same is true for osmotic dehydration (as explained in the paragraph on osmotic dehydration in Chapter 2). This could result in an apparently larger diffusion coefficient than in air. Both allowing $\mu < 1$ and demanding $\mu \geq 1$ was therefore tried.

6.4.4 DIRECT APPROACH FOR FINDING PARAMETERS

In order to find suitable parameters for the model, one can use a direct approach to find these properties from measured data. Several sources give correlations for the parameters, but they differ (see Section 6.5.3). Defining the overall mass transfer coefficient as:

$$\beta_{tot} = \left(\frac{1}{\beta} + \frac{\mu s}{D_a}\right)^{-1} \tag{6.17}$$

it is clear that this parameter is equal to the mass transfer coefficient at the surface when (or if) the dry layer thickness is zero, and smaller than the smallest of β and $\frac{D_a}{\mu s}$ (since its reciprocal must be larger than the largest of the inverse of the two). Assuming that the initial dry layer and the convective effects are small, the overall and perhaps the surface transfer coefficient could be found from rearranging the equation for mass transfer:

$$\beta_{tot} = -\frac{\delta m/\delta t R T_a}{(0.99 p_w^o(T_{ham}) - \phi p_w^o(T_a)) M_w} \tag{6.18}$$

$$\beta = \beta_{tot,t=0}.$$

Then, since s was also known because the mass loss was known (this method was applied to measured data), μ could be found from:

$$\mu = \frac{D_a}{s}\left(\frac{1}{\beta_{tot}} - \frac{1}{\beta_{tot,t=0}}\right).$$

6.4.5 CALCULATIONS

In the Strømmen model, the derivative of the mass is actually a function of the mass. This is because the dry layer thickness or the dry layer is assumed to be a function of the amount of removed water, which is $m(0) - m(t)$. Therefore, it is really a differential equation, and a numerical method has been applied to solve it. Due to the very slow changes and nearly isothermal conditions in the process, a simple, explicit, first order numerical method, the forward Euler method, was used. A time step of 6010 seconds was used for the two first experiments, and a time step of 601 seconds was used in all the remaining ones. As the drying process is very slow, this was assumed to work fine.

For some samples however, the drop in mass turned out to be very high initially, and it was necessary to see if there were numerical errors resulting from this, as the Euler method is only good for slow changes or small time steps relative to the changes. Small time steps would require extremely many time steps and make the numerics more cumbersome and the simulations very slow. An attempt to solve the differential equation was therefore conducted.

Assuming the internal resistance dominates (as several results indicated), $\frac{(p_i)_{lm}}{p} \approx 0$ (which was found to be almost true) and $s = \frac{m(0)-m(t)}{A\rho_{tot,0}X_{wb,0}}$ while the driving force and resistance μ are

both constant, then:

$$\frac{\delta m}{\delta t} = \frac{-M_w(0.99p_w^o(T_{ham}) - \phi p_w^o(T_a))D_a\rho_{tot,0}X_{wb,0}}{RT_a\mu(m(0)-m(t))} = \frac{-C_1}{m(0)-m(t)} \tag{6.19}$$

$$C_1 = \frac{M_w(0.99p_w^o(T_{ham}) - \phi p_w^o(T_a))A^2D_a\rho_{tot,0}X_{wb,0}}{RT_a\mu}$$

$$(m(0)-m(t))dm = -C_1dt$$

$$m(0)m(t) - m(0)^2 - \frac{1}{2}m(t)^2 + \frac{1}{2}m(0)^2 = -C_1(t-0)$$

$$m(t)^2 - 2m(0)m(t) + m(0)^2 - 2C_1t = 0$$

$$m(t) = \frac{-(-2m(0)) \pm \sqrt{(-2m(0))^2 - 4(m(0)^2 - 2C_1t)}}{2}$$

$$m(t) = m(0) \pm \sqrt{2C_1t} \tag{6.20}$$

The sign should be negative, since the mass decreases in drying.

Eventually, including that both the mass transfer coefficient and initial dry layer thickness might have effects, one can find:

$$\frac{\delta m}{\delta t} = \frac{-C_1}{A\rho_{tot,0}X_{wb,0}(\frac{D_a}{\beta\mu} + s_0) + m(0) - m(t)} \tag{6.21}$$

$$\frac{\delta m}{\delta t} = \frac{-C_1}{C_2 + m(0) - m(t)}$$

$$C_2 = A\rho_{tot,0}X_{wb,0}(\frac{D_a}{\beta\mu} + s_0)$$

$$(C_2 + m(0) - m(t))dm = -C_1dt$$

$$(m(0)+C_2)m(t) - m(0)^2 - m(0)C_2 - \frac{1}{2}m(t)^2 + \frac{1}{2}m(0)^2 = -C_1(t-0)$$

$$m(t)^2 - 2(m(0)+C_2)m(t) + m(0)^2 + 2C_2m(0) - 2C_1t = 0$$

$$m(t) = \frac{-(-2(m(0)+C_2)) \pm \sqrt{(-2(m(0)+C_2))^2 - 4(m(0)^2 + 2C_2m(0) - 2C_1t)}}{2}$$

$$m(t) = m(0) + C_2 \pm \sqrt{C_2^2 + 2C_1t} \tag{6.22}$$

Again, the sign should be negative.

If the method with $s = 1$ mm and constant, whereas the internal resistance varies as $\mu = \mu_0 + d\mu(m(0) - m(t))$ is used instead, then

$$\frac{\delta m}{\delta t} = \frac{-M_w}{RT_a}\frac{A(0.99p_w^o(T_{ham}) - \phi p_w^o(T_a))}{\frac{1}{\beta} + \frac{(\mu_0 + d\mu)(m(0)-m(t))s}{D_a}}. \tag{6.23}$$

In this expression, the dependence of the evaporation on the surface area is to the first power. This is really the same equation as (6.21), but with a slightly different constant. It therefore has

the solution

$$m(t) = m(0) + C_4 \pm \sqrt{C_4^2 + 2C_3 t},$$

where

$$C_3 = \frac{M_w A(0.99 p_w^o(T_{ham}) - \phi p_w^o(T_a)) D_a}{R T_a \; s \; d\mu}$$

and

$$C_4 = \frac{1}{d\mu}\left(\frac{D_a}{\beta s} + \mu_0\right).$$

Applying this expression would give practically equal results as the numerical method if the numerics are not unstable. But with one exception: The decrease in internal vapour pressure is not included in this model, thus it is only valid above the moisture content at which this pressure decreases ($X = 1.33$ for unsalted samples at 13 ^{o}C and relative humidity of 68 %). Therefore, some modelling involved a combination of this explicit method, until a certain moisture content was reached, and then the numerical method was used for the rest of the simulation. Since the large changes that could cause numerical instability are only present at the start, this should work well.

6.5 General

The Fickean and Weibull model utilize the same moisture ratio MR or Ψ. These are equal, but belong to two different models to not confuse them with one another. β is a parameter in the Weibull model, but has nothing to do with β in the other models, where it represents the mass transfer coefficient on the surface.

6.5.1 Error measure

The error was calculated by:

$$\sigma^2 = \sum_{j=1}^{n} \frac{(W_{modelled,j} - W_{measured,j})^2}{n - \text{DOF}}, \tag{6.24}$$

where n is the total number of measurements. The sum is divided by $n - \text{DOF}$ instead of n since the choice of parameters offers degrees of freedom, DOF. The Fickean model has one (D_{eff}); the Strømmen model two (s_0 and μ) and the Weibull model two (α and β).

6.5.2 Heat transfer

Heat calculations were only performed for the two first samples supplied, Salt and Unsalt, because heat calculations were not the main focus and it seemed sensible to choose some samples, not all for this research. A third reason was that experimental results for these two samples were supplied much earlier than for the other samples, and the final data for the last experiments

arrived so late it was impractical to do more than this.

The heat needed for the process can be calculated as the product of the enthalpy of vaporization of water and the actual amount of water evaporated. Salt content might have an effect on the heat needed for evaporation. To see if it matters, a calculation of its maximum possible impact is performed here.

The enthalpy of solution is about 3.9 $\frac{kJ}{mole}$ [Wik, 2014, New, 2012], and the heat of vaporization for water at 13 ^oC is 2470.8 $\frac{kJ}{kg}$. Actually, the value at the wet bulb temperature should be used, but the difference is small. The advantage with the value at the highest applied temperature is that it is also the lowest value for the enthalpy of vaporization, and to investigate maximum possible impact of salt, the lowest possible value for the heat of vaporization should be used. Salt has molar mass 58.44 $\frac{kg}{kmole}$. The enthalpy of solution is then

$$\frac{3900\frac{kJ}{kmole}}{58.44\frac{kg}{kmole}} \approx 66.74\frac{kJ}{kgsalt}$$

Salt content can be up to 9 % on wet basis, and water content as low as 54 % on wet basis [Raiser, 2014, Petrova, 2015]. Thus at the highest applied salt contents, there are $\frac{54}{9} = 6$ kg of water for every kg of salt. Removing 1 kg of water then requires

$$2470.8\,\frac{kJ}{kg} - \frac{66.74\,\frac{kJ}{kg}}{6} \approx 2459.7\,\frac{kJ}{kg}$$

corresponding to a change of 0.45 % compared to the value of pure water, and this was the absolutely highest possible effect it could have if salt content was 9% (the highest applied salt concentration was 5.2 % but this was unknown at the time). Considering the small size and that the number of significant digits in the enthalpy of solution is 2, this difference cannot be said to be important. Hence, the assumption that the latent heat of water can be used was considered as appropriate.

As explained in Section 6.4, heat transport $\dot{Q}$ into the ham is found from:

$$\dot{Q} = \frac{A(T_a - T_{wet})}{\frac{1}{h} + \frac{s_T}{k}} \tag{6.25}$$

where T_a is the air temperature, T_{wet} the wet bulb temperature, s_T the thermal thickness or the distance the heat must be conducted, and should be equal to the dry layer thickness. k is the thermal conductivity of the product and h the heat transfer coefficient on the surface. This means that $\frac{1}{h}$ is an external resistance to heat transfer and $\frac{s_T}{k}$ is an internal resistance. A could be the total surface area of the ham, but in the experiments, evaporation was only allowed from one surface. Therefore it is more likely that heat will mainly flow through this one side of the ham where the heat for evaporation is needed, and the same area was used in heat calculations as in the mass flux calculations.

Because isothermal models have been reasonable many times before [Okos et al., 2006], heat supply was assumed to always be sufficient. The thermal conductivity of ham will probably differ upon evaporation as the water content changes it according to [Marcotte et al., 2008],

Product	T [^{o}C]	p [Pa]	k [$\frac{W}{mK}$]	Medium
Beef	-18 to 65	24	0.032	water vapour
Beef	-18 to 65	7456	0.021	air
Beef	-18 to 65	785	0.036	air and water vapour
Turkey	-18 to 65	7456	0.194	air, water vapour, Freon-12, CO_2, helium
Ham	10	101325	0.310	air
Ham	13	101325	0.319	air
Water	10	101325	0.58	air

Table 6.1: Thermal conductivities k, for various products at temperature T and pressure p in different surrounding media: Data in the first four rows are taken from table 11.3 in [Marinos-Kouris and Maroulis, 2006, p. 276], data in rows five and six from [Marcotte et al., 2008].

from which the used value was found by interpolation according to:

$$k_{ham} = 0.34\frac{W}{mK} + \frac{(T - 293.15)(0.37 - 0.34)}{303.15 - 293.15}\frac{W}{mK}$$

This was measured in hams with 72.7 % water content, and is therefore only valid in the first part of the process. Values at relevant temperatures are shown in rows five and six in Table 6.1. Conductivity decreases as moisture is removed[Marinos-Kouris and Maroulis, 2006]. Various conductivities for other substances are shown in Table 6.1. This gives an indication of which value the conductivity can have in dry ham: the value must be lower than that of water and higher than those of freeze dried products under vacuum[Marinos-Kouris and Maroulis, 2006].

However, the undried hams have higher conductivity than dried hams, as the meat structure has low conductivity and only the water allows it to be this high (see Table 6.1) . No measured conductivity of dried hams was found, but measurements for beef and turkey was given by [Marinos-Kouris and Maroulis, 2006, p. 276] in table 11.3 , the most relevant data in that table for this project are also shown in the first four rows of Table 6.1. These were obtained for freeze dried meat at very low pressures, and would have been significantly higher if the pressure had been atmospheric [Marinos-Kouris and Maroulis, 2006]. Temperatures were reported to be in the range -18 to 65 ^{o}C. The value for water was found by interpolation in[Bergman et al., 2011, p. 1003].

The convective heat transfer coefficient h was found from the formulas and properties in [Bergman et al., 2011, p. 995]. Since heat calculations were only performed for the two first experiments, Unsalt and Salt, only the parameters relevant for those cases are shown here. The Reynolds number Re and critical length for onset of turbulence z_{cr} for these first samples were:

$$Re = \frac{vL}{\nu_a} = \frac{0.4 \cdot 0.05}{1.4459 \cdot 10^{-5}} = 1,383$$

$$z_{cr} = 5 \cdot 10^5 \nu / v = 5 \cdot 10^5 \dot{1}.4459 \cdot 10^{-5} \frac{m^2}{s} / 0.4 \frac{m}{s} = 18.07\, m$$

The Prandtl number was:

$$Pr = \rho_a c_{p,a} \nu / k_a = \frac{1.232 \frac{kg}{m^3} 1007 \frac{J}{kg} 14.48 \cdot 10^{-6} \frac{m^2}{s}}{25.2 \cdot 10^{-3} \frac{W}{mK}} \approx 0.7129$$

Since the length of the sample is much smaller than the critical length and $Pr \approx 0.6$ one can use equation 7.30 for average Nusselt number in [Bergman et al., 2011]:

$$Nu = 0.664 Re^{\frac{1}{2}} Pr^{\frac{1}{3}} = 0.664 \cdot 1383^{\frac{1}{2}} \cdot 0.7129^{\frac{1}{3}} = 22.06$$

This gives the heat transfer coefficient:

$$h = Nu\ k_a / L = 22.06 \cdot 0.0252 \frac{W}{mK} / 0.05m = 11.16 \frac{W}{m^2 K}$$

In some cases, the heat transport is completely internally or externally controlled, thus one can assume an isothermal substance or isothermal surrounding medium. Calculating the Biot number is convenient to determine if this is the case [Bergman et al., 2011, p. 284]. The Biot number is the ratio between the internal and the external resistance to heat transfer. It is dimensionless and if its value exceeds 10, then the heat transport is internally controlled, thus the surrounding medium can be taken as isothermal. Opposite if it is smaller than 0.1, internal resistance to heat flow is negligible and the substance is as good as isothermal. For the experiments at 13 ^{o}C, the highest possible value of the Biot number was then (using the thermal conductivity of beef at 7456 Pa as a lower limit, the real number is likely to be lower):

$$Bi < \frac{hL}{k} = \frac{11.16 \frac{W}{m^2 K} \dot{0}.05m}{0.036 \frac{W}{mK}} = 15.5$$

And the lower, initial Biot number at the start of drying is

$$Bi_0 = \frac{hL}{k} = \frac{11.16 \frac{W}{m^2 K} \dot{0}.05m}{0.319 \frac{W}{mK}} = 1.75$$

This shows that both resistances to heat transport matters initially and must be included, but after some time, the external coefficient might be negligible. Then, there will be a time during drying when the air most likely can be seen as isothermal, but exactly when and how the thermal conductivity of the ham develops is unknown.

This should also mean that there will be temperature gradients within the ham, unlike what others have found. If so, many properties should actually be taken at some intermediate temperature [Bergman et al., 2011]. The saturated vapour pressure at 13 ^{o}C is much higher than at 10 ^{o}C, and exchanging the lower with the higher will increase the driving forces by 135 %, but since the vaporization must take place at the wet bulb temperature, this property should be taken at this lowest temperature, which was approximately 10 ^{o}C for the samples dried at 13 ^{o}C and 68 % relative humidity, and 2.75 ^{o}C for the samples dried at 4 ^{o}C and 80 % humidity. This was found from a Molliere diagram.If heat supply exactly balances the heat for

vaporization, then

$$\dot{m}h_{fg} = \frac{A(T_a - T_{wb})}{\frac{1}{h} + \frac{s_T}{k}}$$

$$s_T = k(\frac{A(T_a - T_{wb})}{\dot{Q}} - \frac{1}{h}) \tag{6.26}$$

s_T is here called the thermal thickness, and represents the distance from the surface to the humidity front in the ham. This could be equal to the dry layer thickness in the Strømmen model, but this is not certain.

A part of the ham, where evaporation takes place, will be cooled due to evaporation. Thus, the supplied heat might be less than the heat for evaporation at the start of drying, so that the expression does not balance: s_T could become negative in Equation 6.26 since it demands that the length heat must be conducted is small enough to allow all the necessary heat supply and thus no cooling of the ham. This period should be short.

6.5.3 Mass transfer parameters

Diffusion of water in air, $D_{w,a}$ was modelled as

$$D_{w,a} = 1.4738\dot{1}0^{-4}e^{\frac{-523.78}{T}} \tag{6.27}$$

The expression was taken from [Clemente et al., 2011], and gives $2.208\dot{1}0^{-5}\frac{m^2}{s}$ at 2.75 ^oC, the lowest temperature in these experiments (the wet bulb temperature for the experiments at 4 ^oC) and $2.318\dot{1}0^{-5}\frac{m^2}{s}$ at 10 ^oC.

The mass transfer coefficient β could be found experimentally by placing an open tank of water in the same drying conditions as the samples and obtaining the mass flux of water by measurement. The coefficient of mass transfer would then be

$$\frac{RT_{wet}\dot{m}_w}{M_w(p_w^o - p_{w,a})}$$

This would be convenient to verify that the β used is correct and not effecting other parameters, but was not done. Instead, it was calculated.

[Clemente et al., 2011] found that the mass transfer coefficient was quite accurately modelled by:

$$\beta = \frac{StScD_{w,a}Re}{d} = \frac{Nu\nu_a D_{w,a}Re}{Re\ Pr\ D_{w,a}d} = \frac{22.06 \cdot 14.66 \cdot 10^{-6}\frac{m^2}{s}}{0.7129 \cdot 0.05m} \approx 0.0091\frac{m}{s}$$

whereas [Strømmen, 1980] successfully applied:

$$\frac{9.05v^{0.8}}{c_{p,a}\rho_a} = \frac{9.05 \cdot 0.4^{0.8}}{1007 \cdot 1.234} \approx 0.0035\frac{m}{s}$$

d is here the diameter of the meat, or for other geometries, a characteristic length or hydraulic diameter could be used. St is Stanton number, Sc the Schmidt number and Re the Reynolds number, all using this same length scale L, which is the length of the drying surface, v is

air velocity. However, from the definitions of Stanton, Reynolds and Schmidt numbers, this correlation gives $\beta = \beta(Le)^{\frac{2}{3}}$. It is not uncommon to assume a Lewis number of 1, but in this case the Lewis number is around 0.86 (for the first samples of 5 cm). In [Bantle et al., 2014], this has been taken into account.

All sources report that the internal resistance dominates, thus, even though different sources give different values, the coefficient should not be highly important during most of the process. On the contrary, it can be very important at the beginning when the surfaces are wet. Several values for this parameter were tried for reasons that will be explained in the Results and discussion chapter, Section 7.4.

As for heat transfer, it can be determined whether or not the mass transfer is internally or externally controlled by the Biot number for mass [Bergman et al., 2011, p. 408]:

$$Bi_m = \frac{\beta L}{D_{w,ham}} \geq \frac{0.0035\frac{m}{s}\dot{0}.04m}{2.318 \cdot 10^{-5}\frac{m^2}{s}} = 15.5$$

where the lowest possible value for β and L were used, and the value used for diffusion is the diffusion coefficient in air. The true Biot number is likely to be significantly higher, so the value is the absolutely minimum value possible. Therefore, it seems clear that mass transport is completely internally controlled, except for, perhaps, at the start.

6.5.4 SORPTION ISOTHERMS

It is important in several models to know the relationship between the moisture content and the corresponding equilibrium vapour pressure. This was modelled with good fit by [Comaposada et al., 2000] applying the GAB model:

$$Xe = \frac{M_0 K C a_w}{(1 - K a_w)(1 - K a_w + C K a_w)} \tag{6.28}$$

By trial and error, a good approximation to this that fits well with reported sorption results at 13 ^{o}C is: M0=0.055 K=1 C=10000000 And then an expression for the water activity was found from:

$$a_w = \frac{-b - \sqrt{b^2 - 4ac}}{2a} \tag{6.29}$$

where $a = (1 - C)K^2$ $b = (-2K + CK - M0KC/Xe)$ and $c = 1$. This is shown in Figure 6.1.

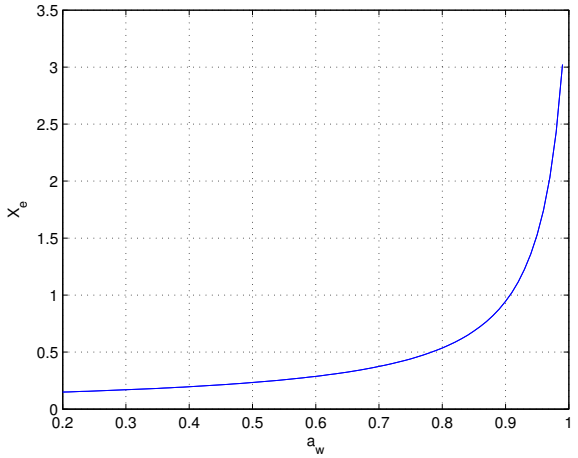

Figure 6.1: Modelled sorption isotherm for unsalted ham using the GAB-equation, showing the equilibrium moisture content as a function of water activity

Chapter 7

Results and discussion

7.1 General

The first results of the salted and unsalted sample at 13 ^oC and 68 % humidity were highly different. For the unsalted sample, an equilibrium was reached as the drying rate decreased to zero, giving the profile a curved shape, whereas the salted samples yielded a straigth line. This make them very suitable for determining which model is the most suitable. Initially, the drying is linear for both, as if there is a constant rate of drying, but for the unsalted sample this step is very short, and there is too much disturbances in the measurement to obtain a derivative that shows a flat line in this period. (Initially a constant drying rate would yield a straight line in the drying curve.) All reported parameters have an accurcay so that the last reported digit cannot be varied without increasing the error for that model and the given conditions.

Some problems in the start phase for the unsalted samples made the weight increase initially. The problem was fixed, and two sets of measurements, before and after the problem were obtained. Measurements with increasing weight were discarded, and the two sets put together. There was a drop in measured mass between the two sets, this was modelled with linear interpolation. Of the 6186 datapoints, 139 were before the error and 17 were made by interpolation. Applying the model to only the last measurements, after the error and to the two curves with interpolation between them yielded almost identical results, so this adjustment was regarded as reasonable. The salted samples were dried for 14 days and the unsalted for 43 days. The weight was measured every 601st second, to the nearest whole gramme.

The measured weight of the ten unsalted samples decreased from 1608 to 1170 (lowest measured value) or 1171 grammes(last measured value). The ten salted samples had measured weights of 3270 grammes before and 3184 grammes after drying. A metal track of 203 grammes and the weight of lard and fat was subtracted. This was done because the fat is not drying and this component has the same effect on measurements as adding another metal track to the weight. For the the salted samples the lard weight was 2293 grammes. For the unsalted samples the measured mass of fat changed slightly before and after drying, so an average value of 784.5 grammes was used.

Since the mass is decreasing and only one measurement for all samples of the same type was supplied, there has been no way to perform a statistical analysis to the deviation or exactness of the measurements. When it comes to numericals applied to the Strømmen model, timesteps of 60.1, 601 and 6010 were all used with equal results, thus the algorithm was stable and the results reliable. All files used to obtain the results are given in Section A.1.

7.2 THE FICKEAN MODEL

The Fickean model required knowledge about the equilibrium moisture content, as this is an important part of the modelled parameter Ψ. In[Corzo et al., 2010] this is taken from the final measured value, giving $X_e = 0.24$ for the unsalted and $X_e = 2.56$ for the salted sample. However, from the plots, it is clear that only the salted sample was dried to equilibrium. From figure 2 in [Comaposada et al., 2000], the value should be around 0.55. Both values were tried for comparison, and the curves are also plotted in Figure 7.1. The obtained values for diffusion coefficent and corresponding errors are shown in Table 7.1 for the cases with realistic equilibrium water contents.

Fick's second law modelled the curve for the unsalted sample very well, and the sine-shaped profile improved its accuracy, even though it is a very simple, one-term expression. The diffusion coefficients were 21.7 and 363.2 % higher for the sine-shaped profile for Unsalt and Salt respectively, and the errors 16.8 to 29.4 % better than for the falt profile. It is peculiar that the resulting curves in Figure 7.1 differ so much in shape for the salted samples when $X_e = 0.55$. Either, the version with flat initial profile cannot predict a straight line, but this seems weird, as the sine-shaped version could. Or perhaps the error measure has local minimuma, so that a value of D_{eff} can be found to be better than values slightly above and below, but very far away from this appearent best value, there can be another, truly best performing value. This is not likely however, as the exponential function, through which the diffusion coefficient influences the curve, is steadily decresing with D_{eff}, and not likely to exhibit such behavior.

Neither the flat nor the sine-shaped version of the model managed to model the salted sample well, regardless of choice of equilibrium moisture content. Especially wrong is it to assume $X_e = 2.56$. This parameter is higly important. One reason for this might be that the value of this parameter is the only way the relative humidity of the air impacts the result. Humidity influences drying to a high extent [Bantle et al., 2014], but it is not included in the model in any other way than through decideing the equilibrium condition.

The values of the diffusion coefficient obtained here are $\approx 10^{-9}$ when realistic values for equilibrium moisture content were used, which is 100 to 1000 times higher than other findings

Sine-shaped		
Sample	$D_{eff} \cdot 10^{10}$	$\sigma^2 \cdot 10^8$
`Unsalt`	11.28	6.455
`Salt`, $X_e = 0.55$	1.76	3.620
Flat		
Sample	$D_{eff} \cdot 10^{10}$	$\sigma^2 \cdot 10^8$
`Unsalt`	9.27	7.752
`Salt`, $X_e = 0.55$	0.38	5.129

Table 7.1: Results from the Fickean model: The values for the diffusion coefficient D_{eff} that gave the lowest errors for a flat initial moisture profile in the hams and a sine-shaped inital profile are shown. The error between model and measurement is given as σ^2.

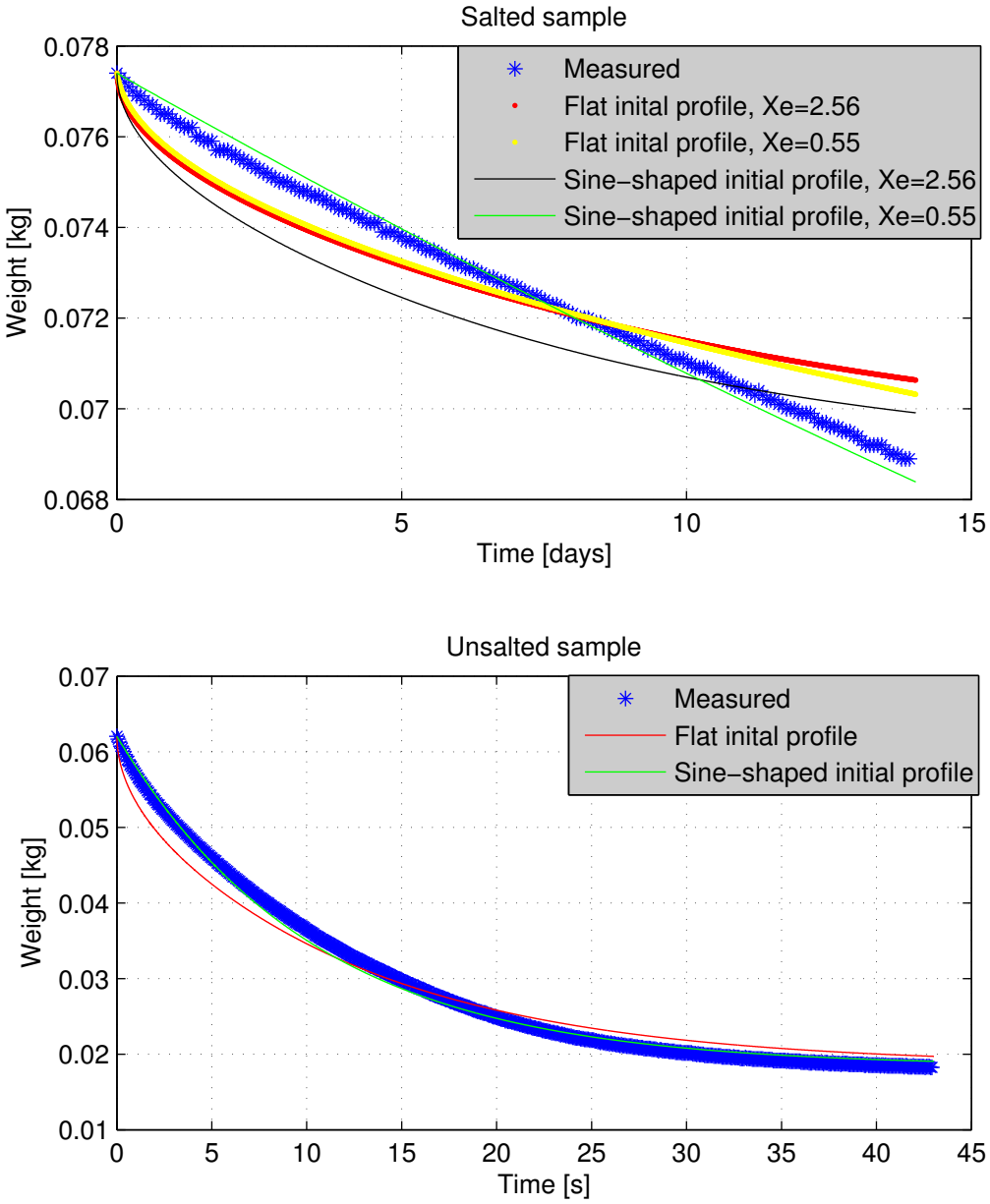

Figure 7.1: Final results for the Fickean model for the experiments named Salt and Unsalt, using sine-shaped or flat initial moisture profile, and applying two different values for the equilibirum moisture content for the salted sample

[Gou et al., 2003, Gou et al., 2002, Raiser, 2014, Bantle et al., 2014]. However, the results in these studies also differ by an order of magnitude, so this could be seen as another sign that the model is not very good, as it is very difficult to know which value to use when they are so inconsistent between studies. Adjusting the value to fit any cure is curve-fitting rather than finding a physical parameter. A good feature with this model is that it dries slowly for a thicker product and can give a visual picture of the moisture distribution, as shown for Unsalt in Figure 7.2.

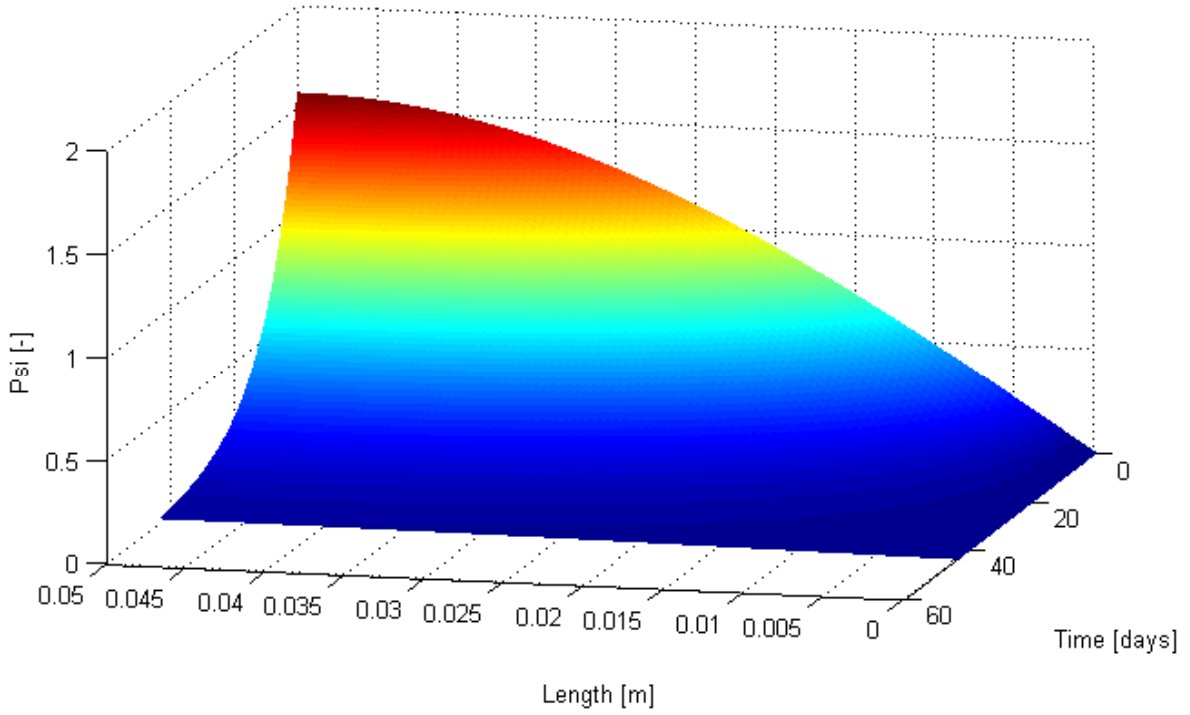

Figure 7.2: Moisture distribution in the hams as a function of time and position for the unsalted sample, modelled by Fick's laws using a sine-shaped initial profile: The dimensionless moisture content Ψ ('Psi' in the figure) exceeds 1 away in the parts away from the surface (surface at L=0) because from the definition of Ψ, its average must be 1.

7.3 The Weibull model

The obtained parameters, errors are shown in Table 7.2 and Table 7.3, and the measured and plotted curves can be seen in Figure 7.5. For the Weibull model, using the linear regression method faced some problems: the time starts at zero, which has the logarithm $-\infty$, and in addition experimental values for the moisture ratio MR were both zero and negative at the end, and some early values were larger than one at the beginning. This is probably due to inaccuracy in the weighing or disturbances from the airflow. The measured weight increases were always only a few grammes, less than one percent of total weight, and this was therefore considered to be an acceptable error, but it made it impossible to apply the method of linear regression without adjustments: To obtain values for the linear plot, the equilibrium water content was found from the miniumum measured weight minus one gramme in stead of the last measured value for Unsalt. For the salted samples, the value was simply set to 0.55 as no equilibrium weight was measured. Instabilities were always present in the beginning, but discarding data to fit a model better is not good practice, therefore, two sets of parameters were found. One discarding the first four and one discarding the first 31 measurements.

If the model is suitable, the linear regression should indeed involve a linear curve. This was seen to be very close to the truth for both samples in Figure 7.3 and Figure 7.4. However, as

can be seen in Figure 7.5, the linear regression model deviates a bit at the end of the drying curve. This is also the case for the Grid method for the salted sample. An important question is how this model would perform if it should predict the rest of the curve for this experiment. It might be, since the model is empirical and not based on physics, that it can be fitted to many curves, but is not applicable for predicting drying curves.

For all methods applied, α and β had similar values for the same sample. β was never much above 1, which is reasonable as the weight should decrease.

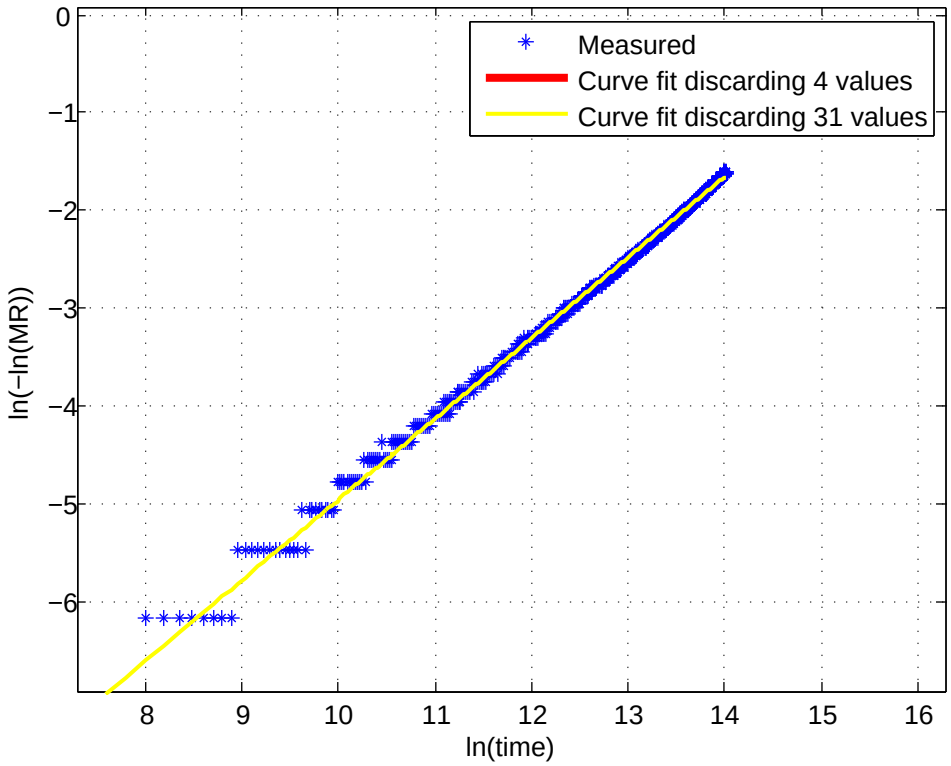

Figure 7.3: Plot of the logarithm of the negative of the logarithm of the moisture ratio MR, versus the logarithm of time, for the salted samples: This should theoretically should be a linear plot where the slope and intersection of the curves could be used to determine the parameters for the Weibull model. The graphs are obtained after discarding either four or 31 of the first values. Discarding four values gave complex or infinitely large numbers, or no numbers at all, and the program did therefore not plot the line, showing the necessity of discarding values. The measurements show an almost completely straight line, suggesting the model is applicable.

The unsalted sample always showed very similar values for both parameters, the fits are good and the errors are small. Both the grid method and the normalized model use a grid to find the parameters, and it is not surprising that these two stategies show more similar results than the linear regression method. No big difference between discarding four or 31 values was found, but discarding more of the unstabilities at the beginning yielded a slightly better result.

For the salted sample, one result using the lowest measured weight as equilibrium weight is also shown. All other methods for finding the parameters using $X_e = 2.56$ gave similar values and plots. These results deviate much from the results using $X_e = 0.55$. The modelled curve for the higest equilibrium moisture content bends up and down were the mesurements are straigth,

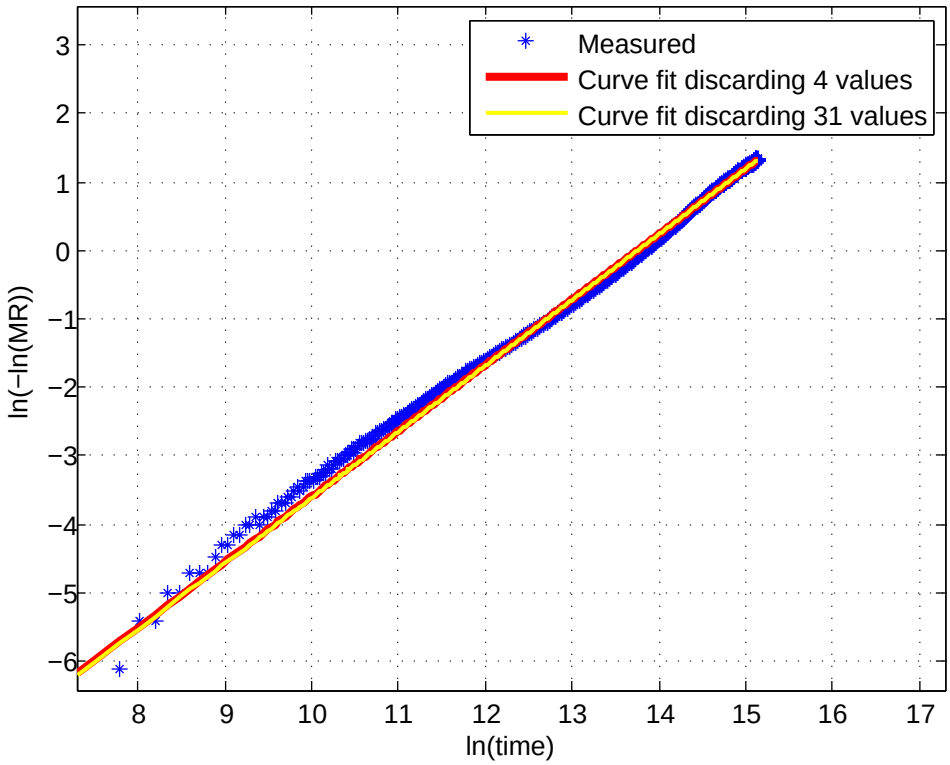

Figure 7.4: Plot of the logarithm of the negative of the logarithm of the moisture ratio MR, versus the logarithm of time, for the unsalted samples: This should theoretically should be a linear plot where the slope and intersection of the curves could be used to determine the parameters for the Weibull model. The graphs are obtained after discarding either four or 31 of the first values, because including all values gave complex or infinitely large numbers or functions of these yielding no numbers at all. Discarding more values gave a line that fitted the main part of the measured curve slightly better. The measurements show an almost completely straight line, suggesting the model is applicable.

Parameter	Grid	Lin.reg., 4	Lin.reg., 31	Normalized
α [s]	9.2186e+5	9.4312e+5	9.4551e+5	9.2186e+5
α, % of t_{tot}	24.81	25.38	25.45	24.81
β	1.0470	0.9563	0.9605	1.0450
σ^2	1.284e-8	2.567e-8	2.501e-8	1.282e-8

Table 7.2: Parameters and errors resulting when applying the Weibull model to the unsalted samples: The columns show the results obtained by applying the Grid method (Grid), Linear regression method (Lin.reg.) discarding four or 31 measurements and the results from the normalized Weibull model. α is given both as a value and as a fraction of total drying time, t_{tot}.

Parameter	Grid	Grid, $X_e = 2.56$	Lin. reg., 31	Normalized
α [s]	5.2475e+6	6.6397e+5	9.0989e+6	8.0354e+6
α, % of t_{tot}	433.1	54.8	751.0	663.2
β	1.0660	1.2970	0.8231	0.8640
σ^2	3.860e-9	3.442e-6	5.996e-10	2.077e-10

Table 7.3: Weibull results for the first salted samples (Salt) using equilibrium moisture content X_e=0.55 in all cases except for in the second result column: The results are obtained by applying the Grid method (Grid), Linear regression method (Lin.reg.) discarding 31 measurements and the normalized Weibull model. Errors and the best parameters obtained are shown. α is given both as a value and as a fraction of total drying time, t_{tot}

.

and the error is much larger than when X_e is 0.55. As can be seen in both Figure 7.5 and Table 7.3, the higher value gives a much worse result, thus the realvX_e is probably closer to 0.55, in agreement with the findings for the Fickean model.

For the salted sample, the parameters differ much more between the methods than for the unsalted, even the two most similar have almost 10 % difference in alpha-values.These are also about ten times higher than the value for the unsalted sample, and it is questionable whether this can truly be less than the total time to equilibrium for the salted sample. This migth indicate that the theory weakly linking this model to physical parameters fails; it gives very good curve fits, but there are no physical relationship between this model and reality. β is about 15 % lower for this salted sample.

The normalized model performed better than the not-normalized. It was strictly speaking the best for the unsalted sample as well,but the difference between it and the not-normalized one was not significant. This is oposite of the results found by [Corzo et al., 2010]. The linear regression method failed when only the four first values were discarded, yielding complex numbers and parameters and errors that MATLAB reports as NaN (not a number). Thus, only the results for discarding 31 values are shown. This method performed quite well, however.

The two best methods for the salted sample, linear regression and normalized Weibull, reached quite different answers than the grid method did, but this is because the grid did not include such high values of α. The procedure was not repeated since the two best methods already have given the better values and these results demonstrate the important limitation of such a grid method: to find the real optimal parameters, the applied ranges for these must include the global minimum for the error.

The normalized model also results in values for D_{eff}, which are reported for both samples in Table 7.4. Reasonably enough, the salted sample has a lower value, this is similar to all other reported results [Bantle et al., 2014, Raiser, 2014, Comaposada et al., 2000, Gou et al., 2003, Gou et al., 2004, Clemente et al., 2011]. They are however one order of magnitude lower than those obtained by [Gou et al., 2004, Gou et al., 2003] but similar to those obtained by [Bantle et al., 2014]. One explanation might be that D_{eff} is not a real physical property, but accounts for all deviations from reality in the model. [Pakowski and Adamski, 2007] reported that it is model dependent. Eventually, this finding strenghtens the idea that there is no link at

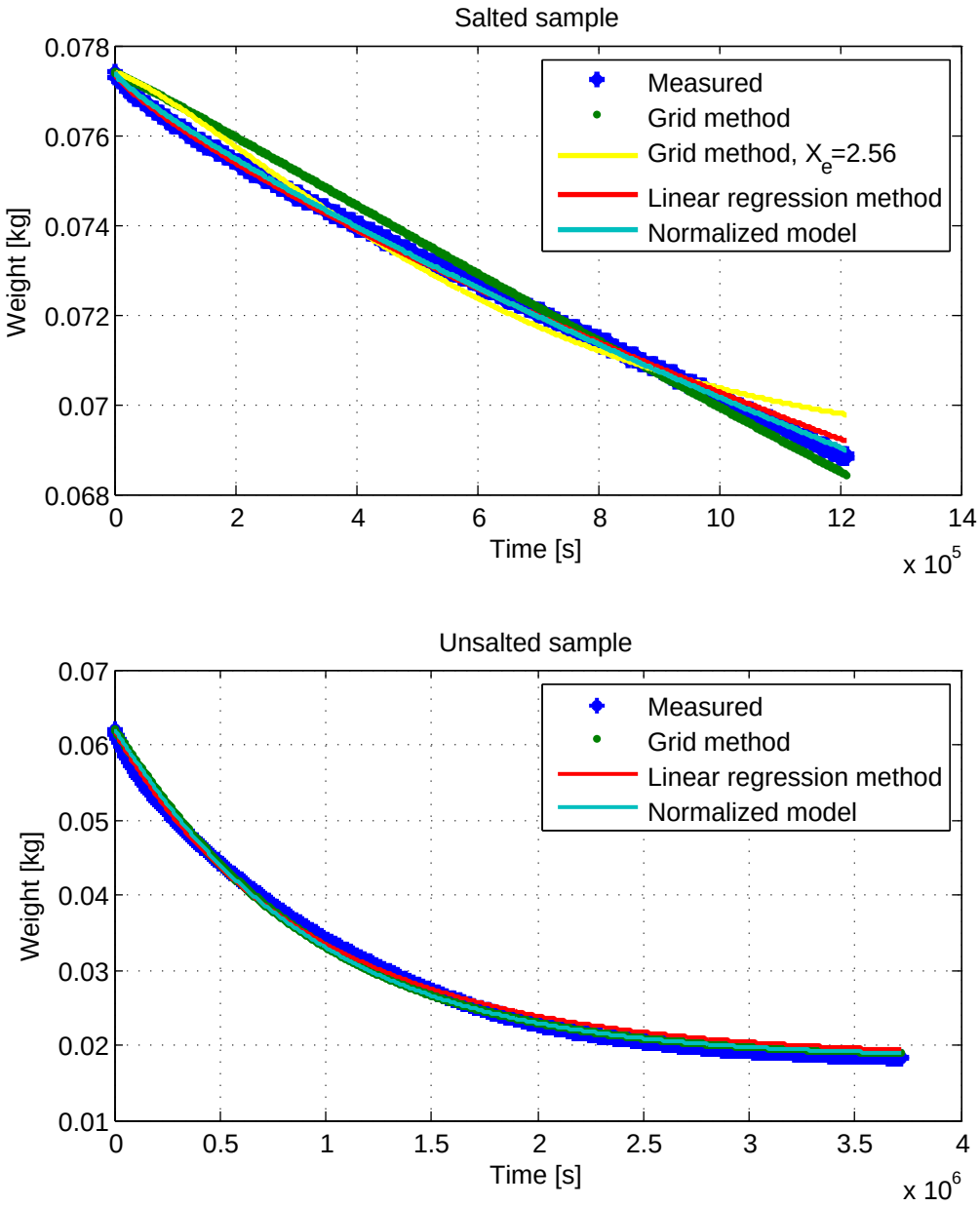

Figure 7.5: The different predictions for the drying curves for experiments Salt and Unsalt using the Weibull model with parameters obtained from the Linear regression method, Grid method or the normalized Weibull model. For the salted samples, one curve with equilibrium moisture content set to the final measured moisture content is shown ($X_e = 2.56$), the rest of the curves use $X_e = 0.55$ from theory. The normalized and Linear regression methods are highly similar. For the unslated samples, the parameters for the Grid method and the normalized model coincide and it is hard to see the difference between them.

Parameter	Salted	Unsalted
D, $[m^2/s]$	7.7780e-11	6.7798e-10
D_{eff}, $[m^2/s]$	2.8293e-12	5.9317e-12
R_g, $D_{eff} = 10^{-10}$	0.794	11.3
R_g, $D_{eff} = 10^{-11}$	7.94	40.7
R_g, $D_{eff} = 10^{-12}$	73.7	290.9
Average R_g	27.5	114.3

Table 7.4: Resulting parameters for the normalized Weibull model: The obtained diffusivities (D) and obtained effective diffusivities (D_{eff}) are shown for salted and unsalted samples at 13 ^oC and 68 % relative humidity, along with geometric factors R_g for the different diffusivities and the average. These differ much from one another, suggesting the model is not applicable for generalization.

all between this model and reality. Another sign of this can be found from studying the values of the geometric factor R_g. In theory, the three obtained values for this factor should be quite similar as in [Corzo et al., 2010]. There, the deviation was less than 10 %. In Table 7.4 it is clear that this was not the case for ham drying. The geometric factor differs by as much as two orders of magnitude, depending on both salt content and modelled diffusivity. The average was used in the final result, but the average does not represent the obtained values, as they differ too much. This will make generalization of the model difficult.

From the linear plots and the obtained results, it could be concluded that the normalized method is the best, but it has the limitation that it requires a grid search for parameters with suitable ranges. This could face the problem previously mentioned in this section. In order to find suitable ranges for the parameters, a first search by linear regression could be made.

7.4 THE STRØMMEN MODEL

Using the Strømmen model, it became clear that the theoretical mass transfer coefficients were much too low to predict the drying rate. Finding the mass transfer parameters by the direct approach described in Section 6.4.4 showed that the overall mass transfer coefficient decreased, as it should, but also that its initial value varied much between the samples. The unsalted sample had value of about 0.019, the salted 0.0045 $\frac{m}{s}$, see Figure 7.10 and Figure 7.11. Therefore, several different values (from 0.0002 to 1800) were tried during modelling, and it appeared that this parameter was quite insensitive for the first samples, as the inner resistance dominates during most of the drying.

The mass transfer from the surface is only important in for the initial slope. However, the start of the drying curve cannot be steep enough if the value is too low, thus, setting it high enough was early found to be important (in Table 7.5 the error for Unsalt is 10^4 times larger for a low value than for a high). From the measured values and the different attempts to model, 0.018 $\frac{m}{s}$, the value from Figure 7.9, was chosen, despite that this is higher than any theoretical value. This was done because even though theory disagrees with the value, this is an actual observed value, and therefore it must be physically correct. Something must

make β larger, if not, it could not have been observed. Enhancement could be due to osmotic dehydration, capillary effects (which are only present initially [Song, 1990, Whitaker, 1977]), interaction between samples or other items causing turbulence in the drying chamber.

The simulated drying curve for the first unsalted samples at 13 ^oC and 68 % relative humidity (Unsalt) did not show the same shape or curvature as the experimental one, as seen from the green curve in Figure 7.6. Adjusting the initial dry layer thickness s_0 to a non-zero value could correct any initial error, as seen from the red 'Fit start only'-curve in Figure 7.6, but caused greater failures later. The problem was that the measured profile of the unsalted sample flattens out at the end, whereas the simulated one decreases more steeply.

For the first salted samples (Salt), the fit was good. Important to notice is that this measurement lasted for a much shorter time than the experiment with the unsalted samples and the initial part of the profile was therefore more important, thus s_0 could be adjusted to give a good initial profile without causing error later. To say whether the model would have fitted further out in the process is uncertain, as the hams were not dried any further. It should also be commented that the modelled curve bends slightly, and this is not completey similar to the slight bending of the measured curve. The result is shown in Figure 7.6 and the parameters are given in Table 7.5.

For the unsalted samples, the problem was that the driving forces never decreased to zero and/or that the resistance did not grow to infinity. Trying to decrease the driving forces (as explained in Section 6.4.2) when the dry layer thickness s reached a certain value clearly gave better fits, as seen in Figure 7.7.

At this time in the work, the modelled value of s could be larger than the length of the sample, which was highly unrealistic. The reason was an error that was found and corrected, as will be explained later in this chapter. (This only affected the value of μ in Table 7.5, but nothing else. All reported values are from after the correction.) The best fits were obtained if the pressure decreased when s reached a value of twice the length of the samples (s grows as long as s<2L, then pressure starts to decrease). However, geometry for hams can vary, but this should not determine whether or not the vapour pressure decreases. Therefore it was desirable to find another, more realistic way to model this change in mechanism. Two solutions were investigated:

The first involved to define dry layer thickness s as a function of heat supply, to see if the length then became reasonable. The heat supply is known from the amount of evaporated water, the enthalpy of vaporization and the temperature of the air and at the humidity front. These were all known, so s could be found from Equation 6.26. Unfortunately, this solution appeared to be very unstable with regard to mathematics, and s could become negative, alternate and have magnitudes of 10^{17} metres. The predicted mass loss was also unsteady and completely unrealistic. This solution was rejected.

The second approach consisted in assuming that it is the end of free water, and the start of removal of bound water that causes the change in mechanism. Therefore, the change should happen at a certain value of the moisture content X. This value was denoted X_P (or XP in Figure 7.7) and was set to 1.33 as this gave the best results by trial and error. This method

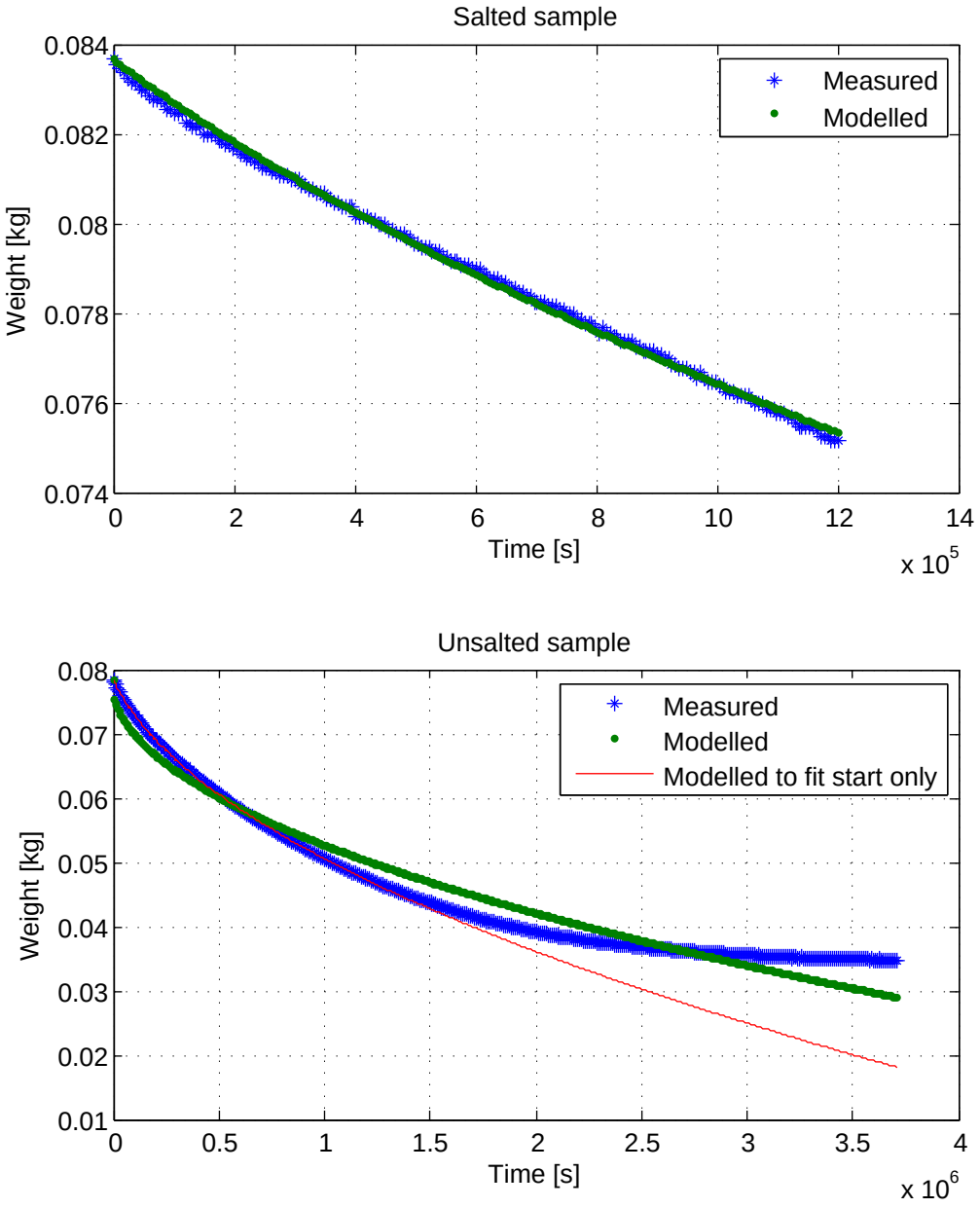

Figure 7.6: The resulting drying curves for the unmodified Strømmen model applied to the experimental curves Salt and Unsalt: For the unsalted samples, two curves are shown. The green is based on minimizing the error throughout the whole drying process; the red is based on minimising the error in the first third of the time.

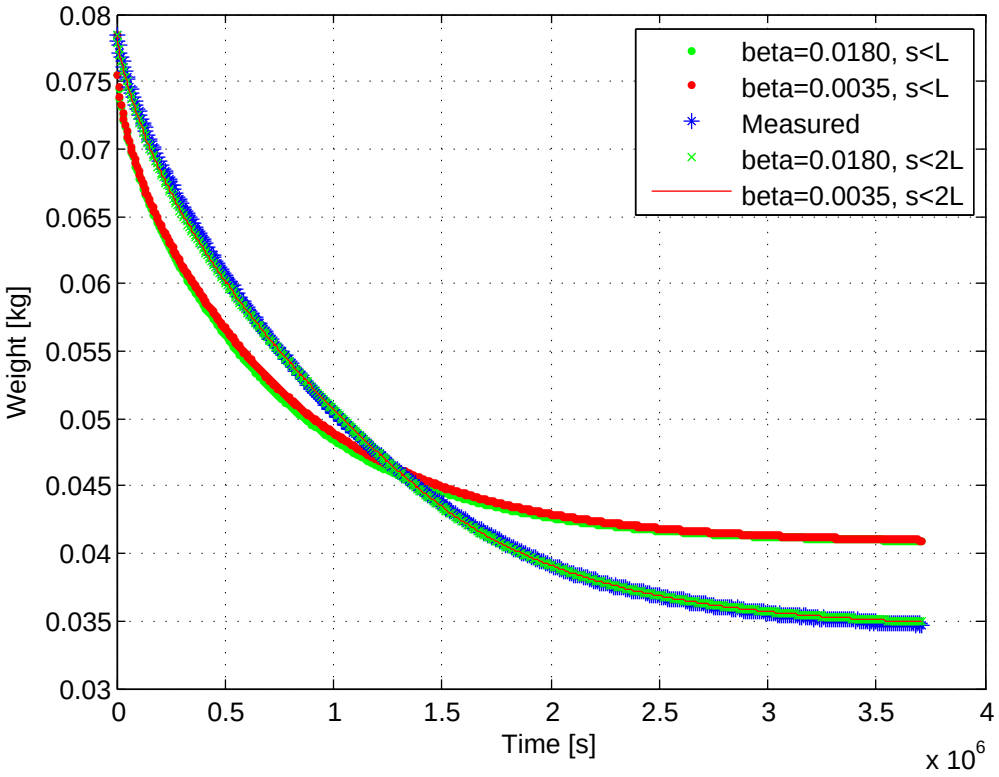

Figure 7.7: The modified Strømmen model applied to Unsalt with several variations: assuming the vapour pressure in the ham decreases when the modelled dry layer thickness s reaches the length of the sample L, denoted 's<L', or when the modelled dry layer becomes twice the length of the sample, denoted 's<2L'. Two different values for the surface mass transfer coefficient β were tried for both cases, but had no significant influence.

involved to allow a dry layer thicker than the sample. However, this was accepted since the dry layer thickness is not a physical size, as the border between the completely dry layer and the wet 'core' of the ham will not be abrupt [Strømmen, 1980]. Hence, this length is an equivalent or effective length of the dry layer, that says something about how fast the internal resistance grows due to the development of this drier layer. It is not the magnitude of s, but the speed of growth that governs the drying.

Pressure decrease was carried out using the sorption isotherm in Section 6.5.2 and a linear decrease was also tried. Both gave equal results, so the model was quite insensitive to *how* the vapour pressure decreased, as long as it decreased, and did so at a reasonable speed. The final curve is seen in Figure 7.8.

The final value of the dry layer thickness became too high in several cases. For the unsalted sample (Figure 7.10), it exceeded the length of the entire sample. It was discovered that the reason for this was that the mass of fat had been subtracted from the measured mass, and then initial density had been calculated as mass of lean meat divided by total volume, yielding a very low value. This was corrected by using a density of $1070\frac{kg}{m^3}$ given by Inna Petrova. This value was then used consistently. If the fat and lard cover was included in the weight for the unsalted sample it gave an initial density of $1124\ \frac{kg}{m^3}$. This is only slightly higher (but it includes the lard cover), so $1070\ \frac{kg}{m^3}$ seemed realistic.

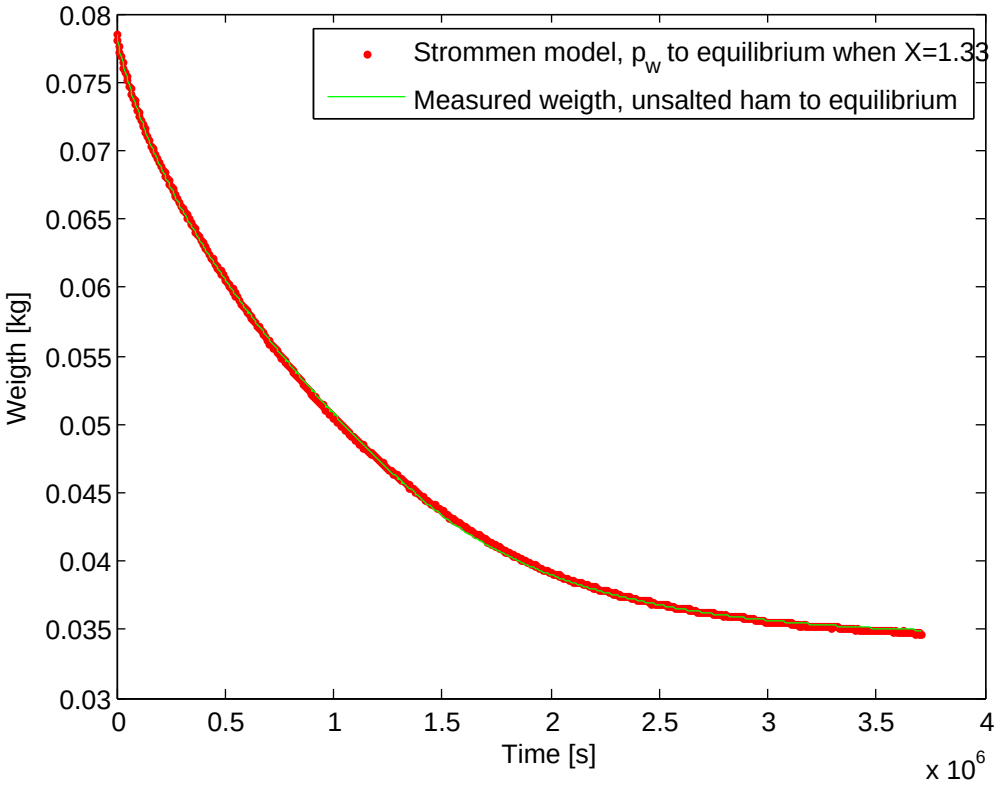

Figure 7.8: The final resulting curve for the first unsalted sample, obtained with modified Strømmen model which involves decrease in the vapour pressure of the ham when the water content reached 1.33

7.5 BEST PERFORMING MODEL

The Strømmen model was the best performing one and used to model all experimental curves. It was also used for the heat calculations. It was chosen as best performing because it managed to model the two first curves quite well, slightly better than the diffusion model, and because it contains physical properties as parameters. If some physical condition is changed, then the model also changes. Also, the Fickean diffusion model does not depend on the relative humidity of the air, which is a huge drawback, as this parameter is highly sensitive [Bantle et al., 2014].

The errors for the chosen model were similar to those of the Weibull model for the unsalted sample (see Table 7.5 and Table 7.2), but much worse than the Weibull model for the salted sample (see Table 7.5 and Table 7.3). However, the inclusion of physical parameters is highly important for simulations, since it is desirable to adjust physical factors. In addition, there were no consistency in the parameters in the Weibull model, as discussed in Section 7.3, so the Strømmen model was seen as superior to the Weibull model even if the errors were higher.

The three other experiments at 13 ^oC and 68 % relative humidity (NotSalt68, LowSalt68 and MedSalt68) showed high measurement error for the medium salted sample MedSalt68, as seen in Figure 7.15. It was therefore an important question how accurate the measurements were, but since only one measurement for each experiment was available, there was no way to check the standard deviations.

The mass transfer coefficient of 0.018 $\frac{m}{s}$ was not sufficient for all later experiments. Thus in some cases the value was set as high as 1. All results assuming another value of the mass transfer coefficient than 0.018 have specified this and which value was used instead.

The results for the three experiments with different salt contents at 13 ^oC and 68 % relative humidity were quite good, as seen from Figure 7.13 through Figure 7.15.

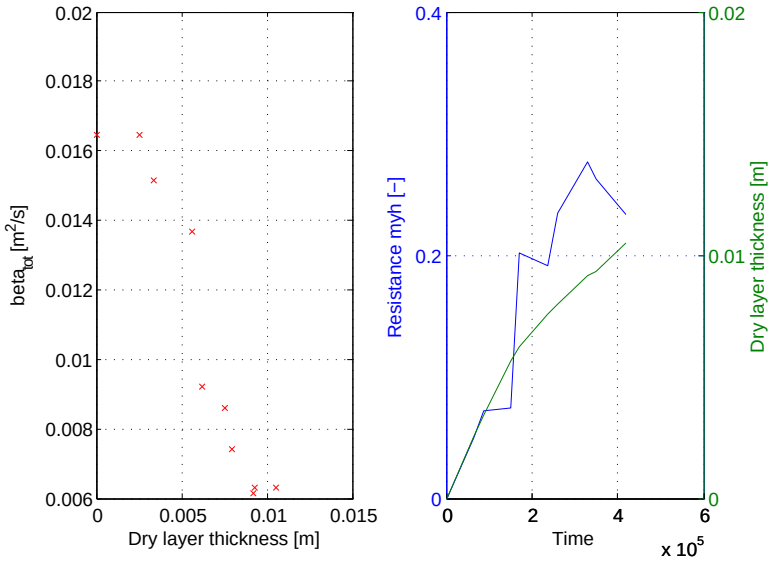

Figure 7.9: Left plot: Measured overall mass transfer coefficient β_{tot} as given in Equation 6.18, as a function of dry layer thickness before the expression for this value was corrected; Right plot: measured value of μ the decrease in diffusion for hams compared to air (left axis), and the dry layer thickness (right axis), both for the experiment NotSalt68

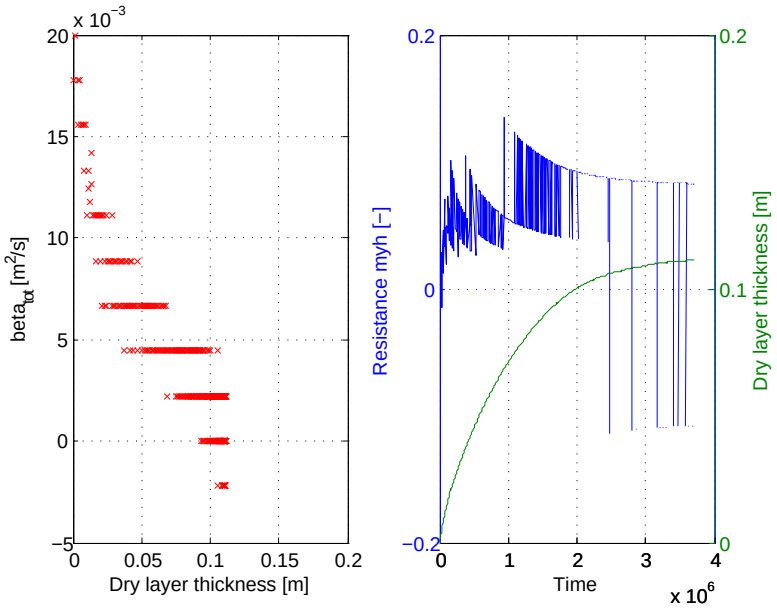

Figure 7.10: Left plot: Measured overall mass transfer coefficient β_{tot} as given in Equation 6.18, as a function of dry layer thickness before the expression for this value was corrected; Right plot: measured value of μ the decrease in diffusion for hams compared to air (left axis), and the dry layer thickness (right axis), both for the experiment Unsalt

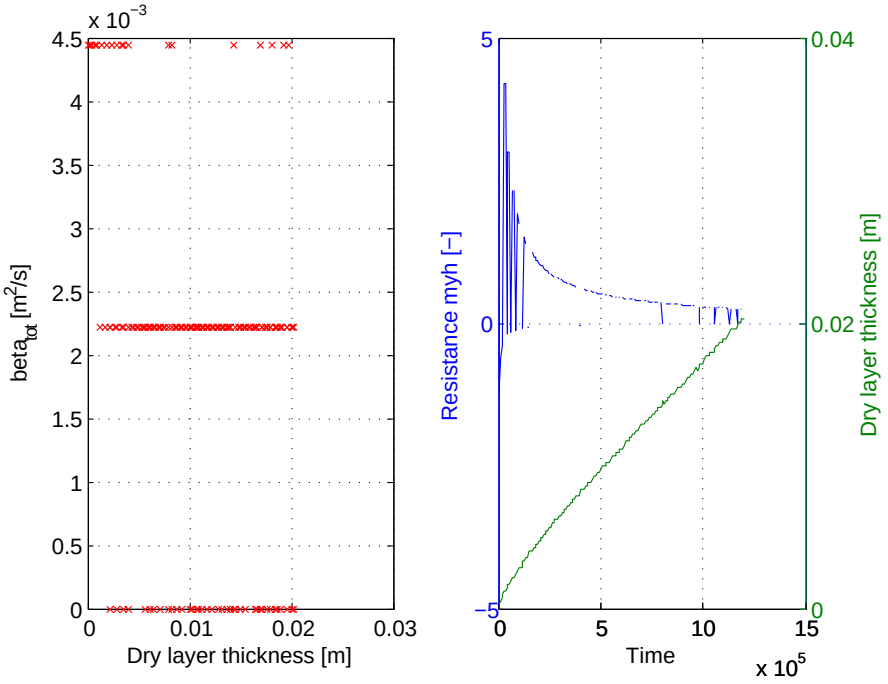

Figure 7.11: Left plot: Measured overall mass transfer coefficient β_{tot} as given in Equation 6.18, as a function of dry layer thickness before the expression for this value was corrected; Right plot: measured value of μ the decrease in diffusion for hams compared to air (left axis), and the dry layer thickness (right axis), both for the experiment Salt

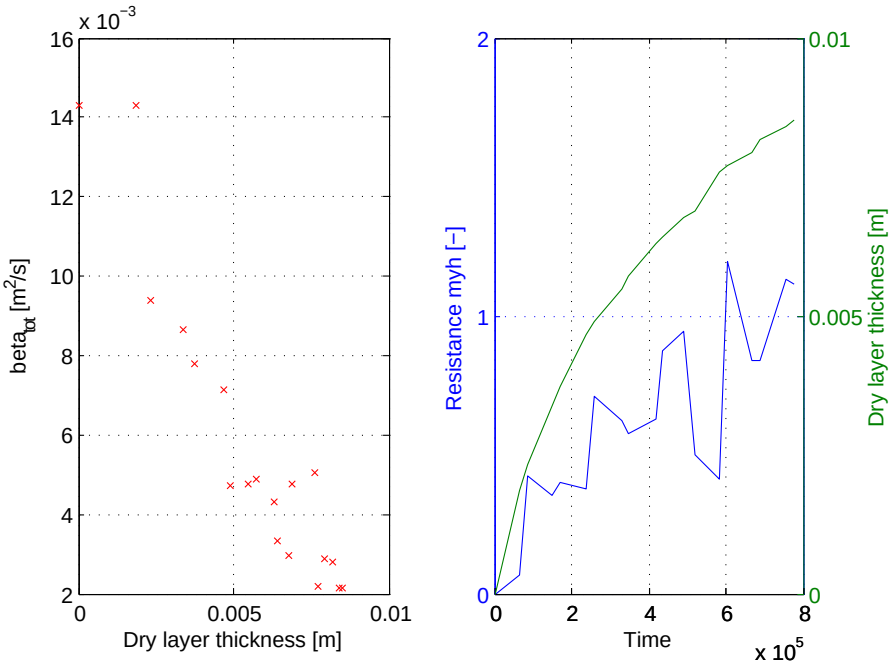

Figure 7.12: Left plot: Measured overall mass transfer coefficient β_{tot} as given in Equation 6.18, as a function of dry layer thickness before the expression for this value was corrected; Right plot: measured value of μ the decrease in diffusion for hams compared to air (left axis), and the dry layer thickness (right axis), both for the experiment LowSalt68

Assumption:	$\mu \propto s^0$		
Sample	μ	s_0 **in mm**	σ^2
`Salted`	2.013	3.7	1.3134e-8
`Unsalted`	0.281	0.0	5.4589e-8
`Unsalted`, $\beta = 0.0035$	0.000	0.0	1.1734e-4
`NotSalt68`	0.198	0.0	8.7012e-7
`NotSalt68`, $\beta = 1$	0.377	1.9	3.6705e-7
`LowSalt68`	0.587	0.0	6.9073e-7
`LowSalt68`, $\beta = 1$	0.803	0.7	1.2341e-7
`MedSalt68`	0.503	0.0	1.3713e-6
`MedSalt68`, $\beta = 1$	0.807	0.4	3.0463e-7

Table 7.5: Optimal parameters and resulting errors for the Strømmen model, depending on different assumptions for mass transfer coefficient β, which was 0.018 $\frac{m}{s}$ unless otherwise stated: s_0 is the initial thickness of the dry layer s, μ is the decrease in diffusion due to the ham and constant and σ^2 is the deviation between model and measurement

Assumption:	$\mu \propto s^1$		
Sample	μ	s_0 **in mm**	σ^2
`NotSalt68`	42.4	0.0	7.7485e-7
`LowSalt68`	124.1	0.0	1.6190e-6
`MedSalt68`	112.3	0.0	2.5524e-6
`Unsalt`	19.3	1.9	3.5685e-7
`Salt`	349.9	3.9	8.4907e-8

Table 7.6: Optimal parameters and resulting errors for the Strømmen model, assuming that the decrease in diffusion coefficient due to the ham was $\mu \propto s$ and $\beta = 0.018\frac{m}{s}$: s_0 is the initial thickness of the dry layer s and σ^2 is the deviation between model and measurement

Assuming the internal resistance μ constant and dry layer thickness s increasing yielded the parameters and errors shown in Table 7.5. μ should be larger than 1, because it is the value the diffusivity of water in air must be divided by to become the diffusivity of water in dried ham. It is clear from Table 7.5, that this was not the case. The best fits required lower values in all cases, except for the first experiment with salted samples. However, the length of the dry layer s, reached lengths of 1-2 cm. This is within the length of the sample, and could be realistic, but it is actually about ten times larger than the values seen in [Gou et al., 2004] and the 1 mm used by [Strømmen, 1980]. Therefore, the approach with $s = 1$ mm was carried out. The inner resistanse should still increase as more water is lost, thus the expression Equation 6.16 was applied.

Assuming a constant dry layer $s = 1$ mm and an increasing μ resulted in the values and errors in Table 7.7, and some plots are shown in Figure 7.13 through Figure 7.15. Generally, bad fits resulted is one demanded $\mu > 1$. For example, modelling LowSalt13 with $\beta = 0.018\frac{m}{s}$ and $\mu_0 = 1$ gave lowest error for $\mu_0 = 1$, that is, as low as possible and made the diffusivity in ham equal to that in air. The error was 3.5256e-06. However, μ grew with time, as it was proportional to mass loss in this version of the model, and the final values were always well

Assumptions:	$\mu \propto \Delta m$	**s=1 mm**		
Sample	μ_0	μ_{end}	$\frac{\Delta\mu}{\Delta m}$	σ^2
Unsalted	1.000	3.5500	77.8418	1.6454e-6
Salted	7.54	15.6563	973.2969	1.3067e-8
Unsalted	0.00	4.5906	281.2	5.4312e-8
MedSalt68	0.000	5.2225	216.38	6.4753e-7
MedSalt68	0.000	4.2780	174.10	1.3839e-6
MedSalt68	0.368	6.8229	274.0	3.0492e-7
MedSalt68	1.000	2.9942	77.86	4.9679e-6
MedSalt68	1.000	5.9816	205.45	7.9515e-7
LowSalt68	0.000	5.1882	203.18	6.9709e-7
LowSalt68	0.577	7.4416	276.30	1.2430e-7
LowSalt68	1.000	3.9217	110.56	3.5253e-6
LowSalt68	1.000	6.8876	233.18	3.1282e-7
NotSalt68	0.000	1.6966	68.546	8.7816e-7
NotSalt68	0.899	3.5421	110.05	2.6115e-7
NotSalt68	1.000	3.4060	99.41	2.9808e-7

Table 7.7: Results for the Strømmen model if $\mu \propto \delta m$ and dry layer thickness $s = 1$ mm, always, was assumed: β was 0.018 $\frac{m}{s}$. In some cases, μ was forced to be at least 1, whereas in other cases, it was allowed to be as low as zero, and the start value μ_0 was optimized with respect to minimizing the error σ^2. The final value of the parameter was also reported in the column denoted 'μ_{end}'.

above 1. The results where μ was allowed to start below 1 are equal to the results where s varied with the amount of evaporated water and μ was constant, and the graphs for the two cases are hence identical, and therefore, resulting curves are only showed for one of the cases in Figure 7.13 to Figure 7.15. The results are reported in Table 7.7.

Is it realistic that μ can have initial value below 1? It seems unreasonable to require that there should be an internal resistance from the beginning of the drying process, but if $s = 1$ mm and one demands $\mu \geq 1$ then there will be an internal resistance from the very beginning. The most physiologically correct would be to set μ constant and let the dry layer grow, thereby allowing no internal resistance to begin with. The reason that this method gave unrealistically low values of μ might be that the expression for the dry layer thickness is wrong, which would also explain why 1: it is ten times higher than others report and 2: why the mass loss in the present model depends on the surface area to the second power during most of the drying process (when β is negligible). This last fact is easily seen from substituting the expression for s ((6.15)) into

$$\dot{m} = \frac{A^2(p_{ws} - p_{wa})D_{w,a}X_{wb,0}\rho_{tot,0}}{R_w T \mu \Delta m}. \tag{7.1}$$

Then, the problem is to find a better expression for s. One attempt was [Bantle et al., 2014]:

$$s = \frac{\Delta m}{A(1-\epsilon)}, \tag{7.2}$$

where ϵ is the porosity of the ham, which must be guessed. Unfortunately, this gave even higher values for the dry layer unless porosity was below 0.197 (at which the two expressions for s

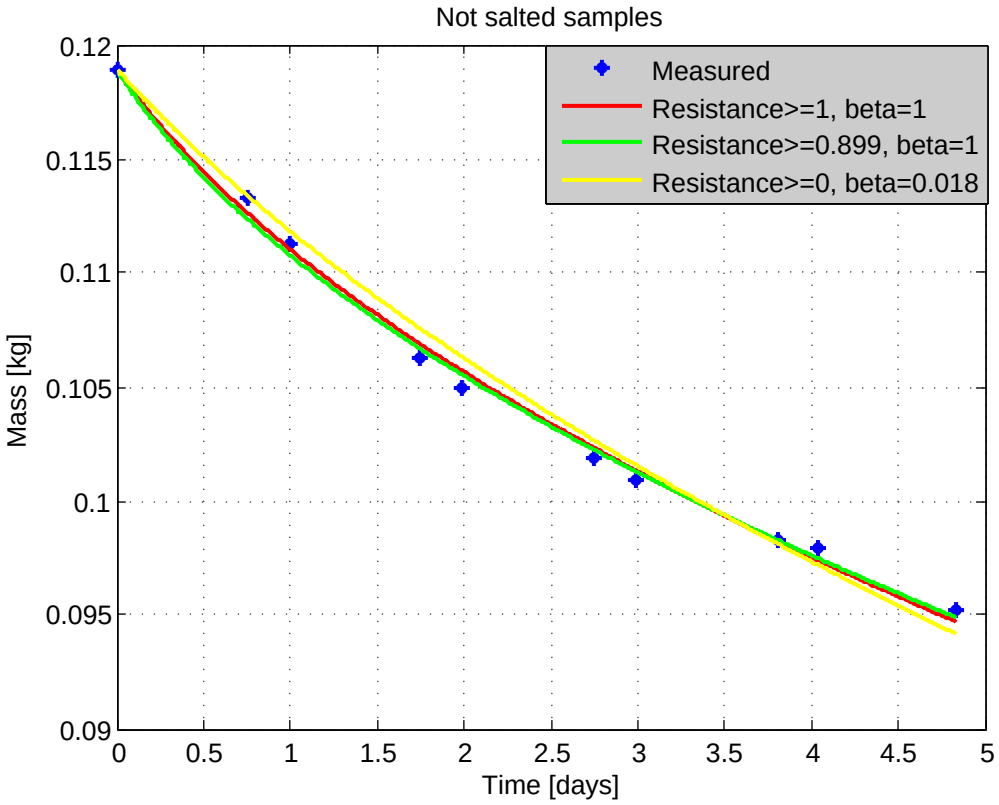

Figure 7.13: Results for the Strømmen model applied to NotSalt68 if $\mu \propto \delta m$ and dry layer thickness $s = 1$ mm, always, was assumed: β was 0.018 or 1 $\frac{m}{s}$. In some cases, μ was forced to be at least 1, whereas in other cases, it was allowed to be as low as zero, giving an optimal start value of 0.000 or 0.889, depending in β. The case $\beta = 0.018\frac{m}{s}$ and $\mu \geq 1$ is not shown, as this only yielded a straight line.

become equal), and the increase in μ if the porosity was set even lower was insignificantly small. In addition, this equation too makes the drying rate dependent on the surface area to the second power. Finding a suitable equation for s would make any value of μ around 0.1 and above in the present model valid, but to find it would require data for different geometries and/or sizes of the hams, which are not available in the present study.

Assuming that μ was a linear function of the dry layer thickness, which Figure 7.9 and Figure 7.12 might indicate that it is, yielded better fits for some samples, but worse for others and the units were no longer correct. Many of the other experiments did not show this trend, and it could be a coincidence, as the different graphs are highly different, regardless of salt content. This was therefore not considered as a realistic solution and this method was not investigated further. The method was not applied to all samples because the last results were supplied very late in the work, and the results for the first samples had not been convincingly better. Values are reported in Table 7.6.

Dry layer thickness $s = 1$ mm gave realistic values for μ during most of the process, but it seems more likely that the dry layer grows and the diffusion coefficient in dried ham stays constant. Since the model with constant μ and changing dry layer thickness performed well except for that the equation for s makes it ten times higher than the realistic value, and μ ten times lower, this model was accepted as realistic. Only the expression for s is considered wrong.

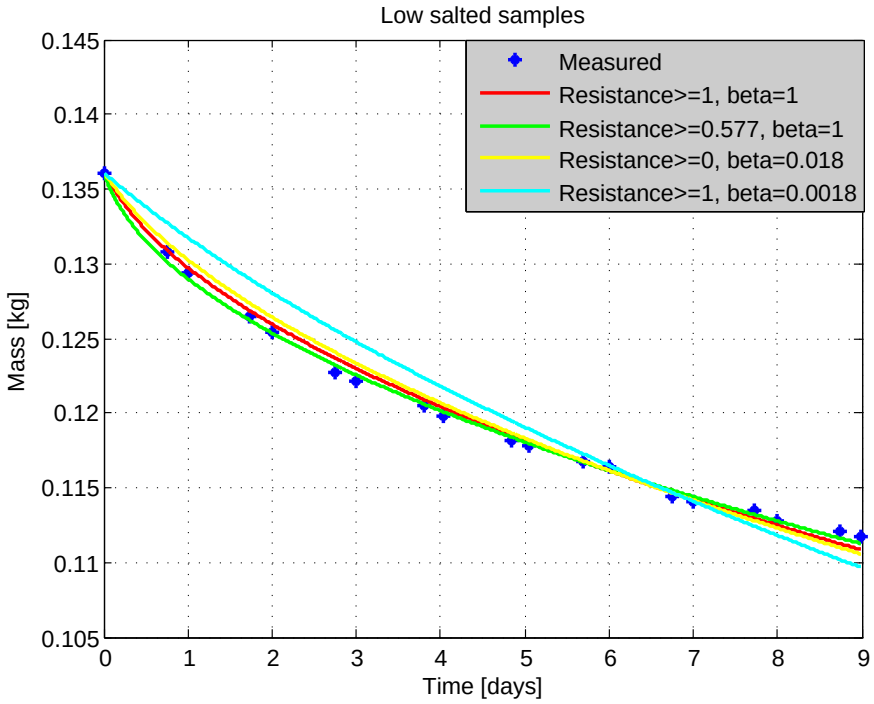

Figure 7.14: Results for the Strømmen model applied to LowSalt68 if $\mu \propto \delta m$ and dry layer thickness $s = 1$ mm, always, was assumed: β was 0.018 or 1 $\frac{m}{s}$. In some cases, μ was forced to be at least 1, whereas in other cases, it was allowed to be as low as zero, giving an optimal start value of 0.000 or 0.577, depending in β.

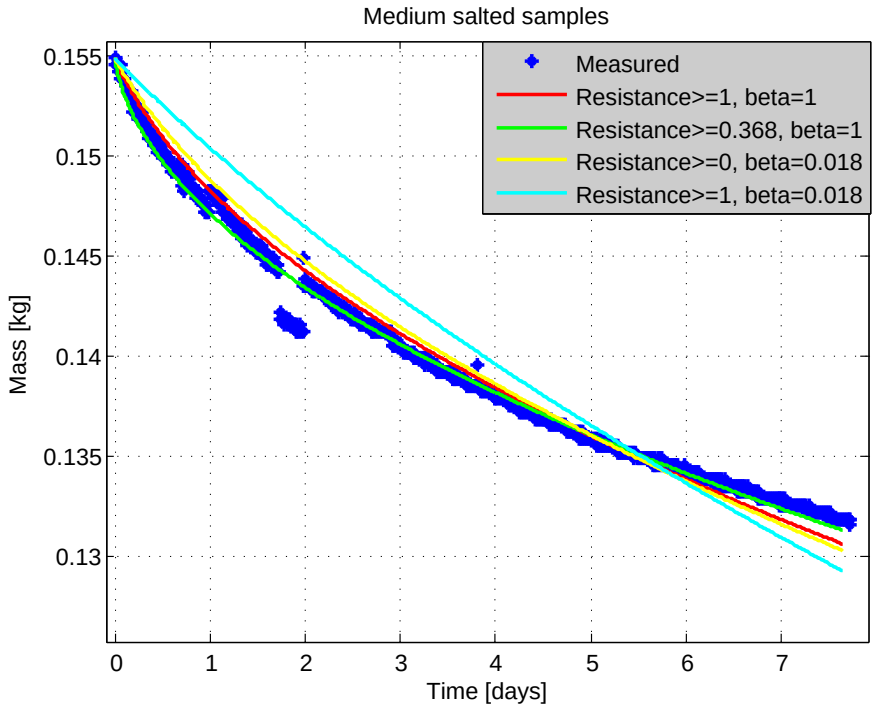

Figure 7.15: Results for the Strømmen model applied to MedSalt68 if $\mu \propto \delta m$ and dry layer thickness $s = 1$ mm, always, was assumed: β was 0.018 or 1 $\frac{m}{s}$. In some cases, μ was forced to be at least 1, whereas in other cases, it was allowed to be as low as zero, giving an optimal start value of 0.000 or 0.368, depending in β.

It is desirable to find another equation for it, preferably one that does not make the drying rate proportional to the square of the surface area. The problem with the excisting one could be that the water content does not only decrease at the surface as the equation assumes. It decreases in the core as well, but much more close to the surface [Gou et al., 2004, fig. 2], making the growth of s more slow. The core is much thicker than the dry layer, so a 90 % reduction of s could be realistic, but it seems much, so maybe this is wrong, and then the entire model must be wrong too (μ simply cannot exceed 1). But again, s is not really a physical size [Strømmen, 1980] as explained in Section 7.4, so the model was accepted.

The last samples were those dried at 4 ^oC and 80 % humidity. A peculiar observation was that the different salted samples dried quite similarily, as if salt content had no effect, which is most easily seen in Figure 7.19. One idea to explanation was that the saturation point of salt in water soultions decreases with temperature, but this relationship was found to be weak, so it is not likely that the decrease from 13 to 4 ^{o}C should matter. Besides, one of the experiments was not salted at all. Results are shown in Table 7.8, where the method with constant μ and dry layer thickness $s \propto \Delta m$ starting from $s = s_0$ was used.

The highest observed mass transfer coefficient by the direct approach was 0.048 for the medium salted samples (except one value at 0.072 halfway through drying but this single value, which was many times higher than all others must be seen as an error). The other samples had around 0.04 and 0.035 as their initial values. Because earlier modelling showed that β should not be set too low, 0.048 $\frac{m}{s}$ was chosen. If the coefficient was set lower, for example 0.018 $\frac{m}{s}$, the best fits required the internal resistance was close to zero, and still, the model could not predict such a high initial mass loss as observed, as seen from the blue line in Figure 7.18 to Figure 7.16.

When β was 0.048 $\frac{m}{s}$, the initial mass loss was good, but quickly became a bit too low (the yellow and black lines in Figure 7.18). This is because the internal resistance increases from the first time step, and therefore the overall mass transfer coefficient quickly decreases, and the value 0.048 in one time step. The problem then becomes that external resistance is limiting the whole drying process. This could suggest that the process should be solely internally controlled. However, removing the external one would give initial resistance of zero, making division problematic. Therefore the value of 1 $\frac{m}{s}$ for β, making it sufficiently high for any initial mass loss, was also tried.

From Figure 7.18 one can conclude that using the highest value of β gave a too steep slope initially, especially the first step show a sudden, vertical fall in mass, and it was a concern whether the numerical method failed at the start, since the applied method requires slow changes. To ensure that the numerics should not cause any error, an explicit expression for the mass was used (derived in Section 6.4.5) to compare. The results showed that the explicit model gives similar shapes and values in all cases. The difference in μ was no more than 0.02, so uncertainty is about $0.02/0.045 \approx 4.5\%$, but there are too few data to give a more precise measure. Both the implicit and the explicit expression give $\mu \in [0.447, 0.477]$ for $\beta = 1$ and $\mu \in [0.327, 0.338]$ for $\beta = 0.048$. The last values are similar to the results for the first unsalted samples (Unsalt). Both also showed deviation at the start and at the end, and both improved in the same manner if a decrease in pressure was allowed. However, the decrease in pressure was modelled to start when

Assumption:	$\mu \propto s^0$		
Sample	μ	s_0 **in mm**	σ^2
`NotSalt80,` $\beta = 1$, `s=0.1`	0.445	0.1	1.9022e-7
`NotSalt80,` $\beta = 1$	0.462	0.0	1.5474e-7
`NotSalt80,` $\beta = 0.048$, `s=0.1`	0.317	0.1	6.6501e-7
`NotSalt80,` $\beta = 0.048$	0.327	0.0	6.1605e-7
`LowSalt80,` $\beta = 1$, `s=0.1`	0.459	0.1	1.6953e-7
`LowSalt80,` $\beta = 1$	0.477	0.0	1.5746e-7
`LowSalt80,` $\beta = 0.048$, `s=0.1`	0.328	0.1	4.9600e-7
`LowSalt80,` $\beta = 0.048$	0.338	0.0	4.5675e-7
`MedSalt80,` $\beta = 1$	0.4470	0.1	6.5827e-8
`MedSalt80,` $\beta = 0.048$	0.328	0.0	2.1681e-7
`MedSalt80,` $\beta = 0.018$	0.112	0.0	1.3837e-6

Table 7.8: Optimal parameters and resulting errors for the Strømmen model applied to samples dried at 4 ^oC and relative humidity $\phi = 80\%$, dependng on different assumptions for mass transfer coefficient β (in $\frac{m}{s}$): s_0 is the initial thickness of the dry layer s, μ is the decrease in diffusion due to the ham and constant and σ^2 is the deviation between model and measurement.

Assumption:	$\mu \propto s^0$		
Sample	μ	s_0 **in mm**	σ^2
`Salt`$\beta = 0.048$	2.018	4.1	1.3163e-8
`Unsalt,` $\beta = 0.048$	0.299	2.3	2.9641e-8
`NotSalt68,` $\beta = 0.048$	0.454	0.0	8.0776e-7
`LowSalt68,` $\beta = 0.048$	0.830	0.0	1.3361e-7
`MedSalt68,` $\beta = 0.048$	0.758	0.0	3.1606e-7

Table 7.9: Optimal parameters and resulting errors for the Strømmen model applied to samples at 13 ^oC and 68 % relative humidity, with mass transfer coefficient $\beta = 0.048\frac{m}{s}$: s_0 is the initial thickness of the dry layer s, μ is the decrease in diffusion due to the ham and constant and σ^2 is the deviation between model and measurement

the water content was 2.65 for emphall the samples, and for all samples, the equilibrium water content must be 2 in order to make the curves flat at the end. The same parameters fitted all three samples well, $\mu \approx 0.3$, as if salt content is unimportant for the drying. Also, the equilibrium moisture content of unsalted meat at 4 ^oC is approximately 0.25-0.3 [Gou et al., 2004](measured at 5 ^oC), so the value necessary to obtain good fits is highly wrong. A more realistic value shows no improvement as the experimental curves seem to flatten towards the end, corresponding to much higher moisture contents (around 1.3, 1.9 and 2.4). The results obtained by this pressure decrease (where X_e was set to 2) must therefore be rejected as unrealistic. The curves with $\beta = 1$ generally are better, as the high value only affects the start, but allows the rest of the drying curve to fit better. Adjusting s_0 could make the initial fit extremely well for all samples, but the rest of the curve deviated much. The results that were assumed to be most realistic are shown in Figure 7.19, and show fits that are not very good, but neither very bad. They could be used in a simulation model unless high accuracy was required. Parameters and errors are given in Table 7.8.

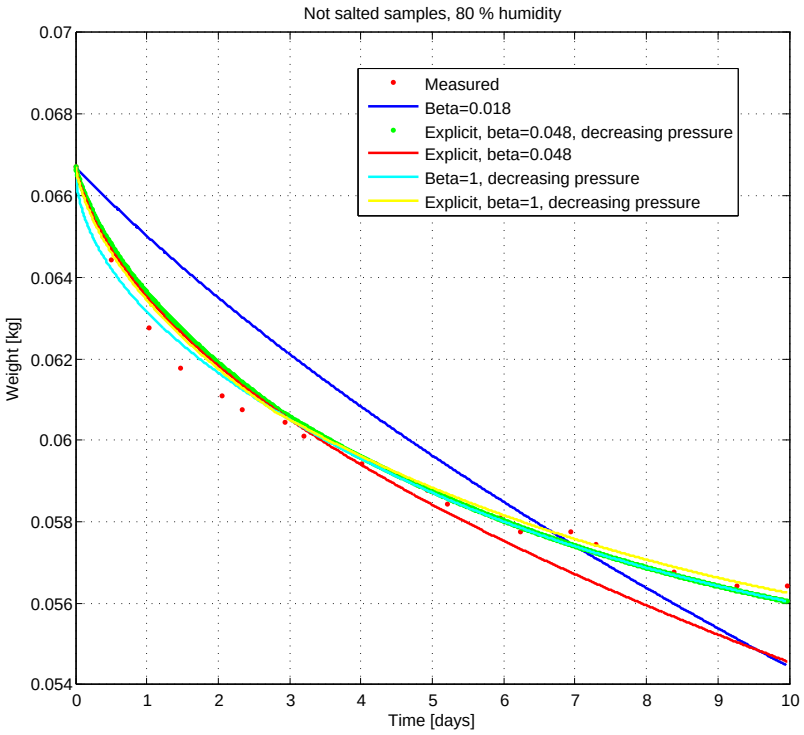

Figure 7.16: Drying curves with different assumptions for the Strømmen model applied to NotSalt80: Modelling was performed with mass transfer coefficient $\beta \in [0.018,\ 0.048,\ 1]\ \frac{m}{s}$, with a numerical or explicit expression for the mass as a function of time and with or without decrease in vapour pressure in the ham when moisture content was 2.65. Equilibrium moisture content was then modelled as 2, which gives good fit but is likely to be unrealistic.

If the model is not simply curve-fitting, then there should be a correlation between the values of μ. A question was then whether the values for the first five samples, dried at 13 ^oC and 68 % humidity, could be compared to the values obtained at lower temperature and higher moisture content, when they had been modelled with different mass transfer coefficients. Therefore, the first samples were modelled again, with $\beta = 0.048$ and the results are shown in table Table 7.9.

The resulting curves were highly similar to those shown in other plots, and are therefore not included. A slight difference was that the initial slope was steeper, so the initial fit was worse (like always with high values of the mass transfer coefficient). This is similar to the observed trend in [Bantle et al., 2014], where the model overpredicted the initial drying rate. This can be easily avoided by giving s_0 a value, but then the curve does not fit at the end and looks like the red line, 'Explicit' in Figure 7.16. For this sample $\beta = 1$ gave a perfect initial fit if s_0 was 0.5 mm, and internal resistance was 0.29. However, with $\beta = 0.048$ the value is zero for a perfect initial fit. Also, when comparing the μs for $\beta = 0.048$, all samples showed $s_0 = 0.0\,mm$, which simplifies a comparison as this factor must not be accounted for. A plot of parameters with $\beta = 0.048$ at the different conditions for the different salt contents is shown in Figure 7.20.

The results for the first salted sample, Salt, is not included as its salt content was unknown until the last days of the work, and both salt and fat content for this experiment was much higher than for any other case. This can explain its unique behaviour, but also makes comparison

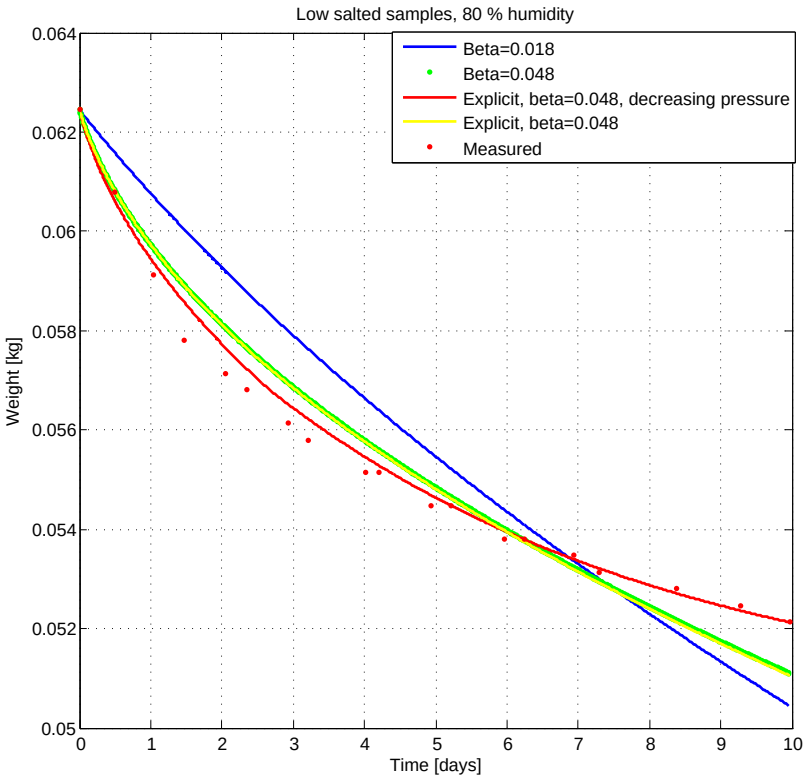

Figure 7.17: Drying curves with different assumptions for the Strømmen model applied to LowSalt80: Modelling was performed with mass transfer coefficient $\beta \in [0.018,\ 0.048,\ 1]\ \frac{m}{s}$, with a numerical or explicit expression for the mass as a function of time and with or without decrease in vapour pressure in the ham when moisture content was 2.65. Equilibrium moisture content was then modelled as 2, which gives good fit but is likely to be unrealistic.

difficult. The fat content includes the lard weight, and was so high compared to that of Unsalt, that the lard is likely to contribute with a large proprtion of it, which also makes inclusion of these results difficult. However, the result for this experiment is very valuable because, all though it does not contribute to understand the relation between the other results better, it is a result for a unique case, the only result for such a high salt content. If one would wish to model hams with higher salt contents, ths could be used. The low salted samples showed higher values than the medium and not salted samples at both temperatures, but the results were very similar to those of the medium salted ones. The difference is of the same order as the uncertainty in the parameters, and therefore not significant; they might be equal. This fits well with [Gou et al., 2002] who found that if enough salt is added, then the effect of salting reaches a constant value. They also reported another work that found the same. According to professor Eikevik, this is probably because the hams become saturated with salt, and any salt added after saturation forms salt crystals and do not bind water, thus the extra salt does not affect the water or vapour flow. However, no value for this salt content has been found, and the experiment with highest salt content, Salt, had even higher values for μ. This could indicate that the other salted samples could not be at the saturation point, but also, since Salt had a very high fat content, such a conclusion cannot be drawn. The results for the two first experiments at 13 ^oC and 68 % relative humidity, and the three others at the same conditions showed different trends in both

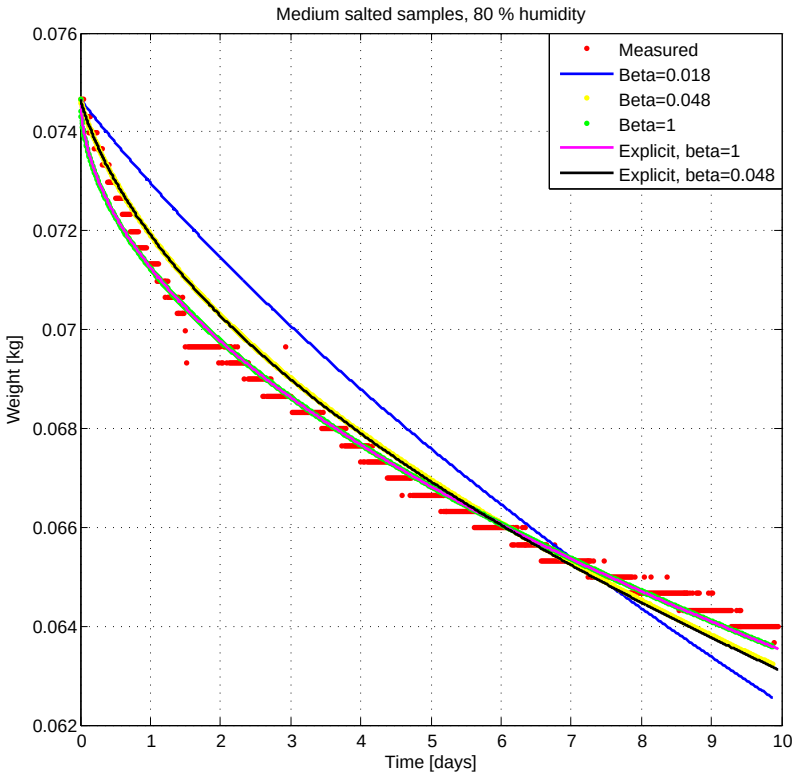

Figure 7.18: Drying curves with different assumptions for the Strømmen model applied to MedSalt80: Modelling was performed with mass transfer coefficient $\beta \in [0.018,\ 0.048,\ 1]\ \frac{m}{s}$, with a numerical or explicit expression for the mass as a function of time but without decrease in vapour pressure.

shape and parameters. Especially the first salted samples deviate much from the rest. It is not certain why. One possibility was that the pre-treatment of the samples had had an influence, since these experiments were arranged by two different persons, but this turned out not to be the case: They had treated the hams similarily.

Clearly, the salt content alone cannot explain the difference between the two conditions. It was discovered that the fat content in the samples differed, and diffusion has been reported to decrease with lipid content [Ruiz-Cabrera et al., 2004]. However, in this work, diffusion increases ($\Leftrightarrow$ μ decreases) with higher fat content as seen in Figure 7.21. The curves shown are just speculations to how a curve could be, and no calculations were used to make them. How the fat is distributed in the hams would of course be important. One question was then if the temperature or humidity could have an effect. The diffusion coefficient already depended on temperature, but a local ham producer reported that the surfaces of hams are much less dry when higher relative humidity is flowing in the drying chambers. Therefore, this would tend to reduce the diffusion resistance in the dry layer, leading to a lower μ. A possible model for μ might be something like the one shown in Figure 7.22, where μ depends on relative humidity. [Bantle et al., 2014] found that D_{eff} depended on ϕ. (The fat percent of Unsalt includes the weight of lard, and is therefore likely to be somewhat too high.)

It must be asked: if adjusting mass transfer coefficient, initial dry layer thickness, when pressure decrease starts and internal resistance freely like this, is this model realistic or simply

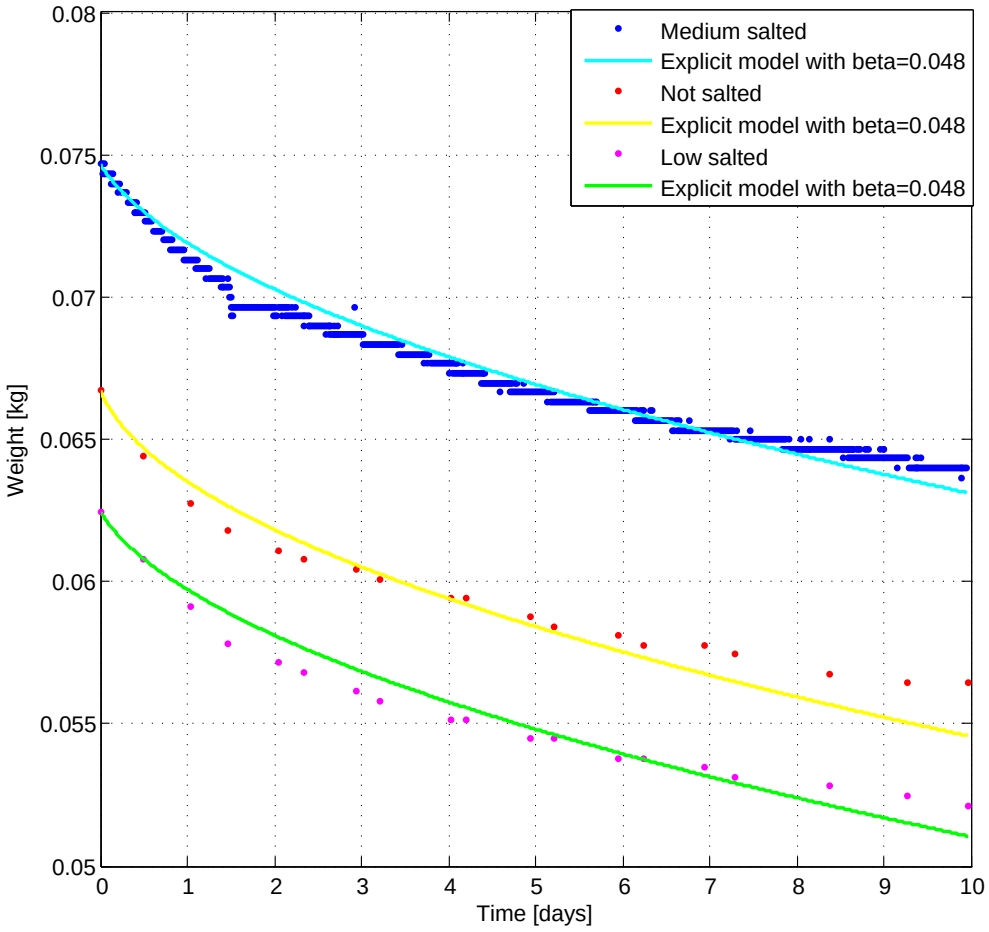

Figure 7.19: Drying curves with the assumptions that seemed to be most physiologically correct for the Strømmen model, applied to all samples dried at 4 ^oC and 80 % relative humidity: Modelling was performed with mass transfer coefficient $\beta = 0.048\ \frac{m}{s}$), with the explicit expression which is free of any numerical error. No decrease in vapour pressure in the hams was used. The results are relatively good, except for the end of the curve for NotSalt80. It is interesting that the measured drying curves are so similar. It looks as if they dry at an approximately equal rate, meaning that salt content was unimportant.

curve fitting? It might be, but there are too few measurements to say anything decisive. It is uncertainity in which values the physical parameters should have that causes all the guessing and speculation, as neither the dry layer thickness, nor the mass transfer coefficient were measured directly. Uncertainty in the physical parameters causes errors in the model parameters, but consequent choices might make the model applicable still, as it will make the errors in model parameters consequent too, and a model that performes well with this error (for example a wrong factor of ten for s and μ) will always perform well with the same error.

Since the Strømmen model did not manage to model the experiments at 4 ^oC and 80 % humidity as well as the first experiments at 13 ^oC and 68 %, and the rejection of the often well-performing Fickean diffusion model was based on only modelling two experiments, the Fickean model was applied to LowSalt80, to see if it could perform better for these last samples. Since sine-shaped profile appeared to give better fits, therefore this condition was used.

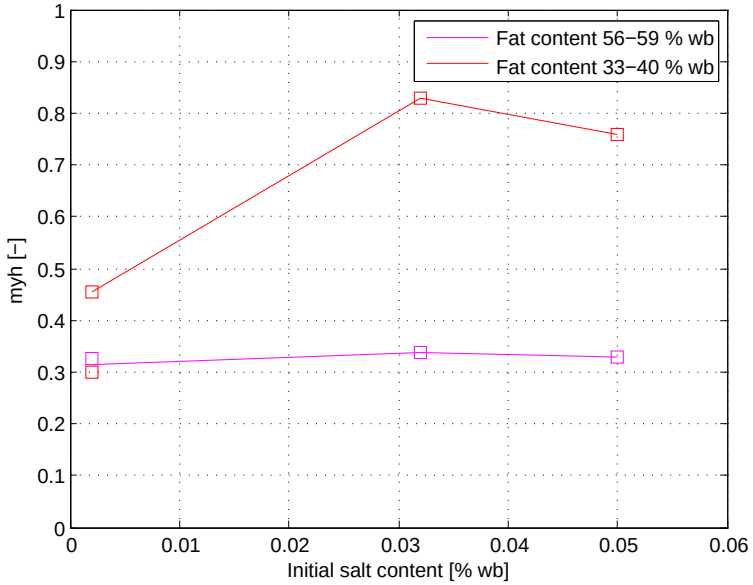

Figure 7.20: Attempt to plot the resistance to vapour diffusion in hams compared to air (μ)as a function of salt content on wet basis: The squares are measured values, the red ones represent samples at 13 ^oC and 68 % relative humidity, the three pink squares those at 4 ^oC and 80 % relative humidity. The three upper values had high fat contents and the four lower values had low fat content, given on wet basis calculated from the initial weights. The lines are only guesses for where other samples with other salt contents could have their values for μ. It is unusual that the samples with highest fat content showed smallest decrease in diffusion coefficients.

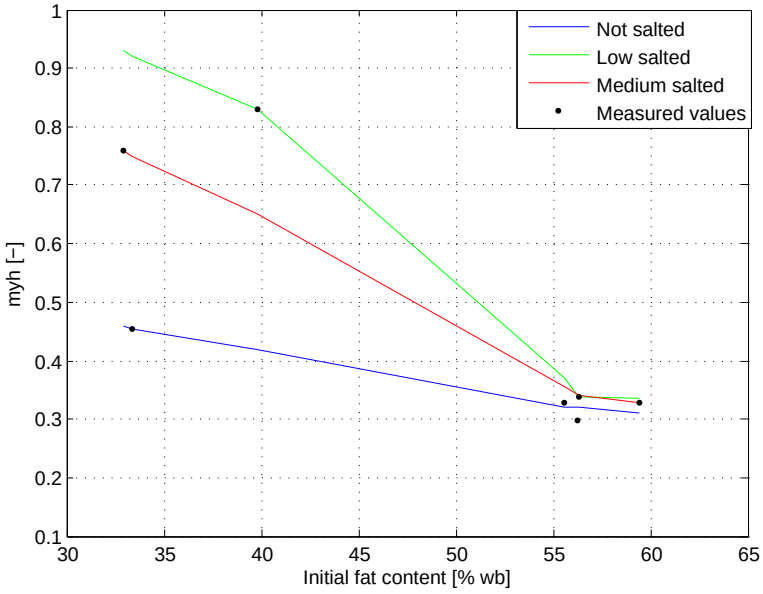

Figure 7.21: Attempt to plot the resistance to vapour diffusion in hams compared to air (μ)as a function of fat content on wet basis, calculated from the initial weights: The dots are measured values, the three values at low fat content were dried at 13 ^oC and 68 % relative humidity, the three highest values at higher fat content at 4 ^oC and 80 % relative humidity. The lowest value at high fat content was also dried at 13 ^oC and 68 % relative humidity. The lines are only guesses for where other samples with otherfat contents could have their values for μ. It is unusual that the samples with highest fat content showed smallest decrease in diffusion coefficients. No realistic pattern was found.

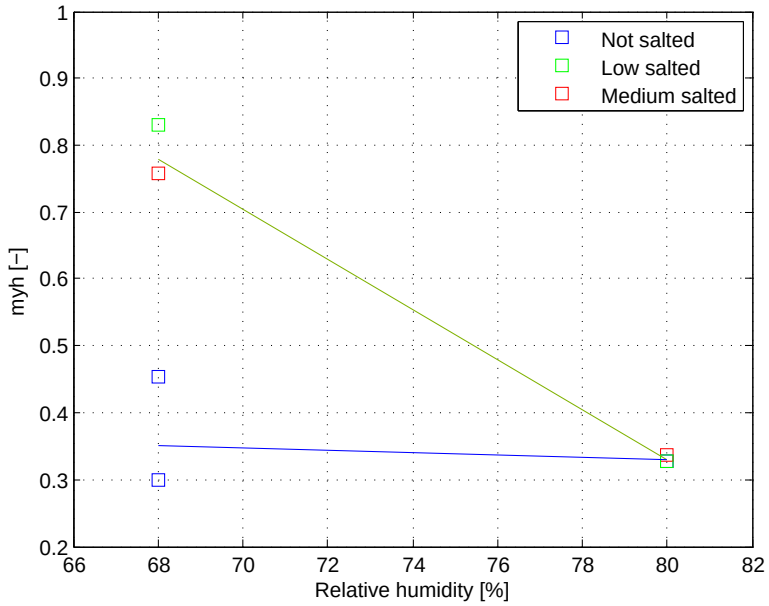

Figure 7.22: Attempt to plot the resistance to vapour diffusion in hams compared to air (μ)as a function of relative humidity as this can keep the dry layer less dry, thereby decreasing μ: The squares are measured values at different salt contents. The two blue point should theoretically be the same, and might show something about the uncertainty in the parameters. The difference is so large that the other experiments that had similar values for μ can be assumed to have identical ones. The lines are only guesses for where other samples dried at other relative humidities contents could have their values for μ. This plot emphcould be correct, but there are way too few values to decide.

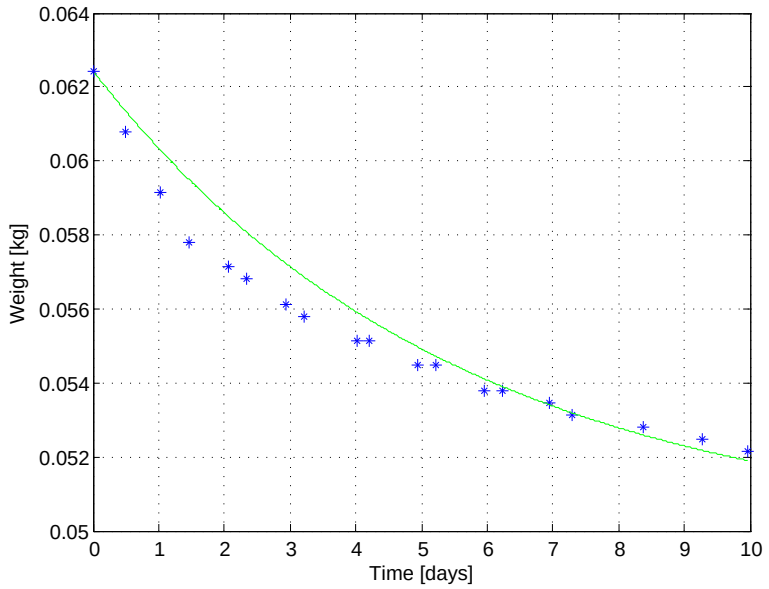

Figure 7.23: Best obtained curve when applying the Fickean diffusion model to the experminent LowSalt80, optimization involved adjusting diffusion coefficient and equilibrium moisture content, the latter was set to 2.2

In Figure 7.23 it is clear that the Fickean model did not perform any better than the Strømmen model did. Since equilibrium moisture content was so important for this model, values from 0.55 to 2.4 were tried, and only the best obtained curve is shown. Low values yielded

straight lines. The model only fitted relatively well for $X_e \in [2, 2.4]$ which is unrealistically high. This high equilibrium water content would correspond to allowing pressure decrease for the Strømmen model (since the modified Strømmen model allows pressure decrease when water content approaches the equilibrium value). This result for the diffusion model should then be compared to the curves with decreasing pressure in Figure 7.17, which gave much better reults. Hence, in this study, the Strømmen model truly seems to be best performing of the two.

7.6 MODEL IN DYMOLA

The Strømmen model was programmed in Dymola, and the code is given in Section A.2. Parameters for Unsalt with $\beta = 0.018\ \frac{m}{s}$ was introduced in it. Running the model, it performed very similar to the experimental curve, see Figure 7.24. The model can scale up the number of hams that are dried, and also allows to have any number of hams after one another, so that the wetter, colder drying air from one ham proceeds to the next ham, as in a real drying chamber or tunnel.

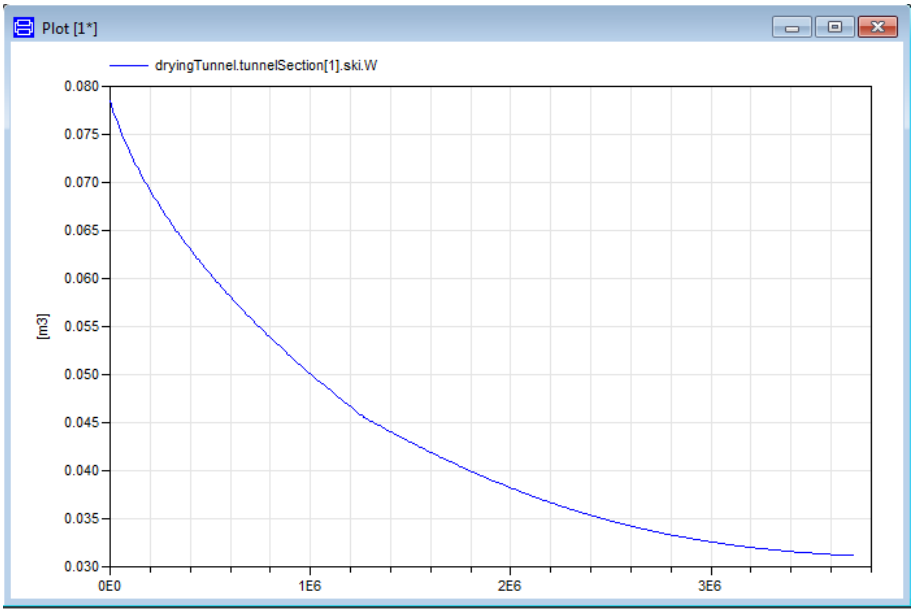

Figure 7.24: Simulated drying curve for Unsalt in DYMOLA, using $\beta = 0.018 \frac{m}{s}$ and $\mu = 0.281$: It is unclear why DYMOLA reports the unit of mass in m^3, but it this error is consequent, also for built in components that measure mass, and is probably not related to this specific model.

Due to the difficulties with the value of β and the initial heat transfer coefficient, no dependency on air speed was included: β was simply given a value. This cannot be improved without further knowlegde about why the drying rate was so high. Because of this limitation, the model assumes heat supply is always sufficient, but a warning appears if the temperature drops below the dew point, as this should not be possible, and also if the amount of removed water is negative.

Another limitation was that the wet bulb temperature and diffusion coefficient of vapour in air, $D_{w,a}$, must be typed in manually. The program did not allow the high accuracy in the expression for $D_{w,a}$. The resistance μ, initial weight and length and many other parameters must also be adjusted manually, but the performance of the model is good when this is done. However, it cannot handle variyng temperature without improvement of the expressions for wet bulb temperature and diffusion coefficient.

7.7 Heat transfer

The highest measured mass flux occurred at the start of drying. For the first unsalted sample (Unsalt) the initial mass loss was about $6.2 \cdot 10^{-8} \frac{kg}{s}$ before the measurement problems. This number is an average of central differences based on measurement points 72 to 151 (very many data points were needed to get reasonable, representative values for the derivative). The mass loss before this was zero and these data were therefore not used in calculations, no mass loss occurred). Using only data from row 72 and 151 (not the ones in between) gave $6.3 \cdot 10^{-8} \frac{kg}{s}$. After the problem the initial mass loss was about $4.5 \cdot 10^{-8} \frac{kg}{s}$ depending on how many of the first data one includes, but always less than the above. For the first salted samples the mass loss was nearly constant and regardless of how many data used. The 18 first measurements gave a slightly higher value than using all measurements though, equal to $\dot{m} \approx 1.9 \cdot 10^{-8} \frac{kg}{s}$. Due to that the measurements involves some increases in mass no and then (normally one gramme), it seemed inappropriate to use fewer values than this. Due to the difficulties in obtaining good

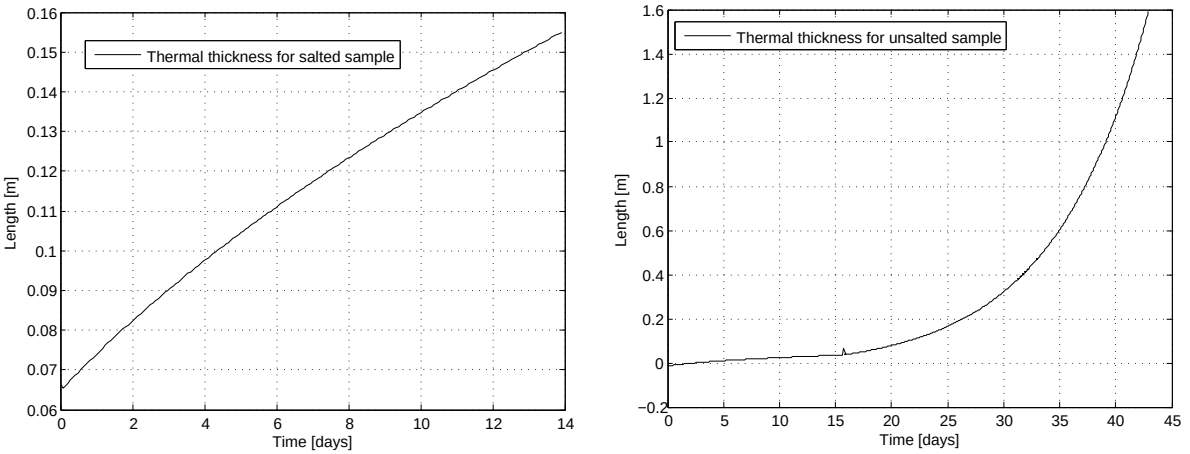

(a) Salted ham **(b)** Unsalted ham

Figure 7.25: The thermal thickness necessary for balanced heat supply and heat for evaporation for the first salted and unsalted samples, calculated from Equation 6.26

derivatives from the measurements (β_{tot} in Figure 7.10 and Figure 7.11 is proportional to the measured derivatives where 39 of 40 data points were discarded, and still alternate very much), the modelled curves were used in the heat calculations. This is strictly wrong to do, but the

modelled curves were highly similar to the measured ones and the same was true for the initial derivatives, so the error in doing so was regarded to be small.

In this work the thermal thickness is defined as the distance heat is conducted if heat supply exactly balances the evaporation rate, or the maximum length heat could be conducted to have sufficient heat transport. For the salted sample, this should be quite high to transport the required amount of heat, thus, it can be assumed that heat supply was always sufficient, and the ham was nearly isothermal at the temperature of the air, only where evaporation took place the temperature would be lower. For the unsalted sample however, the necessary heat supply was not sufficient, as it required a negative resistance to heat flow (s_T becomes negative in Figure 7.25b). This could be explained by an initial cooling period, but as the value was negative for many hours, this cannot be the reason.

If the flow in the drying chamber was not laminar as assumed in the calculation of the surface heat transfer coefficient h, but transient to turbulent, then h should be higher. This is very possible due to swirls and obstacles in the chamber (ten samples were dried together, this might have caused turbulence for the samples further away from the ventilation system, due to disturbances from the ones in front of them). In addition, the measurements were not highly accurate, as mass sometimes increased. However, the derivative was taken as an average over a longer period and Figure 7.25b was based n the steadily decreasing modelled derivative,

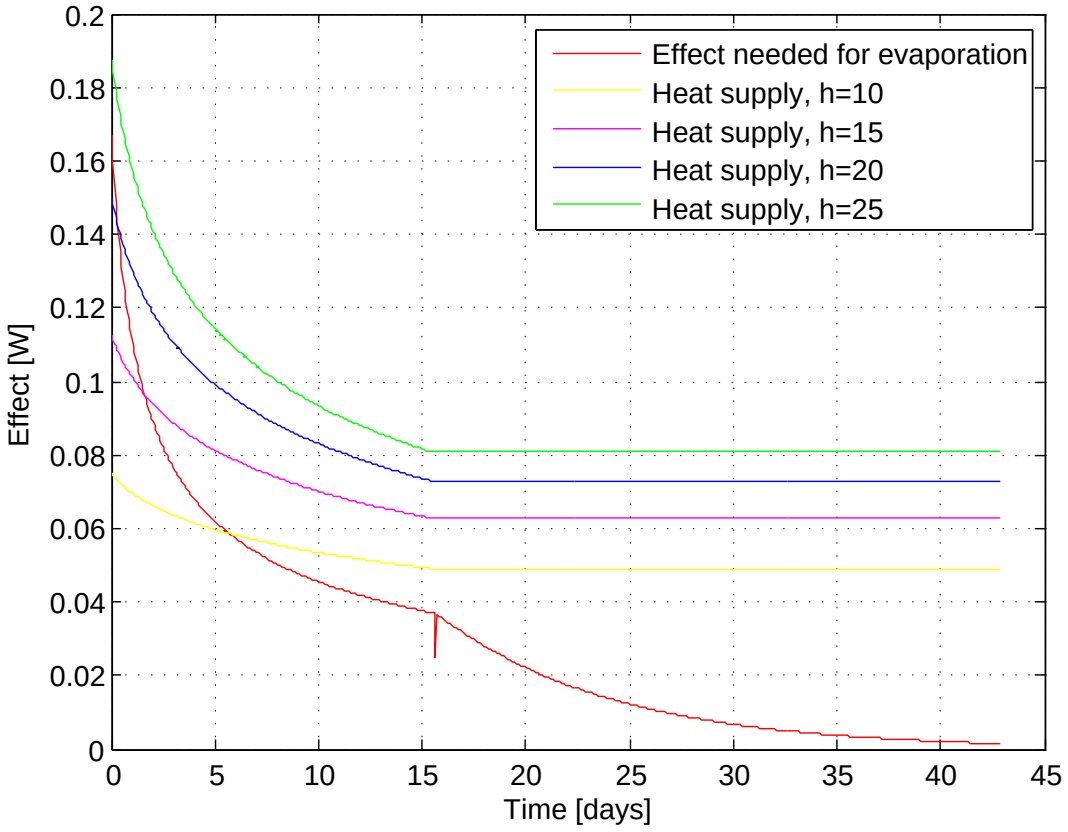

Figure 7.26: Necessary heat for evaporation (red line) and supplied heat from the surrounding air for different values of the heat transfer coefficient h: Heat supply is sufficient during most of the process, but not in the beginning unless $h \approx 22 \frac{W}{m^2 K}$, which is very high.

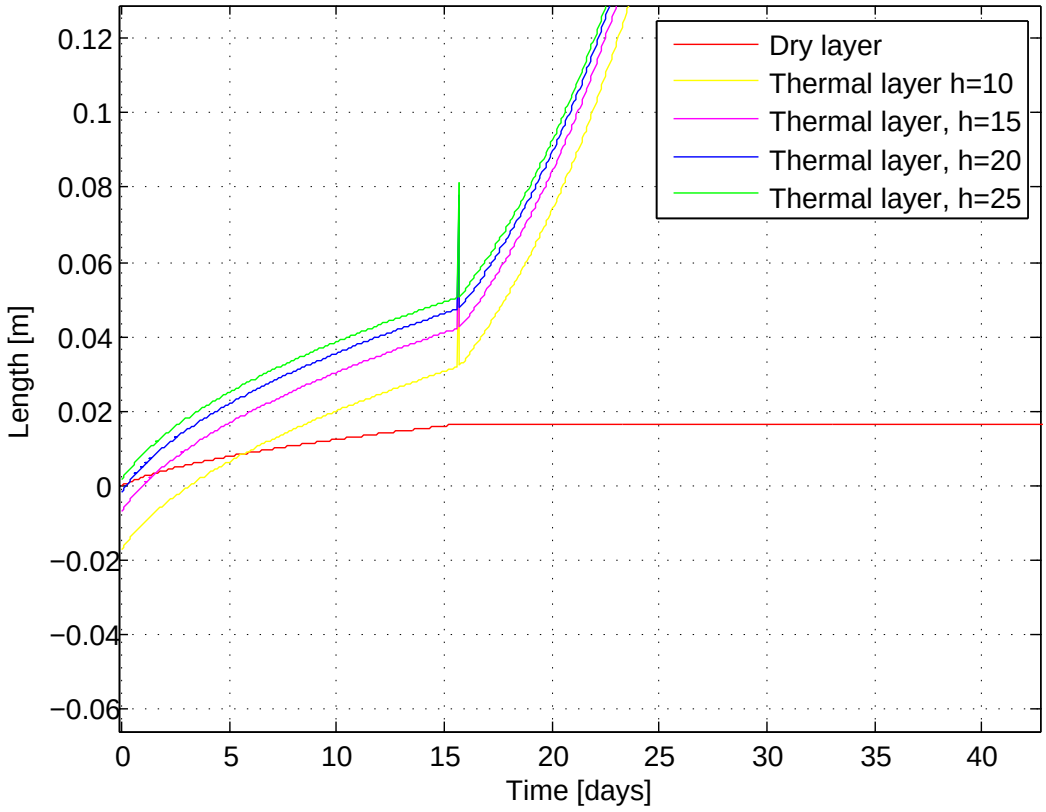

Figure 7.27: Dry layer thickness after (6.15) (red line) and thermal thickness as a function of different values of the heat transfer coefficient h. Thermal thickness is here the length heat must be conducted in the ham during drying if heat supply exactly balances the required amount for evaporation, it should therefore be equal to the dry layer thickness. If heat supply is sufficient,the sizes are equal or the thermal one larger. The thermal thickness reached values of a few metres.

thus there is no reason to believe that the heat required differs much because of this. Increases in mass were never high, normally 1 gramme. The highest error in required effect can be no more than absolutely maximum 2 grammes per final mass. This was 190.48 grammes, giving a maximum deviation of 1.05 %.

Variation of surface heat transfer coefficient for the unsalted sample is shown in Figure 7.27 and the required and supplied effect based on the modelled dry layer (which probably has too high values so that the heat supply should be even larger) are shown in Figure 7.26. All calculations assumed constant thermal activity, all though it should decrease towards the end of the process, but in an unknown manner. Towards the end of the process, the maximum possible heat supply exceeds the needed heat, thus, the case is the same as for the salted sample. The final values were as high as 1.55, but would have been lower if the conductivity had decreased as it should.

It was also clear that the value of h only affects the thermal thickness at the beginning. At the start, only the case where $h = 25\ \frac{W}{m^2K}$ gives sufficient heat at the start, and a value around 22-23 $\frac{W}{m^2K}$ seems to balance the need and supply. This is twice of the laminar value. Correlations for turbulent coefficients gives lower values, since they are based on that the coefficient depends on the Reynolds number to a higher power than the laminar value, and that the Reynolds

number is very high. The Reynolds number here is quite low, and therefore a higher turbulent value could not be found from correlations. Changing the required heat with a 1 or even 2 % did not make any significant change.

There are possible explanations: the accuracy seem to be not too bad except for small oscillations giving errors of only about 1 %, and this does not have any detectable effect on the calculations. The uncertainty of parameters like h and k is more severe. The heat transfer coefficient only matters initially, but is very high in this period. This might be due to turbulence (which could also explain why the observed mass transfer coefficient exceeded all predictions) that causes it to be twice as large (corresponding to a four times higher velocity in laminar flow). Another possibility is that the hams were cooled and therefore heat was conducted from more than one side (as it was assumed here). A six times larger area could be sufficient to double the heat transfer.

A third option is that measurements are not so accurate; especially this sample had some initial problems. Since the mass loss must be halved to balance the need and supply, the error might be as high as 50 % at the start for this experiment. However, the measured curve was steadily decreasing and could not have reached its final values without this high initial evaporation rate. It therefore seems more likely that the measurement error is small and the heat transfer coefficient wrong for some reason, but there is much uncertainty in this. Still, during most of the process, the heat supply was clearly sufficient and the hams could be modelled as isothermal at the surrounding temperature, with a lower temperature only where evaporation takes place.

Chapter 8

Conclusions

Three models were applied and compared, and one was chosen as best performaing and suitable for energy saving simulations, all though too few data were available to say anything decisive about its parameters and realism. This model was implemented in DYMOLA and shows similar behavior as the real process, but has limitations that could be improved.

From the literature review, the important factors for drying were considered to be temperature, salt content and relative humidity of the air. The results however, showed similar results for different salt contents. This could perhaps be partially explained by the saturation of salt, and perhaps not at all. Generally, the results have been somewhat surprising. The curves have behaved quite differently in terms of both shape and initial drying rate.

All models assumed heat transfer was always sufficient. This assumption was investigated for two of the experiments and found to be true during most of the process, but the initial heat supply was too low for a few hours for one of them. No explanation was found, but one possibility was that the flow pattern in the drying chamber was turbulent or transient to turbulent, thereby enhancing the heat transfer coefficient. Salt was found to have negligible effect on the required amount of heat.

The knowledge of true sorption isotherms (and thereby equilibrium moisture content) was highly important for all models. Errors here gave bad results. The model fit was worse for the samples which had drying curves that seemed to flatten out towards the end of drying, but where the moisture content seemed to approach an other equilibrium content than the assumed one. This was especially problem for the experiments dried at 4 ^{o}C and 80 % relative humidity. It would have been very valuable if samples at these conditions could be dried to equilibrium to find out which values the equilibrium contents have, as this is crucial information to apply all the three models.

The three models all performed relatively well in modelling the two initial drying curves (Salt and Unsalt). The smallest errors were obtained by the Weibull model, and the normalized version of this was slightly better than the other methods, however, the assumptions in the model turned out not to be valid for ham drying: The geometric factor differed two orders of magnitude in cases where it should be the same. The model parameter α was supposed to be a fraction of the drying time, but exceeded the drying time manifold.

The model does not involve any dependence on physical properties, and is therefore merely as a curve-fitting technique. It will be very hard to apply to varying conditions, which is likely to be desirable in simulations of ham drying. Therefore, this model was rejected, despite its superior fit. It could however be used as a measure of deviation of the measurements, as it can fit any curve extremely well, and give a measure of how low error could be achieved and how

much measurements deviate about a steadily decreasing line.

The Fickean model performed quite well, and a tiny bit better if a sine-shaped initial profile was assumed. It is highly important to know the true equilibrium moisture content in this model in order for it to perform well. It has the advantages that it gives the moisture profile as a function of both position and time, as the only one of the three models. It has the drawback that neither velocity nor relative humidity is included in the model equation, and the latter is a highly sensitive parameter [Bantle et al., 2014]. Neither does it depend on the size of the surface area available for evaporation. The obtained model parameters differ much between studies, with several orders of magnitude, making its application difficult.

Because of this, and because its performance was slightly worse than that of the Strømmen model (especially the salted case showed differences between modelled and measued curves), this model was also rejected. It could perhaps have performed better if the diffusion coefficient was allowed to depend on the varying moisture content, but the salted samples to which it was compared had a very small water loss, and the model have worked well for cases with much higher water loss, so this was not likely.

Still, the rejection of the Fickean model was based on the results from only two initial experiments. This was done partly because these results were so different they could give a good idea about how suitable the models were and partly because the last data were supplied so late that it was impossible to compare all models to all experiments. But if this had been done, it might have altered which model performed best. Therefore, an additional comparison between the Fickean model and a late supplied experiment was performed, but still, it performed worse than the Strømmen model.

The Strømmen model was seen as the best performing model, and it seems that it can predict most drying curves relatively well. It has the advantages that it depends on physical properties in a realistic way, and therefore varies with varying drying conditions.

The unmodified Strømmen model could not predict drying well if the samples were dried to equilibrium, as the drying rate never decreased to zero. An adjustment involving pressure decrease when water content reached a certain value was necessary, but with this realistic assumption, the model performed very well. It also turned out that the manner of decrease was not important, since both a sorption isotherm-based and a linear model for vapour pressure gave equal results. The surface area on the contrary, was a highly sensitive parameter, as the model depended on this to the second power. This seems unrealistic, and might be a reason for several of the problems related to the model.

The dry layer in the Strømmen model became 1-2 cm, which is ten times higher than measured values, and correspondingly the decrease in diffusion coefficient, μ, became about ten times lower than realistic values. One could argue that the dry layer thickness is not a real size, but an equivalent to the thickness of a theoretical absolutely dry layer, giving the same resistance as the drier part of the ham does in reality. It is the *rate* of growth that matters.

Another explanation is that the equation for the dry layer assumes all water is removed from the surface, but the water content decreases in the entire ham in studies where this was measured, yet, only the surface becomes extra dry, and only here can water gradients be seen

[Gou et al., 2004, Ruiz-Cabrera et al., 2004]. This means that the layer close to the surface is the only part making up an inner resistance, but only a portion of the removed water has created it, thus the dry layer should grow more slowly than in Equation 6.15. This argumentation might be right, and it might be that the entire model is wrong. Thus the dry layers should be measured, to check if one can defend the use of this model, as it is unrealistic unless $\mu \geq 1$.

Another problem was that the dry layer in the model starts to grow from the beginning, whereas it really could take some time before the whole surface is dry. It could therefore be an idea to allow a first drying period at constant rate and then let the dry layer s start to grow after a certain time. Whether or not there was an initial constant drying rate was not certain, as good derivatives were hard to obtain, but the initial slopes look quite straight, so this is a possibility.

Assuming the existence of an initial dry layer s_0 due to osmotic dehydration or drying in the resting period before the experiment can make the initial slope of the modelled curve to fit measurements well, and might be realistic, but again, this could be curve fitting rather than reality. Whether or not s_0 had a value depended on the value of the mass transfer coefficient β, which was highly uncertain. Thus, no conclusions could be made about this parameter.

Many different versions of the model were investigated to find a solution to the possibly wrong expression for dry layer thickness. Using an expression based on the heat equation made the model unstable, and other variations of the model did not appear to be more realistic either. It was assumed that the model is valid, but the expression for dry layer thickness wrong and the model was used despite the high values of s and low values of μ.

A change in the mass transfer coefficient could change the internal resistance μ (and initial dry layer thickness) considerably. The samples at the lowest temperature had μ-values around 0.45 for a high β, and around 0.33 for a low. A mass transfer coefficient of 1 $\frac{m}{s}$ is probably way too high, so the values are probably well below 0.45. They are more likely to be in the range 0.27-0.38. From this range of uncertainty, the values for the last three samples, dried at 4 ^{o}C, do not have significant differences, and should be considered to be the same.

The samples dried at 13 ^{o}C and 68 % relative humidity showed more difference in values for μ, but the two salted experiments had values of about twice as high as the unsalted one. The experiment NotSalt68 had a value of 0.377 to 0.454 depending on whether the mass transfer coefficient β was 0.018 or 0.048 $\frac{m}{s}$, but the fit was worse for the high value. The values of μ varied from 0.587 to 0.830 for LowSalt68 and 0.503 to 0.750 for MedSalt68 depending on β. The similarities might be due to salt saturation.

Clearly, a higher internal resistance in terms of μ was found from assuming a smaller external one (higher β). High vaules of the internal resistance then tends to force the initial dry layer thickness to be zero. This gives initial errors but fits the rest of the curve, and is why no conclusions can be made about this size.

The experiment Unsalt gave $\mu = 0.281$-0.299, not too different from NotSalted68, which is reasonable. The experiment Salt deviates much form all the other results both in terms of μ, salt and fat content, and therefore adds unique, valuable information, but also does not contribute to find the realtionship between the physical factors and model parameters.

There were too few measurements to say anything decisive about how different factors affect μ. Very many experiments showed an optimal value around 0.3, eventually higher if salt was added, but too many factors differed between the experiments: fat content, temperature, humidity and sizes were all different between the sets of samples. The most promising idea for a model for this parameter was that it might be influenced by the relative humidity of the air, but no correlation for μ as a function of the process parameters was found. All graphs shown in this paper only have merely speculative lines plotted in them. More results should complement this work to fill in more values in Figure 7.22, and consistency in size and fat content would be desirable. The fat content and distribution of it is highly important [Ruiz-Cabrera et al., 2004], but not included in the model. If there is no good relationship between μ and physical conditions, then the entire model is simply curve fitting.

Knowledge of the mass transport coefficient was and is a challenge. Even though this parameter has no effect during most of the drying, provided it is large enough, it is highly important for the initial slope, and thus the outset of the entire model curve. Its apparant value can be affected by:

- higher velocity than measured or turbulence which would make the coefficient many times higher.
- pre-treatment - How wet were the surfaces initially, really? Has initial resting allowed dehydration before measurement?
- capillary forces - Drying was only conducted along the fibres, which could create many capillaries between them.
- osmotic dehydration - The highest initial drying rates were observed for the salted samples, and this was only in the beginning. However, the lowest value was also observed for a salted experiment, Salt. This one also had a very high fat content, which might have slowed down the process.

There might be other mechanisms not mentioned here, but no others have been found in the literature, so it is not known what they could be. Pre-treatment did not differ between samples, so this factor cannot explain any differences between experiments that should give equal results (same salt content and conditions).

It would be interesting to measure the velocity and flow pattern inside the chamber to see if it is turbulent. However, all correlations for turbulent heat and mass transfer coefficients are based on that the Reynolds number is above the critical to make these values higher. This was not the case in these experiments, and therefore these correlations did not enhance the coefficients, and if they have other values than the theoretical, these must be found in another way.

No osmotic or capillary dehydration mechanism was included in the model. These effects seemed possible to be incorporated in the model simply by increasing the mass transfer coefficient β. Since a model is supposed to be a simplification excluding everything that can be excluded without notable loss of accuracy, the best solution could be the one applied here: to set the

coefficient high enough not to limit the mass transfer. Since the high values were actually observed, it was regarded as realistic to use these values.

Attempts with higher values than those actually measured generally gave better fits, but there is no physiological reason to do so, as these values were not measured. A too high value (1 for example), gave a way too high mass loss initially. The value 0.048 $\frac{m}{s}$ performed quite well, but for the last dried samples at 4 ^{o}C and 80 % humidity, the drying rate became too low after a while.

In stead of assuming a value of the mass transfer coefficient, one could place small tanks of water in the drying chamber together with the hams and measure their weight in the same way as them. From this one could find out whether the error lies in the correlations, velocity measurements or if the samples actually lose more water than a water surface of the same size does (even though this seems unlikely). Then one could either find the real β from the water measurements, or, if the hams lost water faster than the water tanks, conclude that the difference must be due to salt or capillary effects. If the samples of different salt contents then differed, these differences could be attributed to salt, and the rest to capillary forces.

It is very strange that the required mass transfer coefficient was higher for the samples that were smaller and had lower driving forces for drying in all ways. No theory predicts that the mass transfer coefficient should become higher at higher humidity and lower temperature, but maybe these lower driving forces are actually the reason why β must be higher: If the driving forces decrease too much in the model, then the predicted β would not be sufficiently high. This would indicate that the driving forces in the model are wrong, and then it is difficult to defend its realism. The mass transfer coefficient should differ for the samples as it depends on length (through the Reynolds number), but the difference between observed and theoretical values is too big to be explained by this.

Both heat and mass transfer calculations indicated that the heat and mass transfer coefficients should be much higher. Since both these calculations gave this result, it strengthens the idea that there were turbulence or higher velocity than assumed in the drying chamber. Though, it does not explain that the necessary enhancement of these was several times higher than theoretical values, or why the samples at lowest drying potential required a larger value than the other samples.

Since all measurements were the sum of the weights of many samples and no individual measurements of the samples were made, no deviation statistics could be calculated from the measurements. The average values were used. All hams differ a bit in composition and give slightly different drying curves [Gou et al., 2004], thus, using the average should give a model that is quite close to most real drying curves, but results for a specific ham would not be as exact as the obtained results here.

The error was divided by the number of measurement points minus the degrees of freedom. In the Strømmen model, this was initially two, but later, since both β and X_P, the moisture content for when to start pressure decrease, were chosen, one could argue that the degrees of freedom is three or four. The difference is insignificant for the samples were some hundred measurement points were used, but for the samples with ten it matters.

As this model is the only one that was not explicit, a numerical method was needed, but an explicit expression was also derived when it was discovered that this was possible. The explicit and implicit methods gave similar results both in terms of curves and parameters, thus the use of the numerical method did not give errors in the results. The only mathematical problem was that the selection of parameters was based on the ones that gave the smallest overall error. The parameters are those that fits most data points (lowest value of σ^2 as given in (6.24)), and therefore gives priority to the part of the curve where there are most measurements, generally making the start phase bad.

Changing one parameter changes all the others, and uncertainty about one makes all the other equally uncertain. No clear correlation was found between the all model parameters and process conditions. (But it was found that dry layer should be a function of removed water and pressure should decrease in a way like in sorption isotherms.) This means that overall, there is *one* equation for moisture loss, and *four* unknowns: initial dry layer thickness s_0, dry layer thickness s (its relation to removed water) β and μ. (Not including the parameter for when an eventual pressure decrease should occur.) If some of these were measured (initial and final dry layer thickness and β), this would add value to the model.

Since so many parameters were allowed to vary to fit the curves, one could argue that the model is merely curve fitting. The mass transfer coefficient was extremely high, μ less than 1 and many parameters found by fitting the curve. On the other side, the model gives very good predicitions, even if there might be errors in it. A completely realistic model would have to include extremely many factors, making it slow and cumbersome to use, so any useful model must be a simplification.

If osmotic dehydration and capillary forces can be included simply by enhancing a parameter, this is a very convenient simplification. Simplifications are just what a model should involve, as long as they do not give a poorer result. Inclusion of more details should improve accuracy, but in this project, the accuracy was satisfactory whith enhanced transfer parameters. The Strømmen model is claimed to be suitable for process simulation for energy optimization at constant conditions. This could also be extended to include conditions that vary if further research is conducted.

The model should be used with a high mass transfer coefficient, μ >0.1 and constant, and dry layer growing according to (6.15) as this gives good results, allows for sufficient initial mass transfer and predicts the drying well. All though the dry layer should be ten times smaller and μ ten times larger, the simulations would be good and show a realistic trend for water loss. Hence, this model can be used for energy saving simulations with satisfactory results.

All tasks in the project description have been completed, except that no scientific article was written, because the focus was rather directed to finishing this paper. The article in the project description was optional and not likely to be published, and the remaining time to write it short. This written paper should cover all necessary information.

Chapter 9

Proposal for further work in a master's thesis

To save energy by decreasing the production time of dry-cured ham seems unrealistic from the literature review, as time and moisture are necessary for the chemical and biochemical changes within the hams, developing the desirable taste and structure. However, a local supplier informed that they also produce a low quality ham, which it is both possible and desirable to shorten the production time for, if one can dry it faster. Therefore, a master's thesis could involve:

- improve the model developed in DYMOLA to depend on temperarture.
- investigate if and how the internal resistance decreases if drying is interupted for a while and then started again, and include this in the model.
- test different drying conditions (temperature and relative humidity), both constant, intermittent and time varying, to find promising drying scemes.

This would require further experimental data to verify the drying model at non constant conditions and conditions that were not considered in this work. Another possibility is to look at the energy system, which often involves cooling supplied air, condense out water and then reheat it. The task could then be to:

- simulate the drying if the air is circulated only by convection due to hot pipes in the floor and/or cold pipes in the ceiling (this is done in Spain, according to Erlend Indergård).
- look at different ways to provide dry air, for example:
  - [Gou et al., 2002] reported that the air was dried by silica gel filter, not by cooling and reheating.
  - [AG,] delievers several sorption dehumidifiers.
  - look at how compressing a part of the air could be utilized to heat up other air streams and condense out water, see Figure 9.1.
- find out how much energy that can be saved if extra heat exchangers are placed at strategical points in the system (and where these points are).

The first point would also involve to improve the model in DYMOLA so that it depends on air velocity, which again would require better knowledge of the mass transfer coefficient and thereby laboraty work.

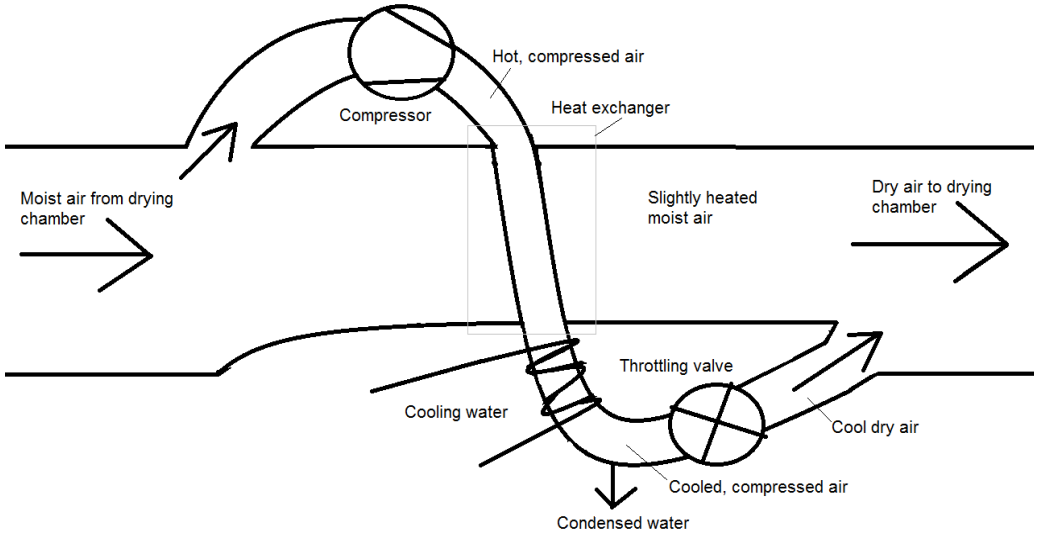

Figure 9.1: A simplified scetch of an energy system for dehumidifying air: The heat exchanger (the grey box) should be more complex than the extremeley simple one in the picture, drawn only to show the working principle. Extra heat exchange after the throttling valve could also be a way to deliver cooling, for example to the cooling water. The optimal solution would probably involve that the air reaches an exact, desired temperature after throttling, though. How water should be removed at high pressure, the amount of air that should be compressed and the temperatures at the different places needs investigation.

Appendix A

APPENDIX

A selection of the scripts used for modeling are given in this section. All other files were equal to these, except that temperature, length of samples, relative humidity and which experminatal data that were imported varied. Several duplicates of each scripts are not given. All results can be found from these files by changing these parameters in the given scripts.

A.1 MATLAB SCRIPTS

Listing A.1: Script finding the optimal parameters for more experiments in the Fickean model

```
%mass in kg, subtracted metal track and lard
mass=0.1*(unsalted()-0.203-0.7845);
massS=0.1*(salted()/1000-0.203-2.293);
%time step in seconds
dt=601;
%time in seconds for each measurement
t=zeros(length(mass),1);
tS=zeros(length(massS),1);
for j=0:length(massS)-1
    t(j+1)=j*dt;
    tS(j+1)=j*dt;
end
%(the unsalted sample needs longer time)
for j=length(massS):length(mass)-1
    t(j+1)=j*dt;
end
%find optimal parameter for the two experiments
u=FindDeffFick(mass,mass(end)*4.01/mass(1)-1);
s=FindDeffFick(massS,0.55);
sXend=FindDeffFick(massS,2.56);

%Optimal diffusion coeffis\cients (D) for the case of flat(Arnau) and
%sin-shaped (Sine) initial profiles, for the unsalted (u), salted sample
%with equilibrium moisture content of 0.55 (s) and eq. moisture of 2.56
%(sXend). Corresponding errors in SSQ_vectors
D_Arnau=[u(1,1) s(1,1), sXend(1,1)];
D_Sine=[u(1,2) s(1,2), sXend(1,2)];
SSQ_Arnau=[u(2,1) s(2,1), sXend(2,1)];
SSQ_Sine=[u(2,2) s(2,2), sXend(2,2)];
```

Listing A.2: Function finding optimal parameters in the Fickean model for one experiment

```
function dqs=FindDeffFick(mass, Xe)
arnau=true; %use flat profile=true
%error measures
m=10^10;
SSQ=zeros(10,1);
```

```
for i=1:20
    %trying different parameters for different samples/equilibrium weights
    if length(mass)>3000
        a=9.2*10^-10;
    elseif Xe>1
        a=10.9*10^-10;
    else
        a=3.6*10^-11;
    end
    Deff=i*10^-12+a; %diffusion coefficient
    %find error from simulation function diff1
    SSQ(i)=diff1(Deff,arnau,mass,Xe);
    if SSQ(i)<m
        mindex=i;%index of the parameter with smallest error
        m=SSQ(i);
    end
end
%save best result and corresponding error
D_Arnau=mindex*10^-12+a;
SSQ_Arnau=SSQ(mindex);

arnau=false; %use sine-shaped profile
%error measure
m=10^10;
SSQ=zeros(10,1);
for i=1:20
    %trying different parameters for different samples/equilibrium weights
    if length(mass)>3000
        a=11.2*10^-10;
    elseif Xe>1
        a=15.0*10^-10;
    else
        a=1.7*10^-10;
    end
    Deff=a+i*10^-12;%diffusion coefficient
    %find error from simulation function diff1
    SSQ(i)=diff1(Deff,arnau,mass, Xe);
    if SSQ(i)<m
        mindex=i;
        m=SSQ(i);
    end
end
%save best result and corresponding error
D_Sine=a+mindex*10^-12;
SSQ_Sine=SSQ(mindex);
dqs=[D_Arnau, D_Sine;%
    SSQ_Arnau, SSQ_Sine];%
end
```

Listing A.3: Function simulating a drying curve by Fick's law for given parameters

```
function SSQ1=diff1(Deff,arnau,Lab, Xe)
%arnau=Use flat inital profile, alternatively, the sine-shaped is used
%number of measurement points
n=length(Lab);
L=0.05;%Length, total, a thicker product dries more slowly
z=0:L/100:L;
dt=601;
Psi=zeros(n,length(z));
%Remaining mass and derivative:
m_sim1=zeros(n,1);
m_dot1=zeros(n-1,1);
m_sim1(1)=Lab(1);
%initial moisture content
X0=3.01;
%dry mass
mdry=Lab(1)*(1-X0/(X0+1));
%At time t=0:
```

```
if arnau
    for j=0:49
        Psi(1,:)=Psi(1,:)+2*sin((2*j+1)*pi/2)/((2*j+1)*pi/2)^2*(-1)^j;
    end
else
    Psi(1,:)=InitialProfile2(L);
end
Xdb=zeros(n,1);
Xdb(1)=max(2/pi,arnau)*Psi(1,end)*(X0-Xe)+Xe;%
for time=2:n
    t=(time-1)*dt;
    if arnau
        for j=0:49
            Psi(time,:)=Psi(time,:)+2*sin((2*j+1)*pi/2)*...
                exp(-Deff*t*(pi*(2*j+1)/2./z).^2)/((2*j+1)*pi/2)^2*(-1)^j;
        end
    else
        %pi/2 gives an initial average of Psi equal to 1, as desired
        Psi(time,:)=pi/2*sin(pi/2*z/L)*exp(-pi^2*Deff*t/(2*L)^2);
    end

    Xdb(time)=Psi(time,end)*max(2/pi,arnau)*(X0-Xe)+Xe;%
end
t=zeros(1,n);
%simulation;
for time=2:n-1
    %Removed water=difference in water concentration detween two time steps
    m_dot1(time)=sum((Xdb(time-1,:)-Xdb(time,:)))*mdry/dt;
    m_sim1(time)=m_sim1(time-1)-m_dot1(time)*dt;
    t(time)=(time-1)*601/24/3600;
end
t(n)=601*(n-1)/24/3600;
m_sim1(n)=m_sim1(n-1)-m_dot1(n-1)*dt;
%error measure
SSQ1=sum(Lab-m_sim1).^2/(n-1);
%mesh(z,t,Psi)
% plot(t,Lab, '*')
% hold on
% grid on
% plot(m_sim1,'g')
% xlabel('Time [days]')
% ylabel('Weight [kg]')
% save('Spes.txt','m_sim1','-ascii')
end
```

Listing A.4: The sine-shaped initial moisture profile used in the Fickean model

```
function f=InitialProfile2(L)
    x=0:L/100:L;
    f=pi/2*sin(pi/2*x/L);
end
```

Listing A.5: The script used to model LowSalt80 by Fick's law

```
clc
clear all
close all
%Using flat inital profile is
arnau=false;
%alternatively, the sine-shaped is used
%measured mass and time
Meas=lowSalted2();
Lab=Meas(:,2);
LabT=Meas(:,1);
%number of simulation steps
n=round(LabT(end)/601)+1;
```

```
T=4+273.15;%%%%%%%%%%%%%%
v=0.4;
L=0.04;%Length, total, a thicker product dries more slowly
%surface area for evaporation
A=L^2; %Only drying from one side
%kg water/kg air in the incomming air:
phi=0.80;%%%%%%%%%%%%%%%%%%%%
z=0:L/100:L;
dt=601;
Psi=zeros(n,length(z));
%simulated remaining mass and derivative:
m_sim1=zeros(n,1);
m_dot1=zeros(n,1);
m_sim1(1)=Lab(1);
%initial moisture content
X0=3.01;
%dry mass
mdry=Lab(1)*(1-X0/(X0+1)); %in grammes!!!!
%equilibrium moisture content
Xe=2.2;
%diffusion coefficient
Deff=13.6*10^-10;
%making initial profile
if arnau
    for j=0:49
        Psi(1,:)=Psi(1,:)+2*sin((2*j+1)*pi/2)/((2*j+1)*pi/2)^2*(-1)^j;
    end
else
    Psi(1,:)=InitialProfile2(L);
end
Xdb=zeros(n,1);
Xdb(1)=max(2/pi,arnau)*Psi(1,end)*(X0-Xe)+Xe;%
%simulating dimensionless water content
for time=2:n
    t=(time-1)*dt;
    if arnau
        for j=0:49
            Psi(time,:)=Psi(time,:)+2*sin((2*j+1)*pi/2)*exp(-Deff*t*(pi*(2*j+1)/2./z).^2)/((2*j+1)*pi/2)^2*(-1)^j;
        end
    else
        %Psi(time,:)=PsiS0+(1-PsiS0)*sin(pi*z/(2*L))*exp(-pi^2*Deff*t/(2*L)^2);
        %pi/2 gives an initial average of Psi equal to 1, as desired
        Psi(time,:)=pi/2*sin(pi/2*z/L)*exp(-pi^2*Deff*t/(2*L)^2);
    end
    Xdb(time)=Psi(time,end)*max(2/pi,arnau)*(X0-Xe)+Xe;%
end
%finding corresponding mass
m_sim1(2)=Lab(1);
for time=2:n-1
    %Removed water=difference in water concentration detween two time steps
    m_dot1(time)=sum((Xdb(time-1,:)-Xdb(time,:)))*mdry/dt;
    m_sim1(time)=m_sim1(time-1)-m_dot1(time)*dt;
end
m_sim1(n)=m_sim1(n-1)-m_dot1(n-1)*dt;
%error measure
    l=length(Lab);
    SSQ=0;
    for i=1:1
        SSQ=SSQ+(Lab(i)-m_sim1(1+round(LabT(i)/dt)))^2/(1-1);
    end
%plot the result
dt=dt/24/3600;
LabT=LabT/24/3600;
plot(LabT,Lab, '*')
hold on
grid on
plot(0:dt:(n-1)*dt,m_sim1,'g')
xlabel('Time [days]')
ylabel('Weight [kg]')
%save('FickSineLow.txt','m_sim1','-ascii')
```

Listing A.6: Script used for plotting the results from the Fickean model

```
clear all
close all
clc
SaltFlatXend=load('FFlatSXend.txt','-ascii');
SaltFlat=load('FFlatS.txt','-ascii');
SaltSineXend=load('FSineSXend.txt','-ascii');
SaltSine=load('FSineS.txt','-ascii');
UnsaltFlat=load('FFlatU.txt','-ascii');
UnsaltSine=load('FSineU.txt','-ascii');
LabS=0.1*(salt()/1000-0.203-2.293);
LabU=0.1*(unsalt()-0.203-0.7845);
timeS=0:601:601*2016;
timeU=0:601:601*6185;
LabStime=0:6010:6010*200;
LabUtime=0:6010:6010*617;
timeS=timeS/24/3600;
timeU=timeU/24/3600;
LabStime=LabStime/24/3600;
LabUtime=LabUtime/24/3600;
subplot(2,1,1)
plot(LabStime,LabS,'b*')
grid on
hold on
plot(timeS, SaltFlatXend, 'r.', timeS, SaltFlat, 'y.',timeS, SaltSineXend, 'k', timeS, SaltSine, 'g')
ylabel('Weight [kg]')
xlabel('Time [days]')
title('Salted sample')
set(gca, 'color', 'none');
legend('Measured', 'Flat inital profile, Xe=2.56','Flat inital profile, Xe=0.55', 'Sine-shaped ...
    initial profile, Xe=2.56', 'Sine-shaped initial profile, Xe=0.55')
hold off
subplot(2,1,2)
plot(LabUtime, LabU, 'b*')
hold on
plot(timeU, UnsaltFlat, 'r', timeU, UnsaltSine, 'g')
grid on
title('Unsalted sample')
ylabel('Weight [kg]')
xlabel('Time [s]')
set(gca, 'color', 'none');
legend('Measured', 'Flat inital profile', 'Sine-shaped initial profile')
hold off
```

Listing A.7: Script finding the optimal parameters for the Weibull model by the grid method

```
clear all
close all
clc
%Script that finds beta by optimising
%number of iterations
nit=100;
%air velocity
v=1.8;
%inital water content on dry basis
Xwi=3.01;
Xwo=Xwi;
%vector containing all measured weigths of the sample
Lab=0.0001*(salted()-203-2293);%0.1*(unsalted()-0.203-0.7845);%xlsread('data2.xlsx', 'B:B'); ...
    %DataA(); %or if you want another file, save it in xlsx-format and
%write the filename in like this: Lab=xlsread('filename.xlsx', 'B:B');
%startvalue for finding beta(should be low):
startbeta=0.5;
%number of measurement times:
n=length(Lab);
%time step between measurements in seconds
dt=10*60+1;
%inital weight
```

```
Wi=Lab(1);
%final weight, modelled as equlibrium weigth in the article Articulo weibull mango 2010 and ...
     therefore the same is done here
Wend=Lab(end);%   1.55*Lab(1)/(1+Xwo);%
%equilibrium water content after eq. 2 in Articulo weibull mango 2010
Xwe=Wend*(Xwi+1)/Wi-1;

%real moisture ratio and content
RX=zeros(n,1);
RMR=RX;
for i=1:n
    RX(i)=(Xwi+1)*Lab(i)/Wi-1;
    RMR(i)=(RX(i)-Xwe)/(Xwi-Xwe);
end
MR=RMR;
%Values to try for alpha and beta
b=1.0:0.033:1.3;%0.75:0.033:1.509;%0.882:0.033:1.311; %
a=0.35:0.033:1;%0.05:0.5:12;%
a=a*(n-1)*dt;
Error=zeros(length(a),length(b));
SSQ=0;
for i=1:length(a)
    for j=1:length(b)
        %generate MR with guessed a and b
        %calculate Sum of SQuares=SSQ
        for t=0:dt:(n-1)*dt
            MR(t/dt+1)=exp(-(t/a(i))^b(j));
            SSQ=SSQ+(MR(t/dt+1)-RMR(t/dt+1))^2;
        end
        Error(i,j)=SSQ;
        SSQ=0;
    end
end
%Find the smallest error and the corresponding alpha and beta
min=exp(1000);
ai=0;
bj=0;
for i=1:length(a)
    for j=1:length(b)
        if Error(i,j)<min
            min=Error(i,j);
            ai=i;
            bj=j;
        end
    end
end
mesh(b,a, Error)
ylabel('alpha')
xlabel('beta')
zlabel('Sum of squares')
alpha=a(ai);
alphaprosent=100*alpha/(n-1)/dt;
beta=b(bj);
%Plotting the best curves and finding SSQ=the Sum of SQuares of deviations
%between modelled and real MR:
SSQ=AllKnown(Lab, alpha, beta, Xwi);
     %SSQ2=AllKnown(Lab, 660330, 1.311, Xwi);
```

Listing A.8: Function used for finding the optimal parameters for the Weibull model by the grid method

```
function [alpha, beta]=FindAlphaBeta(Lab)
%576 simulations for finding alpha and beta by optimising
%Lab= vector containing all measured weigths of the sample
%inital water content on wet basis
Xwi=3.01;
%number of measurement times:
n=length(Lab);
%time step between measurements in seconds
```

```
dt=10*60+1;
%inital weight
Wi=Lab(1);
%final weight, modeled as equlibrium weigth in the article Articulo weibull mango 2010 and ...
     therefore the same is done here
%Wend=Lab(end);
%equilibrium water content after eq. 2 in Articulo weibull mango 2010
Xwe=0.55; %Wend*(Xwi+1)/Wi-1;
%real moisture ratio and content
RX=zeros(n,1);
RMR=RX;
for i=1:n
    RX(i)=(Xwi+1)*Lab(i)/Wi-1;
    RMR(i)=(RX(i)-Xwe)/(Xwi-Xwe);
end
%vector for simulated moisture ratio
MR=RMR;
%parameters to be tried
b=0.6:0.033:1;%beta
a=6.5:0.033:7;%alpha
a=a*(n-1)*dt;
Error=zeros(length(a),length(b));
SSQ=0;
for i=1:length(a)
    for j=1:length(b)
        %generate MR with guessed a and b
        %calculate Sum of SQuares=SSQ
        for t=0:dt:(n-1)*dt
            MR(t/dt+1)=exp(-(t/a(i))^b(j));
            SSQ=SSQ+(MR(t/dt+1)-RMR(t/dt+1))^2;
        end
        Error(i,j)=SSQ;
        SSQ=0;
    end
end
%Find the smallest error and the corresponding alpha and beta
min=exp(1000);
ai=0;
bj=0;
for i=1:length(a)
    for j=1:length(b)
        if Error(i,j)<min
            min=Error(i,j);
            ai=i;
            bj=j;
        end
    end
end
% mesh(a, b, Error)
% ylabel('alpha')
% xlabel('beta')
% zlabel('Sum of squares')
%AllKnown(Lab, a(ai), b(bj), Xwi);
alpha=a(ai);
beta=b(bj);
end
```

Listing A.9: The script used for finding the optimal parameters for the Weibull model by linear regression

```
%Finds alpha and beta by linear regression, which ensures that the values
%represent what they are supposed to.
close all
clear all
%measured
Lab=0.1*(unsalted()-0.203-0.7845);%0.1*(salted()/1000-0.203-2.293);%
n=length(Lab);
%time step
```

```
dt=60*10+1;
%Make abscissa:
lnt=Lab;
for i=1:n
    lnt(i)=log(dt*(i-1));
end
%Find Real Moisture Ratio RMR
RMR=Lab;
RX=Lab;
Xwi=3.01;
Xwe=(Xwi+1)*(min(Lab)-0.001)/Lab(1)-1; %0.55;%it should be Lab(end) in stead of min(Lab)-0.001, but ...
     due to oscillations in weigth, this change is necessary
for i=1:n
    RX(i)=(Xwi+1)*Lab(i)/Lab(1)-1;
    RMR(i)=(RX(i)-Xwe)/(Xwi-Xwe);
end
%make the logarithmic function and plot it
linear=log(-log(RMR));
plot(lnt,linear,'*')
grid on
hold on
%Finding 2 sets of coeffients, 1 set discarding the first four measurements as they cause
%data trouble, another discarding the first 31 to fit the main curve better.
for c=5:27:32
sumxy=0;
sumx=0;
sumy=0;
sumx2=0;
for i=c:n
    sumxy=sumxy+lnt(i)*linear(i);
    sumx=sumx+lnt(i);
    sumx2=sumx2+lnt(i)^2;
    sumy=sumy+linear(i);
end
if c==5
    beta5=((n-c+1)*sumxy-sumx*sumy)/((n-c+1)*sumx2-sumx^2);
    minusbeta_ln_alpha=(sumy-beta5*sumx)/(n-c+1);
    hold on %plot the linear line:
   plot(lnt,minusbeta_ln_alpha+beta5*lnt, 'r', 'linewidth',3)
    alpha5=exp(-minusbeta_ln_alpha/beta5);
else
    beta32=((n-c+1)*sumxy-sumx*sumy)/((n-c+1)*sumx2-sumx^2);
    minusbeta_ln_alpha=(sumy-beta32*sumx)/(n-c+1);
    alpha32=exp(-minusbeta_ln_alpha/beta32);
    hold on %plot the linear line:
   plot(lnt,minusbeta_ln_alpha+beta32*lnt, 'y','linewidth',1.5)
end
end
xlabel('ln(time)')
ylabel('ln(-ln(MR))')
legend('Measured', 'Curve fit discarding 4 values','Curve fit discarding 31 values')
hold off
aplpha5=alpha5*100/dt/(n-2);
%Errors and plots using the variables:
SSQ5=AllKnown(Lab,alpha5,beta5,Xwi);
SSQ32=AllKnown(Lab, alpha32, beta32, Xwi);
```

Listing A.10: The script used for finding the optimal parameters for the normalized Weibull model

```
clear all
clc
close all
%Measured data:
Lab= 0.0001*(salted()-203-2293);%0.1*(unsalted()-0.203-0.7845);
%number of measurements
n=length(Lab);
%time step
dt=60*10+1;
```

```
%Characteristic length=half thickness, this value was used in experiment
L=0.025;
%Initial moisture content
Xwi=3.01;
%geometric factors (to be found)
rg=[1; 1; 1];
%creating three sets of simulated results
Sim=SimulateCurves(n,dt,L);%(First column of Sim corresponds to Deff=10^-10, then 10^-11...)
for i=1:3
%finding optimal parameters for the simulated results
[a, b]=FindAlphaBeta(Sim(:,i));
%diffusion coefficient and geometric factor are then
D=L^2/a;
rg(i)=D/exp((-9-i)*log(10));
end
%average geometric factor
Rg=sum(rg)/3;
%finding alpha, beta, D and Deff
[alpha, beta]=FindAlphaBeta(Lab);
D=L^2/alpha;
Deff=D/Rg;
alphaprosent=100*alpha/dt/(n-1);
SSQ=AllKnown(Lab,L^2/D,beta,Xwi);
```

Listing A.11: Function simulating drying curves for the normalized Weibull model

```
function MR_noise=SimulateCurves(n,dt,L)
%Simulates drying curves by Fick's law as in the article by Corzo, Bracho and Alvarez
%Matrix for the simulated results, rows=time and column=different Deff
MR_noise=zeros(n,3);
for i=3:-1:1
    %Modelled Deff values are 10^-10, 10^-11 and 10^-12 like in the article (in that order)
    De=exp((i-13)*log(10));
    for t=0:dt:dt*(n-1)
        F=0;
        for k=0:3 %using the first four terms
            F=F+exp(-De*t*((2*k+1)*pi/L)^2)/(2*k+1)^2;
        end
        %add disturbance:
        MR_noise(1+t/dt,4-i)=(1+rand()/30)*8*F/pi^2; %(first column corresponds to 10^-10, second ...
            to 10^-11 etc.
    end

end
end
```

Listing A.12: Function that generates a drying curve in the Weibull model for given parameters

```
function ok=AllKnown(Lab, a, b, Xwi)
%models the not normalized weibull when beta is known
%Lab=vector containing all measured weigths of the sample
%Xwi=inital water content on dry basis
Xwo=Xwi;

%number of measurement times:
n=length(Lab);
%time step between measurements in seconds
dt=10*60+1;
%inital weight
Wi=Lab(1);
%final weight, modeled as equlibrium weigth in the article Articulo weibull mango 2010 and ...
    therefore the same is done here
Wend=Lab(end);
%equilibrium water content after eq. 2 in Articulo weibull mango 2010
Xwe=Wend*(Xwi+1)/Wi-1; % 0.55;%
%real moisture ratio and content
```

```
RX=zeros(n,1);
RMR=RX;
for i=1:n
    RX(i)=(Xwi+1)*Lab(i)/Wi-1;
    RMR(i)=(RX(i)-Xwe)/(Xwi-Xwe);
end
%Calculating the drying curve values for normal Weibull
MR=zeros(n:1);
X=MR;
W=MR;
t=MR;
SSQ=0;
  for i=1:n
      %time in seconds:
      t(i)=(i-1)*dt;
      %moisture ratio:
      MR(i)=exp(-(t(i)/a)^b);
      X(i)=(Xwo-Xwe)*MR(i)+Xwe;
      W(i)=(X(i)+1)*Wi/(Xwi+1);
      SSQ=SSQ+(MR(i)-RMR(i))^2;
  end
makePlot(RMR, MR, Lab, W, t)
%save('WeibullUnsaltedLin2.txt', 'W', '-ascii')
ok=SSQ/(n-2);
end
```

Listing A.13: Script for plotting the results from the Weibull model

```
function ok=makePlot(RMR, MR, Lab, W, t)
figure
subplot(2,1,1)
plot(t, RMR, '*', t, MR, 'g');
ylabel('MR')
subplot(2,1,2)
plot(t,Lab,'*', t, W, 'g');
ylabel('Weigth [kg]')
xlabel('Time [s]')
ok=1;
end
```

Listing A.14: Finds measured mass transfer coefficient and inner resistance for Strømmen model

```
clear all
close all
clc
%SIMPLIFIED measurements to get good derivatives
Meas=medSalted2();
%Length of samples
L=0.04;
%Surface area
A=L^2;
%Lab=mass, use every l'th measurement
l=10;
linv=l^-1;
if max(size(Meas))>1000
    Lab0=Meas(:,2);
    time0=Meas(:,1);
    Lab=zeros(floor(linv*length(Lab0)),1);
    time=Lab;
    for j=1:length(Lab0)*linv
        Lab(j)=Lab0(j*l-l+1);
        time(j)=time0(j*l-l+1);
    end
else
    Lab=Meas(:,2);
    time=Meas(:,1);
```

```
25 end
26 if Lab(1)>100 %ensure the unit is kg
27     Lab=Lab/1000;
28 end
29
30 %suppposed water acivity
31 aw=0.9+0.1*(Lab-Lab(end))/(Lab(1)-Lab(end));
32 %Relative humidity
33 phi=0.80;
34 %Molecular weight of water
35 Mw=18.015;
36 %Air temperature
37 T=277.15;
38 %Gas constant
39 R=8314;
40 %Wet bul temperature
41 Ts=273.15+2.75;
42
43 %diffusion coefficient of water in air
44 Da=0.00014738*exp(-523.78/T); %from 4models, very similar to the value in the heat and mass book
45 %moisture content initiall on wet basis:
46 Xwb0=3.01/4.01;
47 %initial density of sample
48 rhoT0=Lab(1)/L^3;
49 Xwb=(Lab()-Lab(1)/4.01)./Lab();
50 %Dry layer thickness
51 s=(Lab(1)-Lab())/(A*rhoT0*Xwb0);
52 %mass transfer coefficient (at the surface)
53 beta=Lab;
54 %mass transfer coefficient (overall)
55 betaTot=Lab;
56
57 for t=2:length(Lab)-1
58
59     mut=(Lab(t+1)-Lab(t-1))/(time(t+1)-time(t-1)); %this is generally <0!!!
60     beta(t)=-(mut*R*T)/(aw(t)*psatw(Ts)-phi*psatw(T))/(A*Mw);
61     betaTot(t)=-(mut*R*T)/(0.99*psatw(Ts)-phi*psatw(T))/(A*Mw);
62
63 end
64 beta(1)=beta(2);
65 beta(end)=beta(end-1);
66 betaTot(1)=betaTot(2);
67 betaTot(end)=betaTot(end-1);
68
69 %Internal resistance
70 myh=zeros(length(Lab),1);
71 myhc=myh;
72
73 for j=1:length(Lab)
74     if s(j)>0
75         myh(j)=(1/betaTot(j)-1/beta(j))*Da/(s(j));
76         myhc(j)=(1/betaTot(j)-1/beta(1))*Da/(s(j));
77     end
78
79 end
80
81 subplot(1,2,1)
82 plot(s, betaTot, 'rx')
83  grid on
84 ylabel('beta_t_o_t [m^2/s]')
85 xlabel('Dry layer thickness [m]')
86 hold off
87 subplot(1,2,2)
88 [ax, p1, p2]=plotyy(time, myhc,time,s,'plot','plot');
89 grid on
90 xlabel('Time')
91 ylabel(ax(1),'Resistance myh [-]')
92 ylabel(ax(2), 'Dry layer thickness [m]')
93
94 mysend=3*Da/(betaTot(end-3)+betaTot(end-1)+betaTot(end-2));
```

Listing A.15: The script used for finding the optimal parameters in the Strømmen model

```
clf
clc
clear all
close all
% Meas=medSalted();
% %Labkg=mass, use every l'th measurement
% l=10;
% linv=1^-1;
% if max(size(Meas))>1000
%     Lab0=Meas(:,2);
%     time0=Meas(:,1);
%     Labkg=zeros(floor(linv*length(Lab0)),1);
%     Lab_t=Labkg;
%     for j=1:length(Lab0)*linv
%         Labkg(j)=Lab0(j*l-l+1);
%         Lab_t(j)=time0(j*l-l+1);
%     end
% else
%     Labkg=Meas(:,2);
%     Lab_t=Meas(:,1);
% end
% if Labkg(1)>100 %ensure the unit is kg
%     Labkg=Labkg/1000;
% end
% n=ceil(Lab_t(end)/601);
%
% Labkg=0.0001*(salt()-3207+774);
% mystart=2.01;%427.5;0.048
% dmy=0.001;
% s0start=0.0029;%0.0045;
% ds0=0.0001;
Labkg=0.1*(unsalt()-1.608+0.7845);
mystart=0.28;
dmy=0.001;
s0start=0.00;
ds0=0.0001;
n=length(Labkg);
%time for Salt and Unsalt
Lab_t=0:6010:(n-1)*6010;

%error
mini=100000;
%number of values to be tried for each parameter
x=30;
%error matrix, containing all errors obtained
SSQ=zeros(x);
%parameters to be tried
s0=zeros(1,x);
myh=s0;
for j=1:x
    myh(j)=(mystart+j*dmy-dmy);
    for k=1:x
        s0(k)=s0start+(k-1)*ds0;
        SSQ(j,k)=stromFinal(n,s0(k),myh(j),Labkg,Lab_t, 0.2425, false, true);
        if SSQ(j,k)<mini
            sk=k;
            mj=j;
            mini=SSQ(j,k);
        end
    end
end
%mesh(s0,myh,SSQ)
mass=stromFinal(n,s0(sk),myh(mj),Labkg,Lab_t, 0.2425, true, false);
%save('StromMed.txt', 'mass','-ascii');
s0(sk)
myh(mj)
```

Listing A.16: Function used for simulating the drying curves in the Strømmen model for constant μ

```
function out=stromFinal(n,s0,myh,Labkg, Lab_t, Xe, graf,ssq)
%Air temperature
T=13+273.15;
%Wet bulb temperature
Ts=10+273.15;
p=101325; %Pa
v=0.4; %m/s
%length of sample
L=0.05;%meters
%area open for convection, that is, lean meat, not covered with fat or anything else
A=L^2;%This is higly sensitive!!! and says that it only dries from one side!!
R=8314; % kJ/kmol K
%molar mass of water
Mw=18.015;
%molar mass of NaCl
Msalt=58.4428; %kg/kmol
%relative humidity (often called RH)
phi=0.68;
%initial salt concentration
Csalt=0.021;
%initial water content, dry basis
X0=3.01;
%initial moisture on wet basis
Xwb0=X0/(1+X0);
%time step
dt=6010;%s
%dry mass if all water is removed
mdry=(Labkg(1)/(1+X0));
%initial density of sample
rhoT0=1070;%Labkg(1)/L^3;%
%simulated remaining mass and its derivative:
m_sim=zeros(n,1);
m_dot=m_sim;
m_sim(1)=Labkg(1);
%Transport calculations
Da=0.00014738*exp(-523.78/T); %from 4models, very similar to the value in the heat and mass book
%mass transfer coefficient
beta=0.048;%035;%Nu*(Sc/Pr)^(1/3)*Da/L;%27; %(9.05*v^0.8)/(cpAir*rhoAir); ...
     %*(Sc/Pr)^(2/3)Insensitive to SMALL changes in this
%dry layer thickness
s=s0;
S=s0;
%relative humidity in the ham
part=0.99;
%The mass per dry mass at the time when pressure decreases
XP=0;
m_dot(1)=(0.99*psatw(Ts)-phi*psatw(T))*A*Mw/(1/beta+myh*s/Da)/R/T;
for time=2:n
    %find the log mean pressure
    RH=0.9+0.1*(m_sim(time-1)-Labkg(end))/(Labkg(1)-Labkg(end)); %relationship is quite linear ...
         according to kapsalis in Okos
    plm=psatw(T)*(phi-RH)/log(phi/RH);
    %sinulated derivative of mass and mass
    m_dot(time)=A*(part*psatw(Ts)-phi*psatw(T))*Mw/(1/beta+myh*s*(1-plm/p)/Da)/(R*T);
    m_sim(time)=m_sim(time-1)-m_dot(time)*dt;
    if m_sim(time)/mdry>2.33
        %updating s as long as the vapour pressure in the ham is
        %saturated, that is, as long as mass/dry mass > 2.33
        s=s0+(m_sim(1)-m_sim(time))/(rhoT0*A*Xwb0);
        S=s;
    else
        if XP
            part=phi+(0.99-phi)*(m_sim(time)/mdry-1-Xe)/(XP-Xe);
        else
            XP=m_sim(time)/mdry-1;
            part=wa(m_sim(time)/mdry-1);
        end
        S=s0+(m_sim(1)-m_sim(time))/(rhoT0*A*Xwb0);
    end
```

```
end
%error measure
SSQ=0;
m=length(Labkg);
for j=1:m
    SSQ=SSQ+(Labkg(j)-m_sim(floor(Lab_t(j)/dt)+1))^2/(m-2);
end
if graf
    t=m_sim;
    for time=0:n-1
        t(time+1)=time*dt;
    end
    plot(Lab_t,Labkg,'r.')
    hold on
    plot(t,m_sim,'g')
    ylabel('Weigth [kg]')
    xlabel('Time [s]')
    legend('Strommen model','Measured weigth')
    hold off
end
%Output is error or simulated mass depending on whether ssq is true/false
if ssq
    out=SSQ;
else
    out=m_sim;
end
end
```

Listing A.17: Script simulating drying curves in the Strømmen model by the explicit expression

```
clear all
close all
clc
%measured data
Meas=notSalted2();
Labkg=Meas(:,2);
Lab_t=Meas(:,1);
%time step
dt=601; %s
%number of timesteps
n=ceil(Lab_t(end)/dt);
l=round(length(Labkg)/3);
%initial density of sample
rhoT0=1070;
%Initial moisture content on dry and wet basis
X0=3.01;
Xwb0=X0/(1+X0);
%initial mass:
m0=Labkg(1);
%equilibrium mass
mdry=Labkg(1)/(X0+1);
%Relatve humidity in the ham, sligthly less than one due to sorption effects
RH=0.99;
%Relative humidity of the air
phi=0.80;
%area
A=0.04^2;
%Air temperature
T=4+273.15;
%Wet bulb T
Ts=2.75+273.15;
R=8314;
Mw=18.015;
p=101325;
Da=0.00014738*exp(-523.78/Ts); %from 4models, very similar to the value in the heat and mass book
%vapour pressures at the two temperatures
pwa=psatw(T)*phi;
pwham=psatw(Ts)*RH;
```

```
%time
t=0:dt:n*dt;
%error measure
mini=10000;
%optimal parameters
my=0;
si=0;
%assumes that heat supply is sufficient
%to include heat, the C1 should be moved to inside the for-loop, and phi
%depend on T, and mass transfer be set to minimum of what is possible with
%the available heat and mass flow predictions (and psat should be updated).
beta=1;
for myh=0.10:0.01:0.4
for s0=0.000:0.0001:0.001
C1=A^2*(pwham-pwa)*Mw*Da*Xwb0*rhoT0/(myh*R*T);
C2=A*rhoT0*Xwb0*(Da/beta/myh+s0);
%simulated mass
m=m0+C2-sqrt(C2^2+2*C1.*t);
%error measure
SSQ=0;
for i=1:l
    SSQ=SSQ+(m(1+round(Lab_t(i)/dt))-Labkg(i))^2/(l-2);
end
 if SSQ<mini
     mini=SSQ;
     si=s0;
     my=myh;
 end
end
end
%the best obtained results, parameters C1 and C2 and the simulated mass m:
C1=A^2*(pwham-pwa)*Mw*Da*Xwb0*rhoT0/(my*R*T);
C2=A*rhoT0*Xwb0*(Da/beta/my+si);
m=m0+C2-sqrt(C2^2+2*C1.*t);
%save('OnlyLow48.txt','m','-ascii')
plot(t,m,'Color',[0.6 0.2 0.67])
hold on
grid on
plot(Lab_t,Labkg,'r.')%'Color', [0.9 0.7 0])
hold off
```

Listing A.18: Script simulating the drying curves in the Strømmen model by the explicit expression before the vapour pressure of the hams decreases, and the rest of the curve numerically

```
clear all
close all
clc
%measured data
Meas=medSalted2();
Labkg=Meas(:,2);
Lab_t=Meas(:,1);
%mass per dry mass when pressure should decrease
XP=2.65;
%mass at that time
mP=XP+1;
%assume an equilibrium moisture content of
Xe=2;
%time step
dt=601; %s
%number of timesteps
n=round(Lab_t(end)/dt)+1;
l=round(length(Labkg)/1);
%initial density of sample
rhoT0=1070;
%Initial moisture content on dry and wet basis
X0=3.01;
Xwb0=X0/(1+X0);
%initial mass:
```

```
m0=Labkg(1);
%equilibrium mass
mdry=Labkg(1)/(X0+1);
%Relatve humidity in the ham and air
RH=0.99;
phi=0.80;
%area
A=0.04^2;
%Air temperature
T=4+273.15;
%Wet bulb temperature
Ts=2.75+273.15;
R=8314;
Mw=18.015;
p=101325;
%diffusion coeff. of water in air
Da=0.00014738*exp(-523.78/Ts); %from Clemente2011,
%vapour pressures in the air and ham
pwa=psatw(T)*phi;
pwham=psatw(Ts)*RH;
%time
t=0:dt:(n-1)*dt;
%error
mini=10000;
%optimal parameters
my=0;
si=0;
%simulated mass
m=zeros(n,1);
beta=1;
%parameters to be tried
for myh=0.26:0.01:0.32
for s0=0.000:0.0001:0.002
C1=A^2*(pwham-pwa)*Mw*Da*Xwb0*rhoT0/(myh*R*T);
C2=A*rhoT0*Xwb0*(Da/beta/myh+s0);
m(1)=m0;
for i=2:n
    if m(i-1)<mP*mdry %check if pressure should decrease
        part=phi+(0.99-phi)*(m(i-1)/mdry-1-Xe)/(XP-Xe);
        m(i)=m(i-1)-dt*A*(part*psatw(Ts)-pwa)*Mw/(1/beta+myh*(s0+(m0-mdry*mP)/(A*Xwb0*rhoT0))/Da)/(R*T);
    else
        m(i)=m0+C2-sqrt(C2^2+2*C1*t(i));
    end
end
SSQ=0;
for j=1:l
    SSQ=SSQ+(m(1+round(Lab_t(j)/dt))-Labkg(j))^2/(l-2);
end
 if SSQ<mini
     mini=SSQ;
     si=s0;
     my=myh;
 end
end
end
%best results found (simulated again to be plotted):
C1=A^2*(pwham-pwa)*Mw*Da*Xwb0*rhoT0/(my*R*T);
C2=A*rhoT0*Xwb0*(Da/beta/myh+si);
m(1)=m0;
for i=2:n
    if m(i-1)<mP*mdry
        part=phi+(0.99-phi)*(m(i-1)/mdry-1-Xe)/(XP-Xe);
        m(i)=m(i-1)-dt*A*(part*psatw(Ts)-pwa)*Mw/(1/beta+myh*(s0+(m0-mdry*mP)/(A*Xwb0*rhoT0))/Da)/(R*T);
    else
        m(i)=m0+C2-sqrt(C2^2+2*C1*t(i));
    end
end
plot(t,m,'Color',[0.6 0.2 0.67])
hold on
grid on
```

```
95 plot(Lab_t,Labkg,'r.')
96 hold off
97 %save('OnlyMedP.txt','m','-ascii')
```

Listing A.19: Script finding optimal parameters in the Strømmen model for constant dry layer thickness

```
1  clf
2  clc
3  clear all
4  close all
5  Meas=lowSalted();
6  %Labkg=mass, use every l'th measurement
7  l=10;
8  linv=l^-1;
9  if max(size(Meas))>1000
10     Lab0=Meas(:,2);
11     time0=Meas(:,1);
12     Labkg=zeros(floor(linv*length(Lab0)),1);
13     Lab_t=Labkg;
14     for j=1:length(Lab0)*linv
15         Labkg(j)=Lab0(j*l-l+1);
16         Lab_t(j)=time0(j*l-l+1);
17     end
18 else
19     Labkg=Meas(:,2); %3 samples, use average
20     Lab_t=Meas(:,1);
21 end
22 if Labkg(1)>100 %ensure the unit is kg
23     Labkg=Labkg/1000;
24 end
25 n=ceil(Lab_t(end)/601);
26 %parameters: startvalues and increments
27 increasestart=77.8;
28 increment=0.01;
29 myh0start=1;
30 dmyh0=0.001;
31 %error and number of values to be tried for each parameter
32 mini=100000;
33 x=20;
34 %matrix containing errors for all sets of values that are tried
35 SSQ=zeros(x);
36 %parameters
37 myh0=zeros(1,x);
38 increase=myh0;
39 for j=1:x
40     increase(j)=increasestart+(j-1)*increment;
41     for k=1:x
42         myh0(k)=myh0start+(k-1)*dmyh0;
43         SSQ(j,k)=strom3(n,myh0(k),increase(j),Labkg,Lab_t, 0.2425 , false, true);
44         if SSQ(j,k)<mini
45             mk=k;
46             mj=j;
47             mini=SSQ(j,k);
48         end
49     end
50 end
51 %mesh(s0,myh,SSQ)
52 mass=strom3(n,myh0(mk),increase(mj),Labkg,Lab_t, 0.2425, true, false);
53 % sim_t=0:601:(length(mass)-1)*601;
54 %save('myh00Low.txt', 'mass','-ascii');
55 myh0(mk)
56 increase(mj)
```

Listing A.20: Function simulating drying curves in the Strømmen model for constant dry layer thickness

```
function out=strom3(n,myh0,mmm, Labkg, Lab_t, Xe, graf,ssq)
%Air temperature
T=13+273.15;
%Wet bulb temperature
Ts=10+273.15;
p=101325; %Pa
v=0.4; %m/s
%length of sample
L=0.06;%meters
%area open for convection, that is, lean meat, not covered with fat or anything else
A=L^2;%This is higly sensitive!!! and says that it only dries from one side!!
R=8314; % kJ/kmol K
%molar mass of water
Mw=18.015;
%molar mass of NaCl
Msalt=58.4428; %kg/kmol
%relative humidity (often called RH)
phi=0.68;
%initial salt concentration
Csalt=0.021;
%initial water content, dry basis
X0=3.01;
%initial moisture on wet basis
Xwb0=X0/(1+X0);
%time step
dt=601;%s
%dry mass if all water is removed
mdry=(Labkg(1)/(1+X0));
%initial density of sample
rhoT0=1070;
%simulated remaining mass and its derivative:
m_sim=zeros(n,1);
m_dot=m_sim;
m_sim(1)=Labkg(1);
%Transport calculations: diffusion coeff of vapour in air
Da=0.00014738*exp(-523.78/T); %from Clemente2011
%mass transfer coefficient
beta=0.018;%Nu*(Sc/Pr)^(1/3)*Da/L;% %(9.05*v^0.8)/(cpAir*rhoAir); %*(Sc/Pr)^(2/3)Insensitive to ...
     SMALL changes in this
%dry layer thickness
s=0.001;
%value of internal resistance
S=myh0;
myh=myh0;
%relative humidity in the ham
part=0.99;
%The mass at the time when s=L is
XP=0;
m_dot(1)=(0.99*psatw(Ts)-phi*psatw(T))*A*Mw/(1/beta+myh*s/Da)/R/T;
for time=2:n
    %find the log mean pressure
    RH=0.9+0.1*(m_sim(time-1)-Labkg(end))/(Labkg(1)-Labkg(end)); %relationship is quite linear ...
         according to kapsalis in Okos
    plm=psatw(T)*(phi-RH)/log(phi/RH);
    %the simulated derivative of mass and mass
    m_dot(time)=A*(part*psatw(Ts)-phi*psatw(T))*Mw/(1/beta+myh*s*(1-plm/p)/Da)/(R*T);
    m_sim(time)=m_sim(time-1)-m_dot(time)*dt;
    if m_sim(time)/mdry>2.33%as long as mass per dry mass is >2.33:
        %increase internl resistance
        myh=myh0+(m_sim(1)-m_sim(time))*mmm;
        S=myh;
    else %decrease the vapour pressure in the ham
        if XP
            part=phi+(0.99-phi)*(m_sim(time)/mdry-1-Xe)/(XP-Xe);
        else
            XP=m_sim(time)/mdry-1;
            part=waMed3(m_sim(time)/mdry-1);
        end
        S=myh0+(m_sim(1)-m_sim(time))/(rhoT0*A*Xwb0);
```

```
68      end
69
70  end
71  %error measure
72  SSQ=0;
73  m=length(Labkg);
74  for j=1:m
75      SSQ=SSQ+(Labkg(j)-m_sim(floor(Lab_t(j)/dt)+1))^2/(m-2);
76  end
77  %Output is error or simulated mass depending on whether ssq is true/false
78  if ssq
79      out=SSQ;
80  else
81      out=m_sim;
82  end
83  if graf %then plot the results
84      t=m_sim;
85      for time=0:n-1
86          t(time+1)=time*dt;
87      end
88      plot(Lab_t,Labkg,'*')
89      hold on
90      plot(t,m_sim,'r')
91      ylabel('Weight [kg]')
92      xlabel('Time [s]')
93  end
94  end
```

Listing A.21: Function that gives the saturated vapour pressure for a given temperature

```
1  function p=psatw(T) %gives saturation pressure as a function of temperature
2  P=[0 4 5 6 7 10 11 12 13 14 15 16 17 18 19 20 21 22 23 24 25 26 27 28 29 30;
3      611 813 872 935 1072 1228 1312 1402 1497 1598 1705 1818 1938 2064 2198 2339 2487 2645 2810 2985 ...
           3169 3363 3567 3782 4008 4246];
4  T=T-273.15;
5  if T<=0
6      p=P(2,1);
7  elseif T>=30
8      p=P(2,end);
9  else
10     i=1;
11     while T>=P(1,i)
12         i=i+1;
13     end
14     p=P(2,i-1)+(T-P(1,i-1))/(P(1,i)-P(1,i-1))*(P(2,i)-P(2,i-1));
15 end
16 end
```

Listing A.22: Function of water content, giving a_w from the modelled sorption isotherm

```
1  function aw=wa(Xe)
2  M0=0.12;
3  K=0.97;
4  C=1000000;
5  a=(1-C)*K^2;
6  b=(-2*K+C*K-M0*K*C/Xe);
7  c=1;
8  aw=(-b-(b.^2-4*a*c).^0.5)/(2*a);
9  end
```

Listing A.23: Compares resistances in the Strømmen model as functions of salt, fat and humidity

```
close all
%Best parameters for changing s, constant myh for all samples when beta was 0.048
%Results for samples at 13 degrees and 68 % humidity
myh13=[0.454; 0.830; 0.758];
s013=[0;0;0];
%salt content on wet basis for the samples
C=[0.002, 0.032, 0.050];
%Best parameters for changing s, constant myh for the samples at 80 % and
%4 degrees
 myh4=[0.327; 0.338; 0.328];
 s04=[0.0;0.0;0.0];
%Fat content on total basis initially;
  F13=[228/(465+228); %med
      179/536; %not
      270/(408+270) %low
      ];
  F4=[250/450;
      241/428;
      328/552
      ];
  F=[F13; F4]*100;
  All=zeros(6,3);%The first index is which fat content a sample has, in
  %increasing order and the second is which salt content it has
  All(2,1)=myh13(1);
  All(3,2)=myh13(2);
  All(1,3)=myh13(3);
  All(4,1)=myh4(1);
  All(5,2)=myh4(2);
  All(6,3)=myh4(3);
  Ex=All;
  All(4,1)=0.32;
  All(1,1)=0.46;
  All(1,2)=0.93;
  All(2,3)=0.75;
  All(2,2)=0.92;
  All(3,1)=0.42;
  All(3,3)=0.65;
  All(4,2)=0.37;
  All(4,3)=0.355;
  All(5,3)=0.34;
  All(6,2)=0.335;
  All(6,1)=0.31;
  All(5,1)=0.32;
myh4guess=myh4;
myh4guess(1)=0.315;
figure(1)
plot(F, All(:,1), 'b', F ,All(:,2), 'g',F,All(:,3), 'r')% 'r',,'g' 'b',
hold on
plot((1608-203-614.73)*100/(1608-203), 0.299, 'k.')%The first unsalted sample
axis([30, 65, 0.1, 1])
xlabel('Initial fat content [% wb]')
ylabel('myh [-]')
plot(F, Ex(:,1),'k.', F ,Ex(:,2),'k.',F,Ex(:,3),'k.')
grid on
legend('Not salted', 'Low salted', 'Medium salted', 'Measured values')
figure(2)
plot(C, myh4guess, 'm', C, myh13, 'r')
hold on
plot(C, myh4, 'ms', C, myh13, 'rs')
hold on
plot(0.002, 0.299, 'rs')%The first unsalted sample
xlabel('Initial salt content [% wb]')
ylabel('myh [-]')
grid on
axis([0, 0.06, 0, 1])
legend('Fat content 56-59 % wb','Fat content 33-40 % wb')
figure(3)
plot(68, myh13(1), 'bs', 68, myh13(2), 'gs', 68 , myh13(3), 'rs', 80, myh4(1),'bs', 80, ...
     myh4(2),'rs',80, myh4(3),'gs',68, 0.299, 'bs')%The first unsalted sample
```

```
hold on
plot([68,80],[0.78, 0.33],'Color',[0.5, 0.7, 0])
hold on
plot([68,80],[0.35, 0.33], 'b')

axis([66, 82, 0.2, 1])
xlabel('Relative humidity [%]')
ylabel('myh [-]')
grid on
legend('Not salted', 'Low salted', 'Medium salted')
```

Listing A.24: The script used for plotting the results in the Strømmen model

```
clear all
close all

Un1=load('myh01.txt','-ascii');
Un0=load('myh00.txt','-ascii');
Lab_U=(unsalt()-1.608+0.7845)*0.1;
Lab_tU=0:6010:6010*(length(Lab_U)-1);
Lab_tU=Lab_tU/24/3600; %unit=days


Sa=load('myh0S.txt','-ascii');
Lab_S=(salt()-3207+774)*0.0001;
Lab_tS=0:6010:6010*(length(Lab_S)-1);
Lab_tS=Lab_tS/24/3600; %unit=days

%01 in text-file-name means beta had to be at least 1, 00 means it could be 0.
Not1=load('myh01notBeta1.txt','-ascii');%Both these have beta=1, density=1070 and parameters in Results
Not0=load('myh00notBeta1.txt','-ascii');
Not=load('myh00Not.txt', '-ascii');%This one has beta=0.018. The combination beta=0.018 and myh>1 ...
    yields a line
Nt=0:601:601*(length(Not1)-1);
Nt=Nt/24/3600; %unit=days
NS=notSalted();
NS_t=NS(:,1)/24/3600;
NS_m=NS(:,2);
%NS_m=NS_m;

Low11=load('myh01LowBeta1.txt','-ascii');%Both these have beta=1, density=1070 and parameters in ...
    Results, this one has myh>=1
Low01=load('myh00LowBeta1.txt','-ascii'); %this one has myh>=0
Low1=load('myh01Low.txt','-ascii');%Both these have beta=0.018, density=1070 and parameters in ...
    Results, this one has myh>=1
Low0=load('myh00Low.txt','-ascii'); %this one has myh>=0
Lt=0:601:601*(length(Low1)-1);
Lt=Lt/24/3600; %unit=days
LS=lowSalted();
LS_t=LS(:,1)/24/3600;
LS_m=LS(:,2);
%LS_m=LS_m;
%L0t=0:601/24/3600:(length(Low0)-1)*601/24/3600;

Med01=load('myh00MedBeta1.txt','-ascii');%Beta=1
Med11=load('myh01MedBeta1.txt','-ascii');%Beta=1
Med0=load('myh00Med.txt','-ascii');%Beta=0.018
Med1=load('myh01Med.txt','-ascii');%Beta=0.018, density=1070, parameters in Results
Mt=0:601:601*(length(Med1)-1);
Mt=Mt/24/3600; %unit=days
MS=medSalted();
MS_t=MS(:,1)/24/3600;
MS_m=MS(:,2);
%MS_m=MS_m;
%M0t=0:601/24/3600:(ceil(MS_t(end)/601)-1)*601/24/3600;

figure(1)
plot(NS_t,NS_m,'*',Nt, Not1, 'r', Nt, Not0,'g', Nt, Not, 'y', 'Linewidth', 1.5)
```

```
grid on
xlabel('Time [days]')
ylabel('Mass [kg]')
set(gca, 'color', 'none');
legend('Measured','Resistance>=1, beta=1','Resistance>=0.899, beta=1', 'Resistance>=0, beta=0.018')
title('Not salted samples')

figure(2)
plot(LS_t,LS_m,'*',Lt, Low11, 'r', Lt, Low01, 'g', Lt, Low0, 'y', Lt, Low1, 'c', 'Linewidth', 1.5)
grid on
xlabel('Time [days]')
ylabel('Mass [kg]')
set(gca, 'color', 'none');
legend('Measured','Resistance>=1, beta=1','Resistance>=0.577, beta=1','Resistance>=0, ...
    beta=0.018','Resistance>=1, beta=0.0018')
title('Low salted samples')

figure(3)
plot(MS_t,MS_m,'*',Mt, Med11, 'r', Mt, Med01, 'g', Mt, Med0, 'y', Mt, Med1, 'c', 'Linewidth',1.5)
grid on
xlabel('Time [days]')
ylabel('Mass [kg]')
set(gca, 'color', 'none');
legend('Measured','Resistance>=1, beta=1','Resistance>=0.368, beta=1','Resistance>=0, ...
    beta=0.018','Resistance>=1, beta=0.018')
title('Medium salted samples')

figure(4)
subplot(2,1,1)
plot(Lab_tU, Lab_U, '*', Lab_tU, Un1, 'r', Lab_tU, Un0, 'g', 'Linewidth', 1.5);
grid on
xlabel('Time [days]')
ylabel('Mass [kg]')
set(gca, 'color', 'none');
legend('Measured','Resistance>=1','Resistance>=0')
title('Unsalted samples')
subplot(2,1,2)
plot(Lab_tS, Lab_S, '*', Lab_tS, Sa, 'r', 'Linewidth', 1.5)
grid on
xlabel('Time [days]')
ylabel('Mass [kg]')
set(gca, 'color', 'none');
legend('Measured','Resistance>=7.54')
title('Salted samples')
```

Listing A.25: The script used for the heat calculations

```
clear all
clc
clf
close all
%mass kg
m=load('s0FinalUnsalt.txt','-ascii');
%mass of dry matter
mdry=m(1)/4.01;
%area m^2
A=0.05^2;
%Air temperature
T=286.15;
%thermal conductivity at wet bulb temperature from Marcotte2008
k=0.310;
%wet bulb temperature
Ts=283.15;
%time
t=0:6010/3600/24:6010*617/3600/24;
td=0:6010/3600/24:6010*616/3600/24;
%dry layer thickness at moisture content X=2.33
sf=(m(1)-2.33*mdry)*4.01/(A*3.01*1070);
```

```
%dry layer thickness as modelled without pressure decrease
S=(m(1)-m)*4.01/(A*3.01*1070);
n=length(S);
%dry layer thickness as modelled with pressure decrease
s=ones(n,1)*sf;
j=1;
while S(j)<sf
    s(j)=S(j);
    j=j+1;
end
%derivative kg/s
mdot=zeros(n-1,1);
for j=1:n-1
    mdot(j)=(m(j)-m(j+1))/6010;
end
%needed heat supply W
P_need=1000.*mdot.*hfg(Ts);
%Heat supplied W
P_in=zeros(4,n);
%thermal length if supply=need
sE=zeros(4,n-1);
for h=10:5:25 %different heat transfer coefficients
P_in(h/5-1,:)=A*(T-Ts)./(1/h+s/k);
Tsurf=T-P_need/(A*h);
sE(h/5-1,:)=(Tsurf-Ts)*A*k./P_need;
%sE(h/5,:)=(T-Ts)*A*k./P_need-k/h;
end
figure(1)
plot(td,P_need,'r',t,P_in(1,:),'y', t,P_in(2,:),'m', t,P_in(3,:),'b',t, P_in(4,:),'g')
grid on
xlabel('Time [days]')
ylabel('Effect [W]')
legend('Effect needed for evaporation', 'Heat supply, h=10','Heat supply, h=15','Heat supply, ...
    h=20','Heat supply, h=25')
hold off
figure(2)
plot(t, s,'r',td, sE(1,:),'y',td, sE(2,:),'m', td, sE(3,:),'b', td, sE(4,:),'g')
grid on
xlabel('Time [days]')
ylabel('Length [m]')
legend('Dry layer', 'Thermal layer h=10','Thermal layer, h=15','Thermal layer, h=20','Thermal ...
    layer, h=25')
hold off
```

Listing A.26: Function that gives the enthalpy of vaporization for water at a given temperature

```
function h=hfg(T) %gives the enthalpy of vaporization as function of temperature
    t=T-273.15;
    H=[0 5 10 15 20 25 30 35;
    2501.6 2489.7 2477.9 2466.1 2454.3 2442.5 2430.7 2418.8];
    i=1;
    while t>=H(1,i)&&i<7
        i=i+1;
    end
    if i==1
        h=H(2,1)+(H(2,2)-H(2,1))*(t-0)/(5);
    else
        h=(H(2,i)-H(2,i-1))*(t-H(1,i-1))/5+H(2,i-1);
    end
end
```

Listing A.27: The script used for plotting the thermal thicknesses in the heat calculations

```
sSalt=load('Thermal_s_salt.txt', '-ascii');
st=0:6010:6010*200;
st=st/3600/24;
figure(1)
plot(st,sSalt(:,2))
xlabel('Time [days]')
ylabel('Thermal thickness [m]')
%axis([0 13*10^5 0.04 0.09])
grid on

sUnsalt=load('Thermal_s_Unsalt.txt', '-ascii');
ut=0:6010:6010*617;
ut=ut/3600/24;
figure(2)
plot(ut,sUnsalt(:,1))
xlabel('Time [days]')
ylabel('Thermal thickness [m]')
grid on
```

A.2 DYMOLA SCRIPTS

Figure A.1: The model developed in DYMOLA consists of three submodels and a function: First, the drying tunnel containing n sections, then the drying section containing a number of hams, then the model for the ham and the function for vapour pressure as a function of moisture content, based on the sorption isotherm used in this project.

Modelica code for the Drying tunnel in DYMOLA

```
model DryingTunnel_multipleSection

 TunnelSection[nCells] tunnelSection(
 each k=1,
 each gasType=gasType)
  annotation (Placement(transformation(extent={{-20,-20},{18,14}})));

 parameter Integer nCells(min=1)=1 "nummer";

 TIL.Connectors.GasPort portA1(gasType=gasType) "Port A"
  annotation (Placement(transformation(extent={{-112,-10},{-92,10}})));
 TIL.Connectors.GasPort port1(gasType=gasType) "Port"
  annotation (Placement(transformation(extent={{92,-10},{112,10}})));
 parameter TILMedia.GasTypes.BaseGas gasType;

equation
connect(tunnelSection[nCells].port1, port1);
connect(tunnelSection[1].portA1, portA1);
 for i in 1:nCells-1 loop
   connect(tunnelSection[i].port1, tunnelSection[i+1].portA1);
 end for;

 annotation (Diagram(coordinateSystem(preserveAspectRatio=false, extent={{-100,
       -100},{100,100}}), graphics),
    uses(
    TIL(version="3.2.1"),
    Modelica(version="3.2"),
    TILMedia(version="3.2.1")));
end DryingTunnel_multipleSection;
```

Modelica code for the sections of the drying tunnel in DYMOLA

```
model TunnelSection

  TIL.GasComponents.Boundaries.BoundaryUnderdetermined boundaryUnderdetermined(
     TFixed=286.05)
    annotation (Placement(transformation(extent={{-32,8},{-24,28}})));
  TIL.GasComponents.Sensors.Sensor_V_flow sensor_V_flow
    annotation (Placement(transformation(extent={{-46,14},{-38,22}})));
  TIL.GasComponents.Sensors.Sensor_T sensor_T
    annotation (Placement(transformation(extent={{-66,26},{-58,34}})));
  TIL.GasComponents.Sensors.Sensor_phi sensor_phi
    annotation (Placement(transformation(extent={{-54,26},{-46,34}})));
  Ski ski annotation (Placement(transformation(extent={{-10,30},{10,50}})));
  inner TIL.SystemInformationManager sim(redeclare
     TILMedia.GasTypes.TILMedia_MoistAir gasType1)
    annotation (Placement(transformation(extent={{-74,80},{-54,100}})));
  Modelica.Blocks.Math.Gain gain(k=1) annotation (Placement(transformation(
       extent={{-10,-10},{10,10}},
       rotation=-90,
       origin={0,-6})));
  TIL.Connectors.GasPort portA1(gasType=gasType) "Port A"
    annotation (Placement(transformation(extent={{-114,8},{-94,28}})));
  TIL.GasComponents.Boundaries.BoundaryOverdetermined boundaryOverdetermined(
    use_temperatureInput=true,
    boundaryType="p, m_flow",
    use_massFlowRateInput=true,
    streamVariablesInputTypeConcentration="phi",
    use_relativeHumidityInput=true,
    use_mixingRatioInput=false)
    annotation (Placement(transformation(extent={{56,28},{64,8}})));
  TIL.Connectors.GasPort port1(gasType=gasType) "Port"
    annotation (Placement(transformation(extent={{94,8},{114,28}})));
  TIL.GasComponents.Sensors.Sensor_m_flow sensor_m_flow
    annotation (Placement(transformation(extent={{-76,22},{-68,14}})));
  Modelica.Blocks.Math.Add add(k2=-1, k1=+1)
    annotation (Placement(transformation(extent={{26,-42},{46,-22}})));
  parameter Real k=1 "Gain value multiplied with input signal";
  parameter TILMedia.GasTypes.BaseGas gasType;
equation
  connect(sensor_V_flow.portB, boundaryUnderdetermined.port) annotation (Line(
     points={{-39,18},{-28,18}},
     color={255,153,0},
     thickness=0.5,
     smooth=Smooth.None));
  connect(sensor_V_flow.sensorValue, ski.m_dot_air) annotation (Line(
     points={{-42,21},{-42,34},{-10.4,34}},
     color={0,0,127},
     smooth=Smooth.None));
  connect(sensor_phi.sensorValue, ski.phi_air) annotation (Line(
     points={{-50,32},{-50,40},{-10.4,40}},
     color={0,0,127},
     smooth=Smooth.None));
  connect(sensor_T.sensorValue, ski.T_air) annotation (Line(
     points={{-62,32},{-62,46},{-10.4,46}},
     color={0,0,127},
     smooth=Smooth.None));
  connect(sensor_phi.port, sensor_V_flow.portA) annotation (Line(
     points={{-50,26},{-50,18},{-45,18}},
     color={255,153,0},
     thickness=0.5,
     smooth=Smooth.None));
  connect(sensor_T.port, sensor_V_flow.portA) annotation (Line(
     points={{-62,26},{-62,18},{-45,18}},
     color={255,153,0},
     thickness=0.5,
     smooth=Smooth.None));
  connect(ski.m_evap, gain.u) annotation (Line(
     points={{0,28.8},{0,6},{2.22045e-015,6}},
     color={0,0,127},
     smooth=Smooth.None));
```

```
  connect(boundaryOverdetermined.port, port1) annotation (Line(
      points={{60,18},{104,18}},
      color={255,153,0},
      thickness=0.5,
      smooth=Smooth.None));
  connect(boundaryOverdetermined.T_in, ski.T_air_out) annotation (Line(
      points={{56,24},{42,24},{42,46},{11,46}},
      color={0,0,127},
      smooth=Smooth.None));
  connect(sensor_m_flow.portA, portA1) annotation (Line(
      points={{-75,18},{-104,18}},
      color={255,153,0},
      thickness=0.5,
      smooth=Smooth.None));
  connect(sensor_m_flow.portB, sensor_V_flow.portA) annotation (Line(
      points={{-69,18},{-45,18}},
      color={255,153,0},
      thickness=0.5,
      smooth=Smooth.None));
  connect(boundaryOverdetermined.m_flow_in, add.y) annotation (Line(
      points={{56,16},{50,16},{50,-32},{47,-32}},
      color={0,0,127},
      smooth=Smooth.None));
  connect(add.u2, sensor_m_flow.sensorValue) annotation (Line(
      points={{24,-38},{-72,-38},{-72,15}},
      color={0,0,127},
      smooth=Smooth.None));
  connect(gain.y, add.u1) annotation (Line(
      points={{-2.22045e-015,-17},{-2.22045e-015,-26},{24,-26}},
      color={0,0,127},
      smooth=Smooth.None));
  connect(boundaryOverdetermined.phi_in, ski.phi_air_out) annotation (Line(
      points={{56,20},{34,20},{34,40},{10.8,40}},
      color={0,0,127},
      smooth=Smooth.None));
  annotation (uses(
      TIL(version="3.2.1"),
      Modelica(version="3.2"),
      TILMedia(version="3.2.1")), Diagram(coordinateSystem(preserveAspectRatio=false,
              extent={{-100,-100},{100,100}}), graphics={Text(
          extent={{-70,-58},{66,-76}},
          lineColor={0,0,255},
          textString="The amount of evaporated water is a negative value(m_evap<0),
as it is the derivative if water in the hams.
Therefore, the mass flow out is the sum of massflow in-m_evap.
Massflows going out from a source are negative in Dymola, thus the
input to mass flow out is -m_flow_in+m_evap")}));
end TunnelSection;
```

Modelica code for the ham in DYMOLA

```
model Ski
/*Always assume that heat is sufficient*/
constant Real A=0.05^2; /*Area*/
constant Real L=0.05; /*Length*/
constant Real W0=0.07845; /*Initial mass*/
constant Real X0=3.01; /*Initial water content(dry basis)*/
constant Real mdry=W0/(1+X0); /*dry mass*/
constant Real Xwb0=X0*mdry; /*Initialwater content(wet basis)*/
constant Real rho_Tot0=1070;/*Initial ham density*/
constant Real myh=0.281;/*Diffusion resistance*/

  Modelica.Blocks.Interfaces.RealInput T_air(start=286.15) annotation (extent=[-120,36; -88,70],
      Placement(transformation(extent={{-122,42},{-86,78}})));
  Modelica.Blocks.Interfaces.RealInput phi_air(min=0, max=100) annotation (extent=[-120,36; -88,70],
      Placement(transformation(extent={{-122,-18},{-86,18}})));
  Modelica.Blocks.Interfaces.RealInput m_dot_air annotation (extent=[-120,36; -88,70],
      Placement(transformation(extent={{-122,-78},{-86,-42}})));
  Modelica.Blocks.Interfaces.RealOutput m_evap              annotation (extent=[92,-68; 112,
        -48], Placement(transformation(extent={{18,-18},{-18,18}},
        rotation=90,
        origin={0,-112})));                 /*PER TIME!!!!!*/
  Modelica.Blocks.Interfaces.RealOutput T_air_out(start=286)
                                       annotation (extent=[92,-68; 112,
        -48], Placement(transformation(extent={{94,44},{126,76}})));
  Modelica.Blocks.Interfaces.RealOutput phi_air_out(start=100)
                                       annotation (extent=[92,-68; 112,
        -48], Placement(transformation(extent={{92,-16},{124,16}})));
  Modelica.Blocks.Interfaces.RealOutput m_dot_out
                                       annotation (extent=[92,-68; 112,
        -48], Placement(transformation(extent={{94,-76},{126,-44}})));
constant Real R=8314; /*Universal gas constant*/
constant Real Mw=18.015; /*Molar mass of H2O*/
constant Real Da=2.3631*10^(-5);/*0.00014738*exp(-523.78/T_air);From Clemente2011, Diffusion of water in air*/
constant Real beta=0.018; /*mass transfer coefficient from surface*/

Real Air_density(start=1);
/*Real Air_density_out;*/
Real pw_air; /*Vapour pressure of the drying air*/
Real RH_Ham(start=0.99);/*"Relative humidity" in the ham, the local vapour pressure divided by the saturated*/
                                                   /*!!!!!!!!!!!!!!!!!!!!!!!!!!!!!!!!!!!!!!!!!*/
Real pw_Ham; /*Vapour pressure in the ham*/
Real W(start=W0); /*Weight*/
Real X;/*Moisture content (dry basis)*/

Modelica.SIunits.Length s(start=0.0001+0.002);/*Har lagt til to mm, Dry layer thickness*/
Real Ts=T_air-3; /*Wet bulb temperature!!!!!!!!!!!!!!!!!!!!!!!!!!!!!!!!!!!!!!!!!!!!!!!!!!!!!!!*/
Real cp_air;
Real Effect(start=0);
Real m_water_in;
Real fraction_water_in_air;
Real pw_sat_out;
Real V_dot_out;
  water ham_water(X_in=X)
 annotation (Placement(transformation(extent={{-10,-10},{10,10}})));

equation
  if X<1.33 then
    RH_Ham=ham_water.activity;
    s=(W0-mdry*2.33)/(1000*A*(1-0.197));
    /*s*A*1000*(1-0.0197)=W0-W;*/

  else
    RH_Ham=0.99;
    s*A*1000*(1-0.197)=(W0-W);
    /*s=(W0-W)/(A*Xwb0*rho_Tot0);*/
  end if;

pw_Ham=RH_Ham*(exp(-5.8002206e3/Ts + 1.3914993 - 4.8640239e-2*Ts + 4.1764768e-5*Ts^2 - 1.4452093e-
8*Ts^3 + 6.5459673 *log(Ts)));
```

```
pw_air = phi_air/100*(exp(-5.8002206e3/T_air + 1.3914993 - 4.8640239e-2*T_air + 4.1764768e-5*T_air^2 - 1.4452093e-
8*T_air^3 + 6.5459673 *log(T_air)));
der(W)=m_evap;
m_evap=(pw_air-pw_Ham)*A*Mw/(R*T_air)/(1/beta+myh*s/Da); /*OBS! <0*/
X=(W-mdry)/mdry;

m_water_in=pw_air*Mw/(R*T_air)*m_dot_air/Air_density;
fraction_water_in_air=m_water_in/m_dot_air;
Air_density=101325*(28.97*(1-fraction_water_in_air)+Mw*fraction_water_in_air)/(T_air*R);
cp_air=(T_air-250)/50*1+1006;
Effect=m_evap*2477900;/*W, 2477.9 kJ/kg is the heat of vapourization at 10 degrees*/
                                                    /*OBS! <0*/
T_air_out=T_air+Effect/(m_dot_air*cp_air); /*Effect<0*/
V_dot_out=(m_dot_air-m_evap)*R*T_air_out/(28.97*101325);
phi_air_out=100*(m_water_in-m_evap)*R*T_air_out/(Mw*pw_sat_out*V_dot_out);
 pw_sat_out=(exp(-5.8002206e3/T_air_out + 1.3914993 - 4.8640239e-2*T_air_out + 4.1764768e-5*T_air_out^2 - 1.4452093e-
8*T_air_out^3 + 6.5459673 *log(T_air_out)));
m_dot_out=m_dot_air-m_evap;
 assert(T_air_out<Ts, "Heat supply is insufficient; the drying air is cooled below the dew point.");
 assert(m_evap > 0, "The hams are absorbing water rather than being dried.");
 annotation (uses(Modelica(version="3.2")), Diagram(coordinateSystem(
        preserveAspectRatio=false, extent={{-100,-100},{100,100}}), graphics));
end Ski;
```

A.3 External effect in the Fickean model

An attempt to include the effect of relative humidity and air velocity through the mass transfer coefficient β was carried out as follows (some material is repeated for convenience): Defining $\Psi = \frac{X-X_e}{X_0-Xe}$ where X is water content, e stands for «equilibrium», 0 for time $t = 0$ and X_e and X_0 are constants, Fick's second law of diffusion is:

$$\frac{\delta\Psi}{\delta t} = D_{eff}\frac{\delta^2\Psi}{\delta z^2}, \tag{A.1}$$

with the general solution:

$$\Psi = \sum_{j=0}^{\infty}\left(C_j e^{\sqrt{B_j}z} + D_j e^{-\sqrt{B_j}z}\right)e^{D_{eff}B_j t} + \text{constant}.$$

The unknown parameters are then the constants B_j, C_j and D_j. Since Ψ must be zero after sufficiently long time, one must demand the constant is zero and that B_j is negative, and then e is raised to the power of a complex number. Using the Euler's formulas

$$e^{iz} = \cos z + i\sin z \quad \text{and} \quad e^{-iz} = \cos(z) - i\sin(z)$$

one gets that

$$\Psi(z,t) = \sum_{j=0}^{\infty}\left[(C_j + D_j)\cos\left(\sqrt{-B_j}z\right) + i(C_j - D_j)\sin\left(\sqrt{-B_j}z\right)\right]e^{B_j D_{eff}t}). \tag{A.2}$$

If external resistance to mass transfer matters, or dependence on humidity is desirable, then one should apply the boundary condition:

$$\rho_{dry}D_{eff}\frac{\delta X}{\delta z}|_{z=0} = \beta(C_{w,a} - C_{w,surf}).$$

Inserting Ψ for X:

$$\rho_{dry}D_{eff}\left((X_0 - X_e)\frac{\delta\Psi}{\delta z}|_{z=0}\right) = \beta(C_{w,a} - C_{w,surf}). \tag{A.3}$$

A relation between the moisture content and vapour concentration in the air is then needed. Assuming that $C_{w,surf} = b(X_e + (X_0 - X_e)\Psi(t,0))$ might be reasonable from sorption isotherms (see [Okos et al., 2006, Comaposada et al., 2000] and Figure 6.1). From equilibrium conditons one must then demand $C_{w,a} = bX_e$.

With the normally applied soultions to the equation, the water content at $z = 0$ is always the equilibrium water content, hence, there is always equilibrium at the surface. Thus, the boundary condition is not valid together with the normally assumed initial moisture distribution. Then

one should use the general expression for Ψ, (A.2) and insert this into (A.3):

$$\begin{aligned}
&\rho_{dry} D_{eff} \left[(X_0 - X_e) \sum_{j=0}^{\infty} \sqrt{-B_j} \left(-(C_j + D_j) \sin(\sqrt{-B_j} z) + i(C_j - D_j) \cos(\sqrt{-B_j} z) \right)_{z=0} e^{B_j D_{eff} t} \right] \\
&= \rho_{dry} D_{eff} \left[(X_0 - X_e) \sum_{j=0}^{\infty} \sqrt{-B_j} i (C_j - D_j) e^{B_j D_{eff} t} \right] \\
&= \beta \Big(C_{w,a} - b \Big(X_e + (X_0 - X_e) \Psi(t, 0) \Big) \Big) \\
&= \beta \Big(C_{w,a} - b \Big(X_e + (X_0 - X_e) \sum_{j=0}^{\infty} \left[(C_j + D_j) \cos(0) + i(C_j - D_j) \sin(0) \right]_{z=0} e^{B_j D_{eff} t} \Big) \Big) \\
&= \beta \Big(C_{w,a} - b \Big(X_e + (X_0 - X_e) \sum_{j=0}^{\infty} (C_j + D_j) e^{B_j D_{eff} t} \Big) \Big).
\end{aligned}$$

Gathering the constants at one side:

$$\beta(C_{w,a} - bX_e) = (X_0 - Xe) \sum_{j=0}^{\infty} \left(\rho_{dry} D_{eff} \sqrt{-B_j} i (C_j - D_j) + \beta b (C_j + D_j) \right) e^{B_j D_{eff} t}.$$

As noted earlier, $C_{w,a} = bX_e$, and thus:

$$0 = \sum_{j=0}^{\infty} \left(\rho_{dry} D_{eff} \sqrt{-B_j} i (C_j - D_j) + \beta b (C_j + D_j) \right) e^{B_j D_{eff} t}. \tag{A.4}$$

But now all dependence on vapour concentration in the air is lost, which is a highly important factor [Bantle et al., 2014] and the inclusion of this was the main motivation for using this approach. It is of course possible that $C_{w,s}$ is a more complicated function of the surface water content, but a boundary conditions should not pose a limit to a physical relationship.

Trying to follow this approach further, one should notice that β, the dependence on air velocity, did not disappear. If one then assumes that (A.4) is valid at all times, then it is also valid when $t = 0$. If one also requires Ψ real, then one could set $C_j = F_j + iG_j$, where F_j and G_j are real, and to make Ψ real, one must demand $D_j = F_j - iG_j$. Inserting this into (A.4) one gets:

$$\begin{aligned}
\sum_{j=0}^{\infty} -\rho_{dry} D_{eff} \sqrt{-B_j} 2 i^2 G_j &= \sum_{j=0}^{\infty} 2\beta b F_j, \\
\sum_{j=0}^{\infty} F_j &= \sum_{j=0}^{\infty} \frac{\rho_{dry} D_{eff} \sqrt{-B_j} G_j}{\beta b}.
\end{aligned} \tag{A.5}$$

This shows that the entire expression for Ψ beomes zero unless both the sine and cosine terms are included. But this is one equation with several unknowns. Another equation is necessary, and one demand must be

$$\frac{1}{L} \int_0^L \Psi(z, 0) dz = 1, \tag{A.6}$$

where L is the length of the sample. Calculating the integral and multiplying both sides with L

leads to:

$$2\sum_{j=0}^{\infty}\left[\frac{F_j}{\sqrt{-B_j}}\sin(\sqrt{-B_j}L)+\frac{G_j}{\sqrt{-B_j}}\left(\cos(\sqrt{-B_j}L)-1\right)\right]=L \tag{A.7}$$

This means that the infinite series of sine and cosine functions should equal a constant. Using the odd Fourier series of 1 with period $4L$:

$$1=\frac{1}{2}+\frac{2}{\pi}\sum_{j=0}^{\infty}\frac{1}{2j+1}\sin\left(\frac{(2j+1)\pi z}{2L}\right),\ z\in[0,2L] \tag{A.8}$$

and the even Fourier series of 1 with period $4L$:

$$1=\frac{1}{2}+\frac{2}{\pi}\sum_{j=0}^{\infty}\frac{(-1)^j}{2j+1}\cos\left(\frac{(2j+1)\pi z}{2L}\right),\ z\in[-L,L] \tag{A.9}$$

If these series should be combined to give (A.7), one should chose $\sqrt{-B_j}=\frac{(2j+1)\pi}{2L}$ and insert this into (A.7):

$$2\sum_{j=0}^{\infty}\left[\frac{2LF_j}{(2j+1)\pi}\sin\left(\frac{(2j+1)\pi}{2}\right)+\frac{2LG_j}{(2j+1)\pi}\left(\cos(\frac{(2j+1)\pi}{2})-1\right)\right]=L,$$

which results in

$$\frac{4}{\pi}\sum_{j=0}^{\infty}\frac{(-1)^jF_j}{(2j+1)}-\frac{G_j}{(2j+1)}=1. \tag{A.10}$$

To solve this equation is beyond the skills of the author.

Trying to obtain even another equation one could argue that if the hams were dried only from one side, as it was in this work, it is reasonable that there is no water gradient in the inner part of the ham at the start, thus:

$$\frac{\delta\Psi}{\delta z}(L,0)=0$$

$$\Leftrightarrow 2\sum_{j=0}^{\infty}-F_j\frac{(2j+1)\pi}{2L}\sin\left(\frac{(2j+1)\pi}{2}\right)-\frac{(2j+1)\pi}{2L}G_j\cos\left(\frac{(2j+1)\pi}{2}\right)=0,$$

which gives:

$$\sum_{j=0}^{\infty}F_j\frac{(2j+1)\pi}{2L}(-1)^j=0. \tag{A.11}$$

Then one must solve this equation together with (A.5):

$$\sum_{j=0}^{\infty}F_j-\frac{\rho_{dry}D_{eff}\sqrt{-B_j}G_j}{\beta b}=0\ \text{ and }\ \frac{4}{\pi}\sum_{j=0}^{\infty}\frac{(-1)^jF_j}{(2j+1)}-\frac{G_j}{(2j+1)}=1.$$

This is beyond what has been achieved in this project.

References

[AG,] Alfsen og gunderson: Luftavfuktning - avfuktere. http://ag.no/produkter-og-tjenester/luftavfuktning-avfuktere-1.aspx. Accessed: 15.12.2014.

[16, 2003] (2003). 1.6. water diffusion in meat. http://www.tdx.cat/bitstream/handle/10803/6675/16DifusivitatIntroduccio.PDF?sequence=16. Accessed 20.10.2014.

[New, 2012] (2012). Newton - ask a scientist. http://www.newton.dep.anl.gov/askasci/chem99/chem99244.htm. Accessed: 12.12.2014.

[Max, 2013] (2013). Maxwell–stefan diffusion. http://en.wikipedia.org/wiki/Maxwell%E2%80%93Stefan_diffusion. Accessed: 20.10.2014.

[Wik, 2014] (2014). Enthalpy change of solution. http://en.wikipedia.org/wiki/Enthalpy_change_of_solution. Accessed: 12.12.2014.

[Álvarez et al., 2009] Álvarez, D., Garrido, M. D., and Bañón, S. (2009). Influence of pre-slaughter process on pork quality: An overview. *Food Reviews International*, 25(3):233–250.

[Anderson and Williams, 1937] Anderson, W. E. and Williams, H. H. (1937). The rôle of fat in the diet. *Physiological Reviews*, 17(3).

[Bantle et al., 2014] Bantle, M., Petrova, I., Raiser, J., and Eikevik, T. M. (2014). Dynamic model and kinetics for convective drying of ham with different salt contents. *19th International drying Symposium (IDS)*.

[Bekhit et al., 2014] Bekhit, A. E.-D. A., van de Ven, R., Suwand, V., Fahri, F., and Hopkins, D. L. (2014). Effect of pulsed electric field treatment on cold-boned muscles of different potential tenderness. *Food and Bioprocess Technology*.

[Berger and Pei, 1973] Berger, D. and Pei, D. C. T. (1973). Drying of hydro scopic capillary porous solids-a theoretical approach. *International Journal of Heat and Transfer*, 16:293–302. in [Whitaker, 1977].

[Bergman et al., 2011] Bergman, T. L., DeWitt, D. P., Incropera, F. P., and Lavine, A. S. (2011). *Heat and mass transfer in capillary porous bodies*. Wiley, New York, 7 edition.

[Berlin et al., 1970] Berlin, E., Kliman, P., and Pallansch, M. (1970). Changes in state of water in proteinaceous systems. *Journal of Colloid and Interface Science*, 34(4):488 – 494.

[Besley, 1942] Besley, A. K. (1942). Improved method for determining the distribution of salt and water in cured hams. *Journal of agricultural research*, 64(5):293–306. Key No A-209.

[Cassens, 1995] Cassens, R. G. (1995). Use of sodium nitrite in cured meats today. *Food Technology*, 49:72–81.

[Cassens, 2000] Cassens, R. G. (2000). Historical perspectives and current aspects of pork meat quality in the usa. *Food Chemistry*, (4):357–363.

[Ceaglske and Hougen, 1937] Ceaglske, N. H. and Hougen, O. A. (1937). Drying granular solids. *Ind. Eng. Chem.*, 29:805–813. in [Whitaker, 1977].

[Cingi et al., 1992] Cingi, M. I., Cingi, C., and Cingi, E. (1992). Influence of dietary nitrate on nitrite level of human saliva. *Bulletin of Environmental Contamination and Toxicology*, 48(1):83–88.

[Clemente et al., 2011] Clemente, G., Bon, J., Sanjuán, N., and Mulet, A. (2011). Drying modelling of defrosted pork meat under forced convection conditions. *Meat Science*, 88(3):374 – 378.

[Comaposada et al., 2000] Comaposada, J., Gou, P., and Arnau, J. (2000). The effect of sodium chloride content and temperature on pork meat isotherms. *Meat Science*, 55(3):291 – 295.

[Corzo et al., 2010] Corzo, O., Bracho, N., and Alvarez, C. (2010). Weibull model for thin-layer drying of mango slices at different maturity stages. *Journal of Food Processing and Preservation*, 34(6):993 – 1008.

[Costa-Corredor et al., 2010] Costa-Corredor, A., Pakowski, Z., Lenczewski, T., and Gou, P. (2010). Simulation of simultaneous water and salt diffusion in dry fermented sausages by the stefan–maxwell equation. *Journal of Food Engineering*, 97(3):311 – 318.

[Crank, 1975] Crank, J. (1975). *The mathematics of diffusion*. Oxford University Press, 2 edition.

[Crapiste et al., 1988] Crapiste, G., Whitaker, S., and Rotstein, E. (1988). Drying of cellular material—i. a mass transfer theory. *Chemical Engineering Science*, 43(11):2919–2928. in [Okos et al., 2006].

[Fortes and Okos, 1981] Fortes, M. and Okos, M. (1981). Non-equilibrium thermodynamics approach to heat and mass transfer in corn kernels. *Transactions of the ASAE*, page 761–769. in [Okos et al., 2006].

[Friedman, 1996] Friedman, M. (1996). Food browning and its prevention: An overview. *J. Agric. Food Chem.*, 44(3):631–653.

[Gal, 1983] Gal, S. (1983). The need for and practical applications of sorption data. In Jowitt, R., F. Escher, B. H., Mefert, H., Spiess, W., and Vos, G., editors, *Physical properties of foods-2*, pages 13–25. Elsevier Applied Science Publishers. in [Okos et al., 2006].

[Gardner and Widtsoe, 1920] Gardner, W. and Widtsoe, J. A. (1920). The movement of soil moisture. *Soil Sci.*, 11:215–232. in [Whitaker, 1977].

[Gou et al., 2002] Gou, P., Comaposada, J., and Arnau, J. (2002). Meat ph and meat fibre direction effects on moisture diffusivity in salted ham muscles dried at 5 ^{o}c. *Meat Science*, 61(1):25 – 31.

[Gou et al., 2003] Gou, P., Comaposada, J., and Arnau, J. (2003). Nacl content and temperature effects on moisture diffusivity in the gluteus medius muscle of pork ham. *Meat Science*, 63(1):29 – 34.

[Gou et al., 2004] Gou, P., Comaposada, J., and Arnau, J. (2004). Moisture diffusivity in the lean tissue of dry-cured ham at different process times. *Meat Science*, 67(2):203 – 209.

[Hankins, 1945] Hankins, O. G. (1945). Quality in meat and meat products. *Ind. Eng. Chem.*, 37(3):220–223.

[H.Burton, 1954] H.Burton (1954). Colour changes in heated and unheated milk. i. the browning of milk on heating. *J. Dairy Research*, 21:194–203. in [Okos et al., 2006].

[Herrmann et al., 2014] Herrmann, S., Duedahl-Olesen, L., and Granby, K. (2014). Simultaneous determination of volatile and non-volatile nitrosamines in processed meat products by liquid chromatography tandem mass spectrometry using atmospheric pressure chemical ionisation and electrospray ionisation. *Journal of Chromatography A*, 1330(0):20 – 29.

[Jaeger et al., 2008] Jaeger, H., Balasa, A., and Knorr, D. (2008). Food industry applications for pulsed electric fields. pages 181–216.

[Kapsalis, 1987] Kapsalis, J. G. (1987). Influences of hysterisis and temperature on moisture sorption isotherms. In Rockland, editor, *Water Activity: Theory and Applications to Food*, chapter 9, pages 173–213. CRC Press. Science and advanced Technology directorate, U.S. Army Natick Research, Development & Engineering Center, Natick, Massachusetts.

[Katekawa and Silva, 2006] Katekawa, M. E. and Silva, M. A. (2006). A review of drying models including shrinkage effects. *Drying Technology*, 24(5–20).

[Krischer, 1940] Krischer, O. (1940). The heat, moisture, and vapor movement during drying porous materials. *VDI z., Beih.*, 1:17–24. in [Whitaker, 1977].

[Kulasiri and Samarasinghe, 1996] Kulasiri, D. and Samarasinghe, S. (1996). Modelling heat and mass transfer in drying of biological materials: a simplified approach to materials with small dimensions. *Ecological Modelling*, 86(2–3):163 – 167. Environmental and Ecological Models for Simulation and Management.

[Kuprianoff, 1958] Kuprianoff, J. (1958). Fundamental aspects of the dehydration of foodstuffs. In *Conference on Fundamental aspects of the Dehydration of Foodstuffs*, pages 14–23. Society of Chemical Industry. in [Okos et al., 2006].

[Lewis, 1921] Lewis, W. K. (1921). The rate of drying of solid materials. *Ind. Eng. Chern.*, pages 427–432. in [Whitaker, 1977].

[Luikov, 1966] Luikov, A. V. (1966). *Fundamentals of heat and mass transfer*. Pergamon, Oxford.

[Marabi et al., 2003] Marabi, A., Livings, S., Jacobson, M., and Saguy, I. (2003). Normalized weibull distribution for modeling rehydration of food particulates. *Eur. Food Res. Technol*, (217):311–318.

[Marcotte et al., 2008] Marcotte, M., Taherian, A. R., and Karimi, Y. (2008). Thermophysical properties of processed meat and poultry products. *Journal of Food Engineering*, 88(3):315 – 322.

[Marinos-Kouris and Maroulis, 2006] Marinos-Kouris, D. and Maroulis, Z. B. (2006). Transport properties in the drying of solids. In Mujumdar, A. S., editor, *Handbook of Industrial Drying*. CRC Press.

[Marriott et al., 1987] Marriott, N., Graham, P., Shaffer, C., and Phelps, S. (1987). Accelerated production of dry cured hams. *Meat Science*, 19(1):53 – 64.

[Marriott et al., 1983] Marriott, N., Graham, P., Tracey, J. B., and Kelly, R. (1983). Accelerated processing of boneless hams to dry-cured state. *J. Food Prot*, 46:717–721. in [Toldrà, 2002].

[Marriott et al., 1992] Marriott, N. G., Graham, P. P., and Claus, J. R. (1992). Accelarated dry curing of pork legs (hams): a review. *Journal of Muscle Foods*, 3:159–168.

[McBryde, 1911] McBryde, C. N. (1911). *A bacteriological study of ham souring*. Washington D. C. : U.S. Department of Agriculture, Bureau of Animal Industry. in [Besley, 1942].

[McDonnell et al., 2014] McDonnell, C., Lyng, J., and Allen, P. (2014). The use of power ultrasound for accelerating the curing of pork. *Meat Science*, 98(2):142 – 149.

[Milroy, 1917] Milroy (1917). The milroy lectures on meat inspection, with special reference to the developments of recent years. *The Lancet*, 190(4905):335 – 341. Originally published as Volume 2, Issue 4905.

[Montgomery et al., 1976] Montgomery, R. E., Kemp, J. D., and Fox, J. D. (1976). Shrinkage, palatability and chemical characteristics of dry-cured country ham as affected by skinning procedure. *Journal of Food Science*, 41(5):1110–1115.

[Mora et al., 2014] Mora, L., Escudero, E., Fraser, P. D., Aristoy, M.-C., and Toldrá, F. (2014). Proteomic identification of antioxidant peptides from 400 to 2500& #xa0;da generated in spanish dry-cured ham contained in a size-exclusion chromatography fraction. *Food Research International*, 56(0):68 – 76.

[Moran and Shapiro, 2006] Moran, M. J. and Shapiro, H. N. (2006). *Fundamentals of Engineering Thermodynamics*. John Wiley & Sons, 5 edition. SI units.

[Motilva et al., 1994] Motilva, M. J., Toldra, F., Nadal, M., and Flores, J. (1994). Prefreezing hams affects hydrolysis during dry-curing. *Journal of food science*, 59:303–305. in [Toldrà, 2002].

[Moyne and Degiovanni, 1985] Moyne, C. and Degiovanni, A. (1985). Importance of gas phase momentum equation in drying above the boiling point of water. In Toei, R. and Mujumdar, A., editors, *Drying '85*, pages 109–116. Springer Berlin Heidelberg. Laboratoire d'Energétique et de Méchanique Théorique et Appliquée Ecole Nationale Supèrieure de la Métallurgie et de l'Industrie des Mines, Parc de Saurupt, 54042 NANCY CEDEX FRANCE.

[Nesse,] Nesse, N. Knudsen-diffusjon. `https://snl.no/Knudsen-diffusjon`. Accessed: 20.10.2014.

[Okos et al., 2006] Okos, M., Narsimhan, G., Singh, R., and Witnauer, A. (2006). Food dehydration. chapter 10. Marcel Dekker/CRC Press, 2 edition.

[Pakowski and Adamski, 2007] Pakowski, Z. and Adamski, A. (2007). The comparison of two models of convective drying of shrinking materials using apple tissue as an example. *Drying Technology: An International Journal*, 25(7-8):1139–1147.

[Palmia et al., 1993] Palmia, F., Pecoraro, M., and Ferri, S. (1993). Essiccazione di prodotti carnei: calcolo del coefficiente di diffusione effettivo (de) dell'acqua in fette di lombo suino. *Industria Conserve*, 68:238–242. in [Gou et al., 2002].

[Parolari, 1994] Parolari, G. (1994). Materia prima ed innovazionetechnologica nell'industria del prosciutto crudo; analisi tecninca del settore. Lecture at the meeting 'Nueve indicazioni dalla ricera tecnologica e zootecnica', Parma, 22 ottobre 1994. in [Parolari, 1996].

[Parolari, 1996] Parolari, G. (1996). Review: Achievments, needs and perspectives in dry-cured ham technology: the example of parma ham. *Fod Science Tech. Int.*, 2(2):69–78.

[Petrova, 2015] Petrova, I. (2015). Drying kinetics and modeling of dry-cured ham with different salt concentrations. Nordic drying conference.

[Prevolnik et al., 2011] Prevolnik, M., Škrlep, M., Janeš, L., Velikonja-Bolta, Š., Škorjanc, D., and Čandek-Potokar, M. (2011). Accuracy of near infrared spectroscopy for prediction of chemical composition, salt content and free amino acids in dry-cured ham. *Meat Science*, 88(2):299 – 304.

[Radford, 1976] Radford, R. D. (1976). Water transport in meat. In *Joint meeting of commissions C2, D1, D2, D3 and E1*, number 62, pages 1–8. International Institute of refrigeration. Australian National Committee. in [Trujillo et al., 2007].

[Radford et al., 1976] Radford, R. D., Herbert, C., and Lovett, D. A. (1976). Chilling of meat-a mathematical model for heat and mass transfer. In *Comm. C2 Meeting, IIR Bull. Annex 1976-1*, pages 323–330. in [Trujillo et al., 2007].

[Raiser, 2014] Raiser, J. (2014). Convective drying and sorption characteristics of cured meat slices. Project work, NTNU and SINTEF Energi AS.

[Richard, 1981] Richard, A. H. (1981). Review of the potential hazard from botulism in cured meats. *Canadian Institute of Food Science and Technology Journal*, 14(3):183 – 195.

[Richards, 1931] Richards, L. A. (1931). Capillary conduction of liquids through porous mediums. *Journal of Applied Physics*, 1(5):318–333.

[Ruiz-Cabrera et al., 2004] Ruiz-Cabrera, M. A., Gou, P., Foucat, L., Renou, J. P., and Daudin, J. D. (2004). Water transfer analysis in pork meat supported by nmr imaging. *Meat Science*, 67(1):169–178.

[Scalettar et al., 1988] Scalettar, B. A., Abney, J. R., and Owicki, J. C. (1988). Theoretical comparison of the self diffusion and mutual diffusion of interacting membrane proteins. *Proc Natl Acad Sci U S A*, 85:6726–6730.

[Schilling et al., 2004] Schilling, M., Marriott, N., Acton, J., Anderson-Cook, C., Alvarado, C., and Wang, H. (2004). Utilization of response surface modeling to evaluate the effects of non-meat adjuncts and combinations of {PSE} and {RFN} pork on water holding capacity and cooked color in the production of boneless cured pork. *Meat Science*, 66(2):371 – 381.

[Sherwood, 1929] Sherwood, T. K. (1929). The drying of solids. i. *Ind. Eng. Chern.*, 21:12–16. in [Whitaker, 1977].

[Song, 1990] Song, X. (1990). *Low temperature, fluidized bed drying with temperature program.* PhD thesis, Norges tekniske høgskole.

[Strømmen, 1980] Strømmen, I. (1980). *Tørking av klippfisk.* PhD thesis, Norges tekniske høgskole.

[Thomas et al., 1980] Thomas, H. R., Morgan, K., and Lewis, R. W. (1980). A fully nonlinear analysis of heat and mass transfer problems in porous bodies. *International Journal for Numerical Methods in Engineering*, 15(9):1381–1393.

[Toldrà, 2002] Toldrà, F. (2002). *Dry-Cured Meat Products.* Food & Nutrition press, Trumbull, Connecticut 06611, USA, 1 edition.

[Trujillo et al., 2007] Trujillo, F. J., Wiangkaew, C., and Pham, Q. T. (2007). Drying modeling and water diffusivity in beef meat. *Journal of Food Engineering*, 78(1):74 – 85.

[Waananena et al., 1993] Waananena, K., Litchfieldb, J., and Okos, M. (1993). Classification of drying models for porous solids. *Drying Technology*, 11(1):1–40.

[Warner et al., 1997] Warner, R. D., Kauffman, R. G., and Russell, R. L. (1997). Muscle protein changes postmortem in relation to prok quality traits. *Meat Science*, 33:359–372. in [Toldrà, 2002].

[Whitaker, 1977] Whitaker, S. (1977). Simultaneous heat, mass, and momentum transfer in porous media: A theory of drying. volume 13 of *Advances in Heat Transfer*, pages 119 – 203. Elsevier.

[Wolf et al., 1972] Wolf, M., Walker, J. E., and Kapsalis, J. G. (1972). Water vapor sorption hysteresis in dehydrated food. *Journal of Agricultural Food Chemistry*, 20(5):1073–1077.